NRC Research and/or Technical Assistance Rept

PDR

EGG-SEMI-6062
October 1982

POSTTEST RELAP5 SIMULATIONS OF THE SEMISCALE MOD-2A FEEDWATER LINE BREAK TESTS S-SF-1, 2, AND 3C

J. E. Streit

Idaho National Engineering Laboratory
Operated by the U.S. Department of Energy

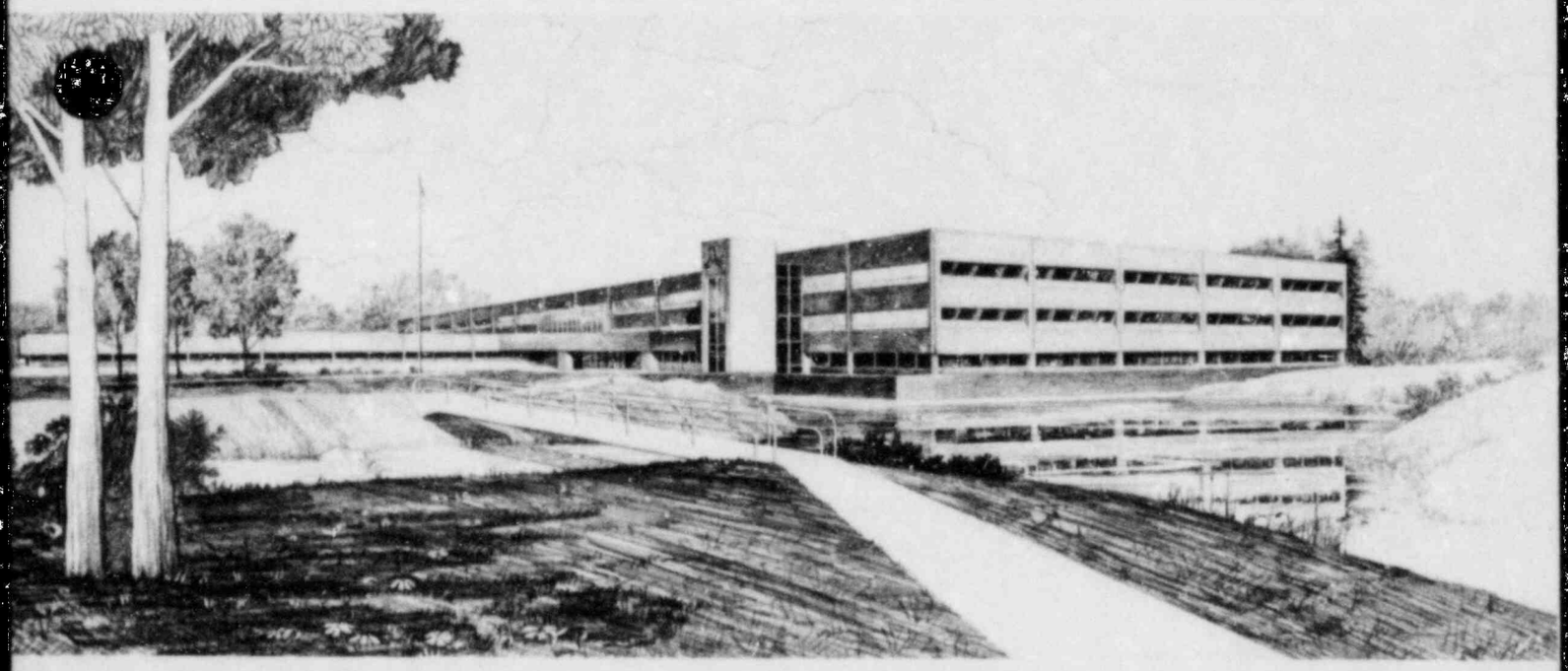

This is an informal report intended for use as a preliminary or working document

Prepared for the
U.S. NUCLEAR REGULATORY COMMISSION
under DOE Contract No. DE-AC07-76ID01570

EG&G Idaho

EG&G Idaho, Inc.

M EG&G-398
(11-79)

INTERIM REPORT

Accession No. _____

Report No. EGG-SEMI-6062

Contract Program or Project Title:

Semiscale

Subject of this Document:

Posttest RELAP5 Simulations of the Semiscale MOD-2A Feedwater Line Break Tests S-SF-1, 2, and 3c

Type of Document:

Posttest Analysis Report

Author(s):

J. E. Streit

Date of Document:

October 1982

Responsible NRC Individual and NRC Office or Division:

R. R. Landry, Reactor Safety Research

This document was prepared primarily for preliminary or internal use. It has not received full review and approval. Since there may be substantive changes, this document should not be considered final.

EG&G Idaho, Inc.
Idaho Falls, Idaho **83415**

Prepared for the
U.S. Nuclear Regulatory Commission
Washington, D.C.
Under DOE Contract No. **DE-AC07-76ID01570**
NRC FIN No. A6038

INTERIM REPORT

POSTTEST RELAP5 SIMULATIONS OF THE SEMISCALE MOD-2A

FEEDWATER LINE BREAK TESTS S-SF-1, 2, AND 3C

Approved: Gary W. Johnsen for

P. North, Manager
Water Reactor REsearch Test Facilities Division

Approved: G. W. Martinell for

G. W. Johnsen, Manager
WRRTF Experiment Planning and Analysis Branch

ABSTRACT

The RELAP5/MOD1 computer code was used to perform posttest best-estimate simulations of three experiments run in the Semiscale Mod-2A facility to investigate the transient behavior of feedwater line breaks. The results of these simulations and corresponding test data are presented in this report. An evaluation is made of the capability of RELAP5 to calculate the thermal-hydraulic response of the Semiscale Mod-2A system over a spectrum of feedwater line break sizes.

FIN No. A6038

Semiscale Program

SUMMARY

Posttest best-estimate RELAP5 calculations were performed for Semiscale Mod-2A feedwater line break (FWLB) simulation Tests S-SF-1, 2, and 3c. The results of the calculations were compared with test data to determine the capability of RELAP5 to calculate the thermal-hydraulic responses of each transient. The modeling approach employed for each of these calculations was consistent with established RELAP5 modeling practices for FWLB transients and other similar transients.

The general trends and characteristics of the tests were calculated. As a result of degradation of the primary-to-secondary heat transfer the primary coolant system (PCS) pressurized to the SCRAM setpoint. Following SCRAM the PCS continued to pressurize slightly, then depressurized continuously thereafter aided by system heat losses, auxiliary feedwater injection, and emergency core coolant (ECC) injection. Some of the more salient characteristics of the tests, however, were not calculated. These included degradation of heat transfer in the broken loop steam generator prior to SCRAM as the secondary coolant inventory was depleted through the break and the steam line. This behavior was not calculated because of preferential depletion of the steam generator downcomer coolant inventory while the coolant in the riser region remained high enough to maintain heat transfer. Degradation of the heat transfer only in the intact loop steam generator prior to SCRAM precipitated a heatup of the PCS. This is in contrast with observed test behavior where degradation of the heat transfer in both steam generators prior to SCRAM caused the PCS to heatup. An exception was Test S-SF-2, where degradation of only the broken loop steam generator heat transfer caused the SCRAM.

Recommendations are presented to improve the quality of future RELAP5 calculations of FWLB transients. In addition, supplementary plots are presented in the appendices for reference.

ACKNOWLEDGEMENTS

The author gratefully acknowledges the assistance of R. A. Shaw and R. A. Dimenna in preparing this report.

CONTENTS

FIGURES

TABLES

1. INTRODUCTION

This report presents the results and analyses of posttest computer code simulations of the feedwater line break (FWLB) transients simulated in the Semiscale Mod-2A facility. These FWLB transients were the first three tests in the Steam and Feedwater Line Break Scoping Test Series (designated S-SF).[1] The calculations were performed with Cycle 18 of the RELAP5/MOD1[2] computer code. Analysis of the calculations is based on comparisons to test data. The data comparisons are presented on an individual test basis, and collectively to show the effects of feedwater line breaks on system behavior over the break size spectrum.

FWLBs cause a loss of heat sink which may result in a overpressurization of the PCS. Depending on break size the initial phase of a FWLB transient may involve an enhanced, degraded, or null effect on primary-to-secondary heat transfer. The location of the break enables the secondary fluid to flow out of the steam generator, and results in a more rapid loss of heat sink and a more severe transient with increasing break size.

The primary objective of the three FWLB tests was to obtain representative thermal-hydraulic response data for assessment of the capabilities of water reactor safety analysis computer codes to predict integral system behavior in response to secondary side transients. Several secondary objectives identified in the Experiment Operation Specification[1] for each test were:

1. To determine the primary-to-secondary heat transfer characteristics as a function of time and steam generator inventory.

2. To characterize the influence of boundary conditions including: break size, loss of offsite power assumptions, and ECC and feedwater train performance.

3. To evaluate the utility of secondary side measurements to interpret liquid level during a blowdown.

The analysis presented in this report is directed toward the primary objective of the test series. This test series represented the first secondary side break simulation in the Semiscale system. RELAP5, which was designed for primary side breaks, had its capabilities tested for the first time for a secondary side break. The break location and modifications to the RELAP5 model are discussed in the following two sections. These are followed by the calculation-to-data comparisons, conclusions, and recommendations.

1. INTRODUCTION

This report presents the results and analyses of posttest computer code simulations of the feedwater line break (FWLB) transients simulated in the Semiscale Mod-2A facility. These FWLB transients were the first three tests in the Steam and Feedwater Line Break Scoping Test Series (designated S-SF).[1] The calculations were performed with Cycle 18 of the RELAP5/MOD1[2] computer code. Analysis of the calculations is based on comparisons to test data. The data comparisons are presented on an individual test basis, and collectively to show the effects of feedwater line breaks on system behavior over the break size spectrum.

FWLBs cause a loss of heat sink which may result in a overpressurization of the PCS. Depending on break size the initial phase of a FWLB transient may involve an enhanced, degraded, or null effect on primary-to-secondary heat transfer. The location of the break enables the secondary fluid to flow out of the steam generator, and results in a more rapid loss of heat sink and a more severe transient with increasing break size.

The primary objective of the three FWLB tests was to obtain representative thermal-hydraulic response data for assessment of the capabilities of water reactor safety analysis computer codes to predict integral system behavior in response to secondary side transients. Several secondary objectives identified in the Experiment Operation Specification[1] for each test were:

1. To determine the primary-to-secondary heat transfer characteristics as a function of time and steam generator inventory.

2. To characterize the influence of boundary conditions including: break size, loss of offsite power assumptions, and ECC and feedwater train performance.

3. To evaluate the utility of secondary side measurements to interpret liquid level during a blowdown.

The analysis presented in this report is directed toward the primary objective of the test series. This test series represented the first secondary side break simulation in the Semiscale system. RELAP5, which was designed for primary side breaks, had its capabilities tested for the first time for a secondary side break. The break location and modifications to the RELAP5 model are discussed in the following two sections. These are followed by the calculation-to-data comparisons, conclusions, and recommendations.

2. SYSTEM DESCRIPTION

The Semiscale Mod-2A system (Figure 1) is a two-loop large pressurized water reactor (LPWR) primary coolant system simulator located at the Idaho National Engineering Laboratory (INEL). The design of the Mod-2A system is based upon a Westinghouse 3411 MW four-loop LPWR. One loop of the Semiscale system (intact loop) is scaled to simulate three loops of the Westinghouse plant; the other loop (broken loop) simulates a single loop in which a postulated steam generator FWLB is simulated. The PCS volume and core power are scaled by approximately 1/1700. Geometric similarity and component layout have been maintained between the Mod-2A system and a Westinghouse LPWR. Specific similarities include a full-elevation (3.66 m) electrically heated core, full-length upper plenum and upper head, two full-elevation steam generators, and the preservation of the relative elevations of various components.

ECC systems include a high pressure injection system (HPIS), passive accumulators, and a low pressure injection system (LPIS), each of which inject coolant (approximately 300 K) into the cold leg of the intact and broken loop. The electrically heated core consists of 25 rods in a 5 x 5 matrix (1.43 cm pitch). Two rods in opposite corners are unpowered and the remaining 23 rods are powered equally, yielding a flat radial profile. The axial profile is a 12-step chopped cosine.

Each steam generator is scaled with respect to both primary and secondary coolant volumes. The intact loop steam generator contains six U-tubes and the broken loop contains two U-tubes. The secondary side of both steam generators consists of a riser (boiler) section, steam separator, and downcomer. Feedwater enters the downcomer and steam exits the top of both steam generators.

The break orifices for these FWLB tests were oriented horizontally to the cold leg centerline and located at the end of an instrumented spool piece attached to the broken loop FWLB port (Figure 2). Instruments for gathering pressure, temperature, density, and mass flow data are included

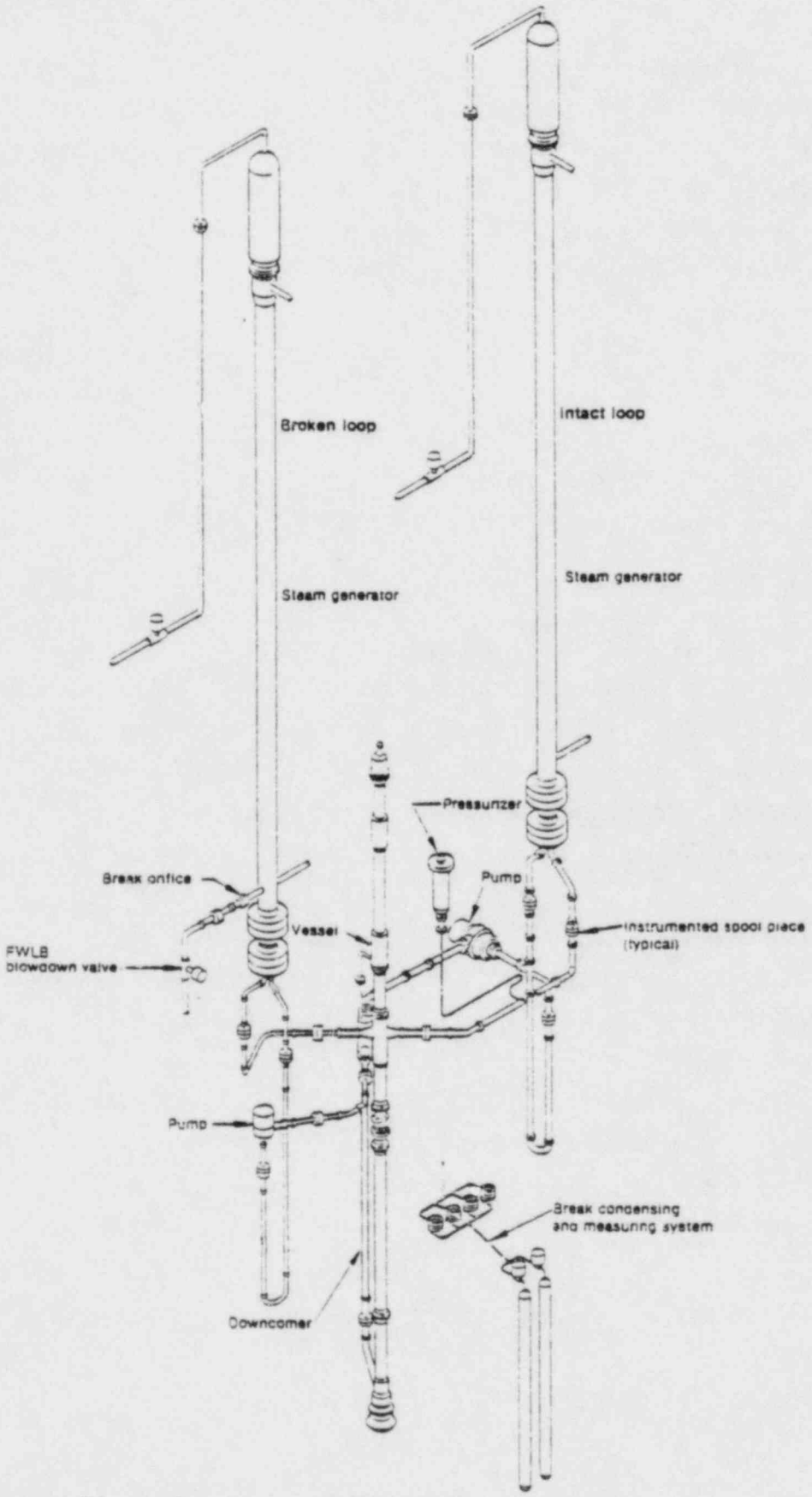

Figure 1. Semiscale Mod-2A system configuration.

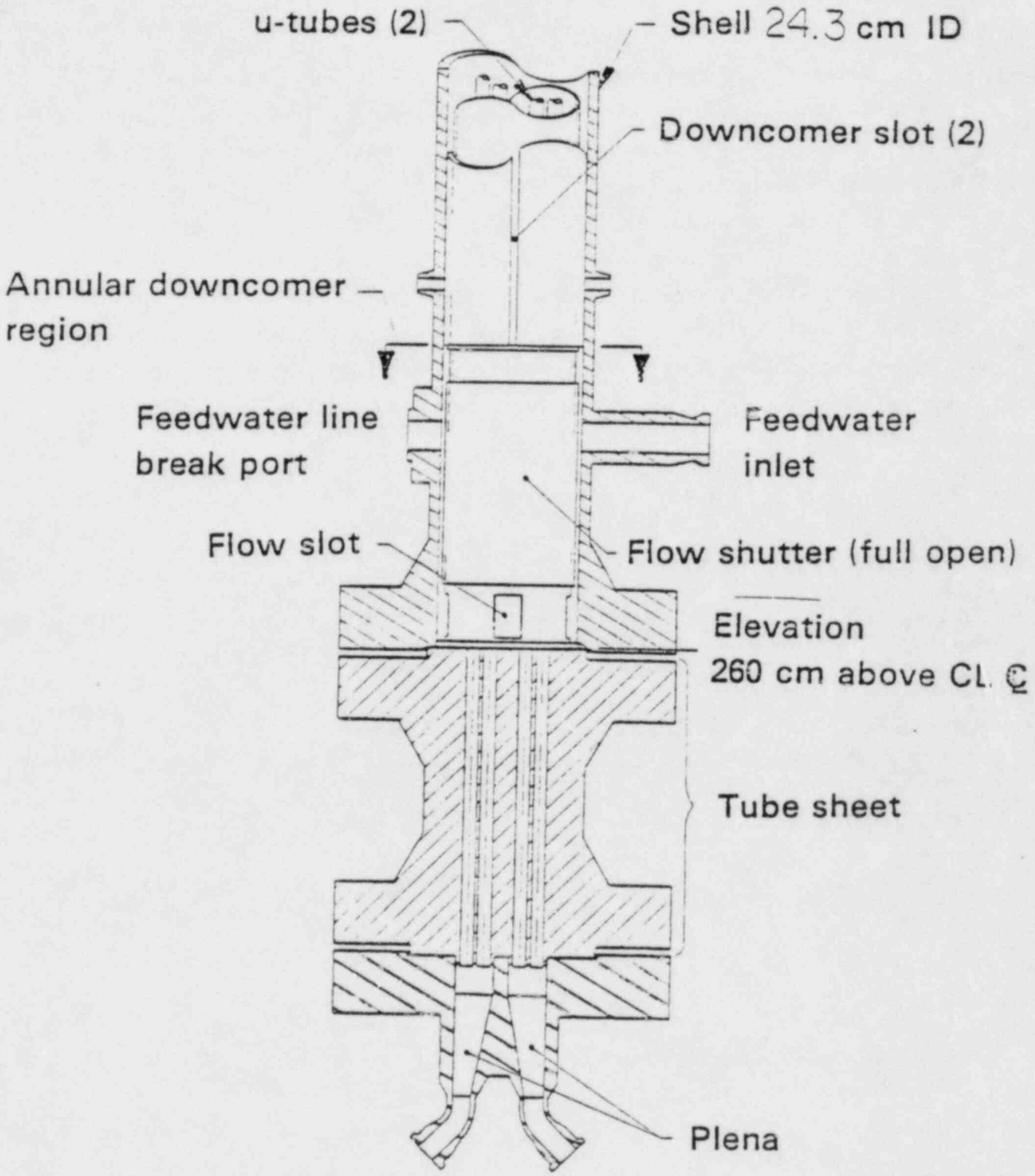

Figure 2. Detail of the Feedwater Line Break Port and Feedwater Inlet.

in the spool piece. Redundant mass flow measurements are obtained by the condensing and measuring system downstream of the elliptical entrance break orifice.

The transients simulated pipe breaks downstream of the check valve in the feedwater line piping of a steam generator in a LPWR at full power conditions. Feedwater flow is terminated to both steam generators due to the pressure differential across the check valve. Communications would normally exist between steam generators through the steam lines until the main steam isolation valves are closed. This is simulated in the Semiscale system by leaving the two independent steam control valves in their initial positions. All safety trips (e.g., low secondary level) were considered to be overridden until a high PCS pressure trip occurs. Auxiliary feedwater was not injected until after the pressurization portion of each transient was over.

3. RELAP5 MODEL DESCRIPTION

RELAP5/MOD1[2] is an advanced, one-dimensional system analysis computer code developed at the INEL for the U.S. Nuclear Regulatory Commission, Office of Reactor Safety Research (USNRC-RSR). It is based on a non-homogeneous, non-equilibrium hydrodynamic model and includes thermal-hydraulic and component models used to describe the processes that occur during the heatup and blowdown of a LPWR. RELAP5/MOD1, Cycle 18, was used for the analyses presented in this report. It is retained, with the code updates used, under INEL computer code configuration management (CCCM) archival number F00885.

The Semiscale Mod-2A system RELAP5 model is represented by the nodalization diagram in Figure 3. It is generally based on the Semiscale Mod-2A Standard RELAP5 Model.[3] The model used for these analyses consists of 187 hydrodynamic volumes and 214 heat structures. All volume parameters are calculated with non-equilibrium code models. Steam generator secondaries, ECC systems, system environmental heat loss, and piping guard heaters are modeled in detail. Table 1 summarizes the ECC systems and guard heater system boundary conditions used in RELAP5. The core axial power profile is modeled with twelve contiguous heat structures over six axial hydrodynamic volumes.

The steam generators are modeled with eight hydrodynamic volumes in the U-tube region (C600 or C700) and nine in the downcomer (C603 or C703). The riser and downcomer are modeled as annulus components to obtain relatively low interphase drag and to minimize the likelihood of flooded conditions in the steam generators.

Two discharge coefficients are applied to the RELAP5 critical flow model at the break, one (CD1) for subcooled flow and another (CD2) for two phase and vapor flow. For liquid with 0-30 K subcooling, the discharge coefficient is expressed as a function of temperature as follows (see Appendix B):

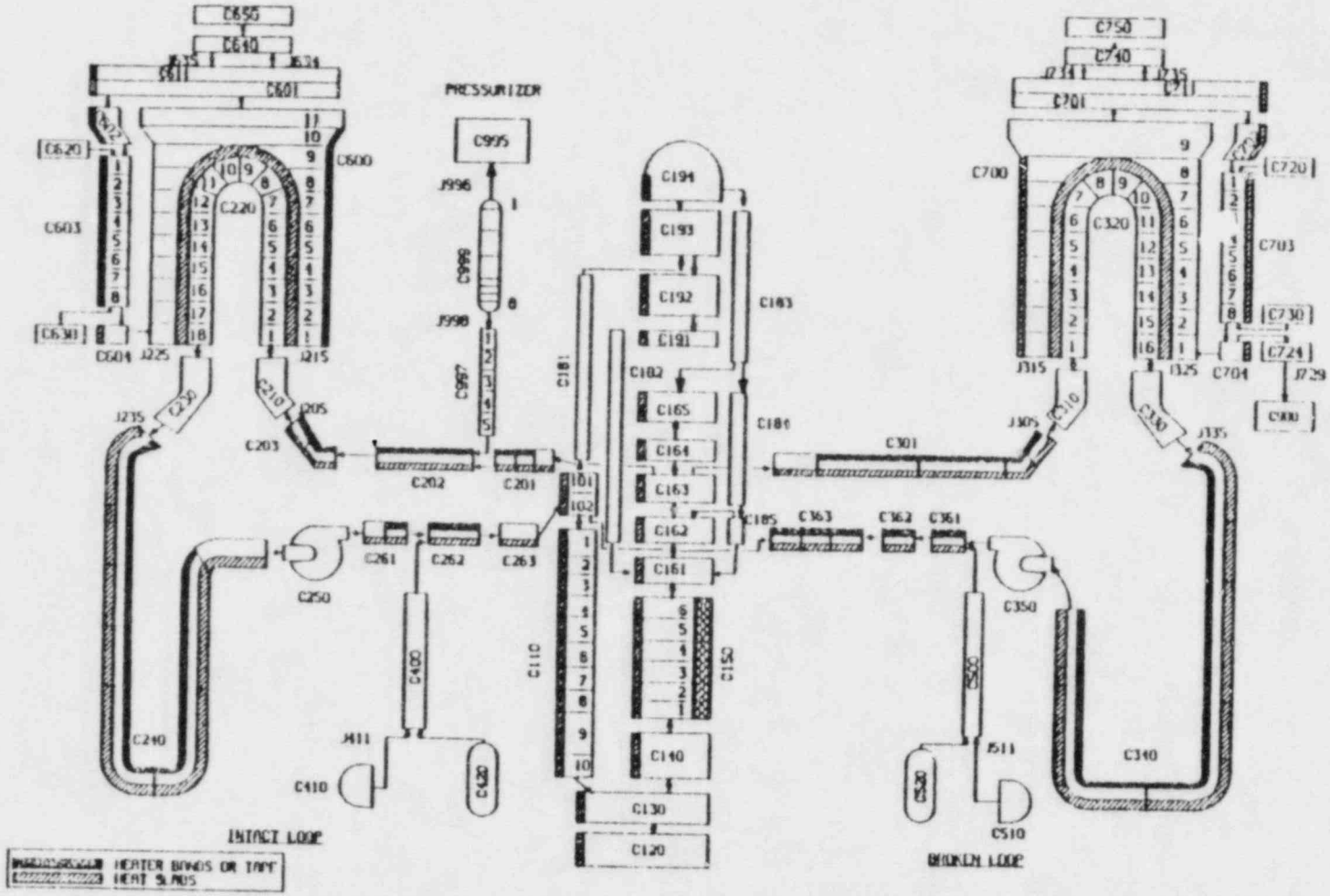

Figure 3. Semiscale Mod-2A system RELAP5 nodalization.

TABLE 1. RELAP5 MODEL BOUNDARY CONDITIONS

ECC Parameters:	All Tests
Intact Loop HPIS	
Actuation Pressure (MPa)	11.24
Injection Rate (kg/s)	See Figure 4
Temperature (K)	300
Delay (s)	25
Intact Loop Accumulator	
Actuation Pressure (MPa)	4.19
Liquid Volume (m^3)	0.045
Gas Volume (m^3)	0.026
Temperature (K)	300
Broken Loop HPIS	
Actuation Pressure (MPa)	11.24
Injection Rate (kg/s)	See Figure 4
Temperature (K)	300
Delay (s)	25
Broken Loop Accumulator	
Actuation Pressure (MPa)	4.19
Liquid Volume (m^3)	0.015
Gas Volume (m^3)	0.0088
Temperature (K)	300

Guard Heater Power:[a]	S-SF-1	S-SF-2	S-SF-3
Broken Loop Pump Suction (kW)	3.9	3.9	4.0
Intact Loop Pump Suction (kW)	8.3	8.3	8.5
Hot Legs (kW)	6.9	6.9	7.0
Cold Legs (kW)	2.9	3.0	1.9
Total (kW)	22.0	22.1	21.4

a. Values are taken from test data.

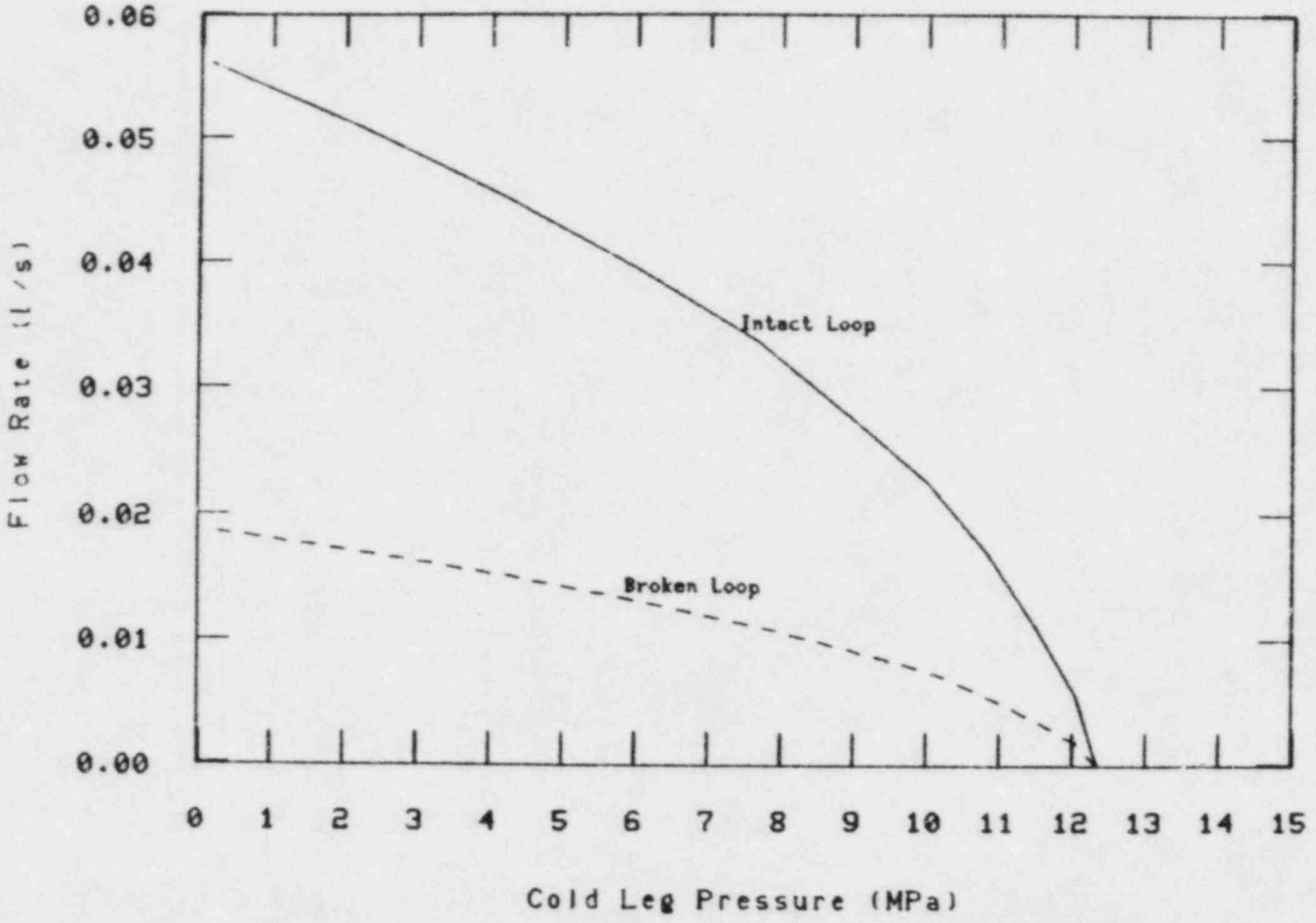

Figure 4. HPIS Flow vs Pressure

$$CD1 = 1.642 - 7.1167 \times 10^{-2}\ SC + 2.9878 \times 10^{-3}\ (SC)^2 - 4.4289 \times 10^{-5}\ (SC)^3$$

where

SC = degrees K subcooling.

Based on analyses of previous test-to-data comparisons, a two-phase discharge coefficient (CD2) of 0.84 has been shown to give good agreement, and was used in Tests S-SF-1 and 3c analyses. However, for Test S-SF-2 the calculated break flow using CD2 of 0.84 was about 45% low. The analysis for Test S-SF-2, therefore, used a higher value for CD2 (1.40) in order to obtain better break flow agreement with data.

4. CALCULATED TEST RESULTS

The equivalent break sizes for a full-size plant[a] for Tests S-SF-1, 2, and 3c were 0.035 m^2, 0.015 m^2, and 0.006 m^2, respectively. Initial conditions were typical LPWR operating conditions. Each test was independently calculated, using a consistent RELAP5 modeling approach. Initialization to steady-state conditions was achieved by allowing the code to calculate a "null transient". A comparison of the calculated steady-state initial conditions with data is given in Table 2.

Operating conditions, especially secondary coolant inventories, were different for each test in the S-SF test series. The initial secondary coolant inventories in the steam generators were determined from the measured break flow rate, steam line flow rate, auxiliary feedwater injection rate, and with the assumption that water was left in the broken loop steam generator below the break orifice (~7 kg) for each test. The uncertainty associated with the initial inventories is, therefore, rather large. For Test S-SF-2 the RELAP5 code could not be initialized to the calculated coolant inventory of 172 kg of water in the broken loop steam generator. The separator component would fill with liquid causing a pressure surge which expelled the liquid out of the steam control valve. Therefore, a steady state initialization was obtained with a lower coolant inventory (160 kg) in the broken loop steam generator.

Figure 5 depicts the total CPU-time consumed by the RELAP5 calculations and indicates an average run-time ratio of approximately 8:1 CPU seconds to transient seconds. The average time step size used was approximately 40 ms.

4.1 General Response

The simulated FWLB transients were initiated from full-power, steady-state conditions. A slight cooldown and depressurization (Figure 6) occurred initially in each test prior to the PCS pressure excursion as a result of terminating the power to the pressurizer heaters at t = 0. In addition, a small depressurization of one or both steam generator

a. Based on postulated 100% feedwater line break (0.13 m^2) in a Combustion Engineering System 80 Plant.

TABLE 2. TESTS S-SF-1, 2, AND 3c CALCULATED AND MEASURED INITIAL CONDITIONS

	S-SF-1		S-SF-2		S-SF-3c	
	Data	RELAP5	Data	RELAP5	Data	RELAP5
System pressure (MPa)	15.16	15.17	15.64	15.51	15.21	15.14
Pressurizer: pressure (MPa)	15.15	15.14	15.53	15.49	15.13	15.12
level (cm)	65.2	65.0	48.5	47.7	83.0	82.5
Hot leg temperature I.L. (K)	596.3	595.2	597.7	594.9	598.1	595.3
B.L. (K)	597.3	595.1	598.6	594.9	598.7	595.3
Cold leg temperature I.L. (K)	562.0	564.5	562.0	563.4	563.0	562.8
B.L. (K)	560.4	561.3	568.9	562.4	561.5	561.6
Core power (MW)	2.0	2.0	2.0	2.0	2.0	2.0
I.L. mass flow rate (kg/s)	8.93	8.93	8.77	8.77	8.45	8.46
B.L. mass flow rate (kg/s)	2.15	2.14	2.18	2.19	2.16	2.16
Bypass mass flow rate (kg/s)	0.22	0.22	0.22	0.21	0.20	0.20
Steam generators:						
Pressure - I.L. (MPa)	6.23	5.77	6.15	5.65	6.31	5.63
B.L. (MPa)	6.31	6.25	7.36	6.36	6.46	6.27
Mass - I.L. (kg)	80.0	80.0	99.1	99.2	114.7	114.8
B.L. (kg)	151.9	152.1	171.6	160.3	126.4	126.4
FDW temp - I.L. (K)	528.1	530.0	529.1	530.0	527.9	530.0
B.L. (K)	522.2	530.0	525.2	530.0	525.0	530.0
Steam temp - I.L. (K)	550.4	546.2	549.1	544.8	551.1	544.7
B.L. (K)	552.2	551.4	561.9	552.6	553.4	551.7

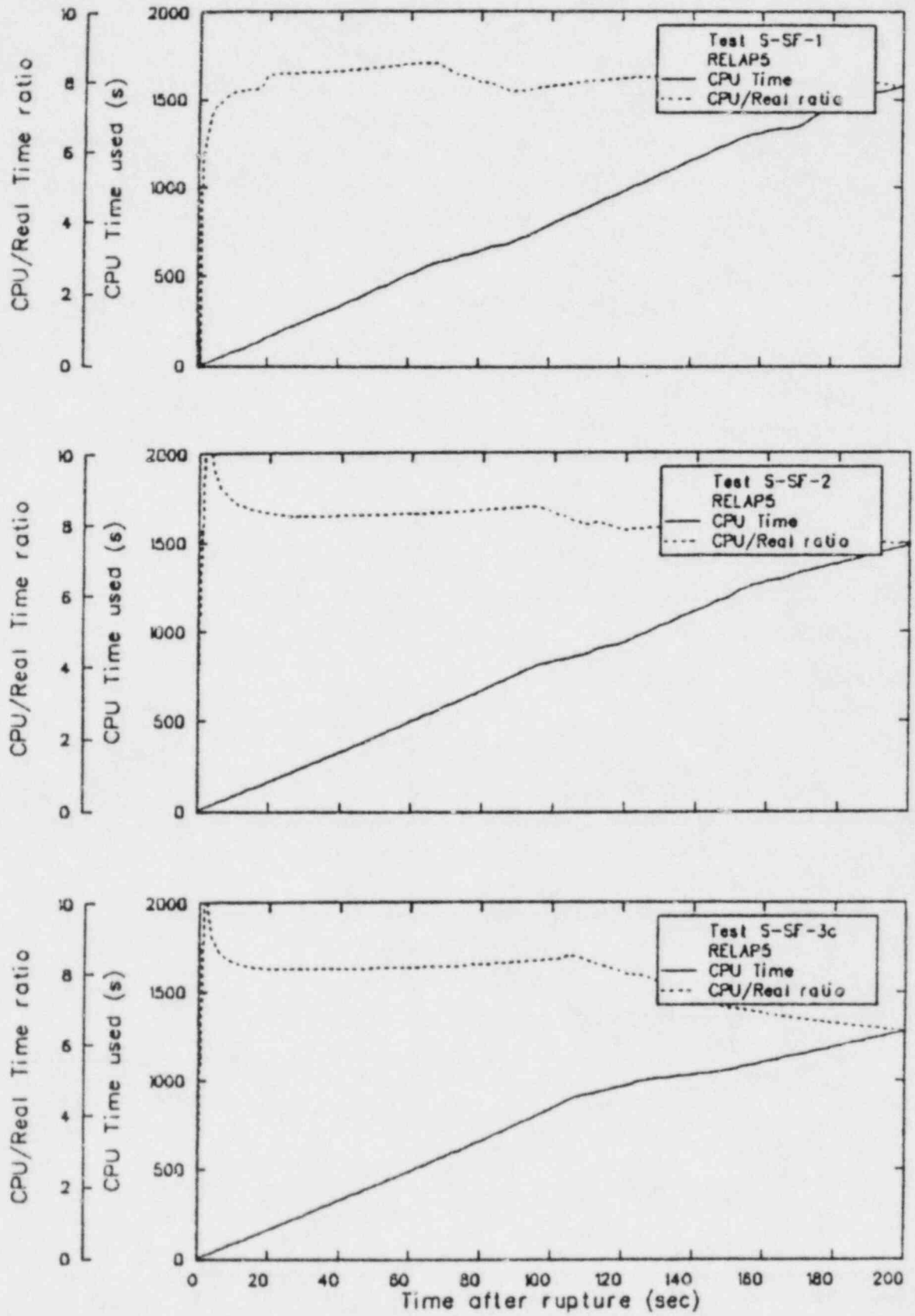

Figure 5. RELAP5 calculation efficiency.

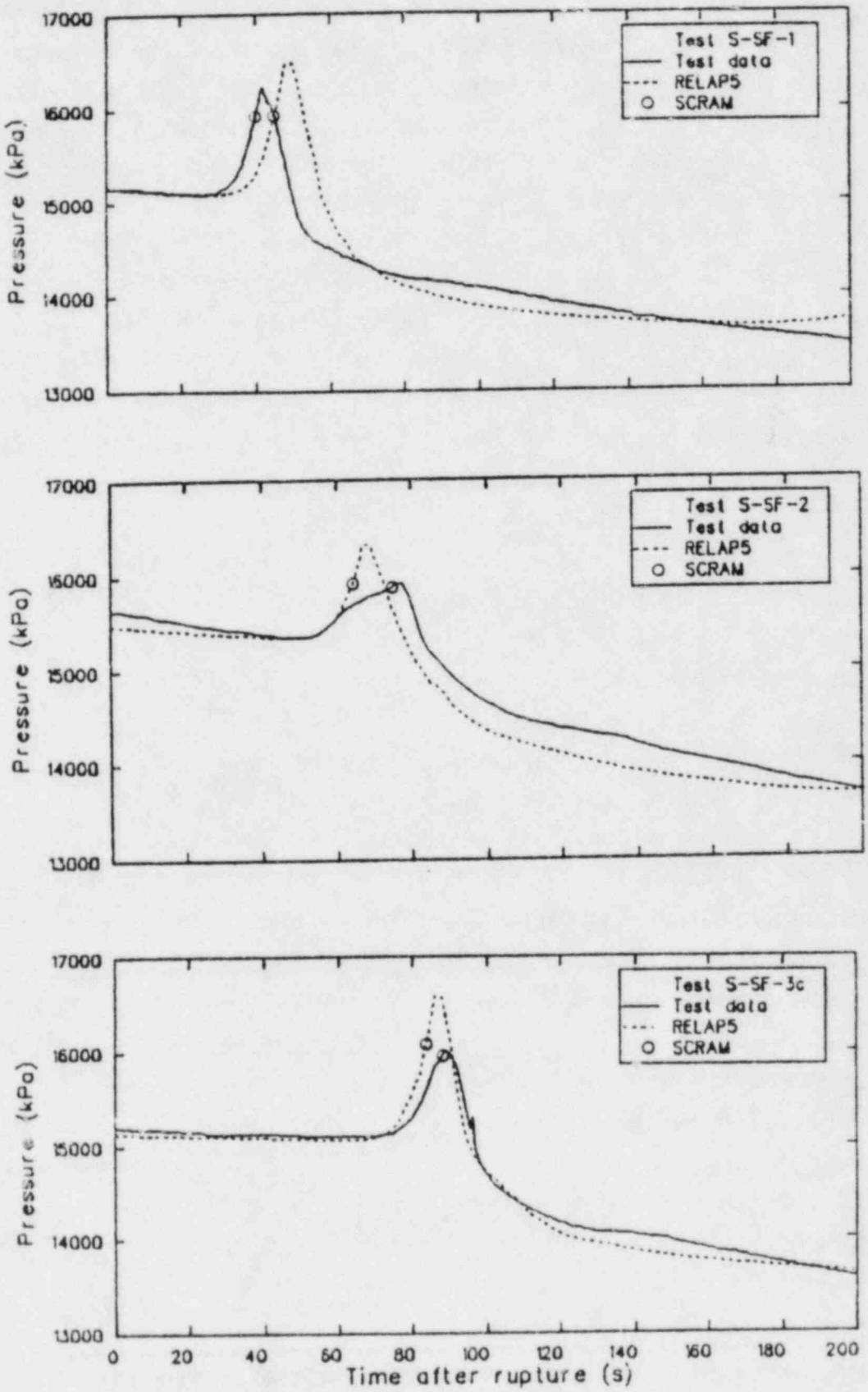

Figure 6. Upper plenum pressure.

secondaries contributed to the slight PCS depressurization. Coincident with break initiation, feedwater to both steam generators was terminated. (A chronology of events is presented in Table 3.) The intact loop steam generator secondary coolant inventory was depleted (prior to steam control valve closure) by boiloff and flashing. The broken loop steam generator secondary coolant was depleted due to flow out the break as well as by boiloff and flashing. Primary-to-secondary heat transfer (Figure 7) was degraded in one or both steam generators as a result of depleting the secondary coolant inventories. This led to a rapid heatup and pressurization of the PCS to the SCRAM setpoint (Table 4) of 15.86 MPa. Concurrent with SCRAM the steam control valves in both steam generators were closed and either one or both of the steam generator secondaries repressurized.

Once the core had SCRAMed the PCS pressure continued to rise briefly, then decreased rapidly to approximately 14 MPa. Thereafter the PCS pressure slowly decreased, aided by the injection of auxiliary feedwater to both steam generators and system heat losses to ambient.

In the RELAP5 analyses the following behavior was calculated. After the break was initiated and the feedwater isolated the PCS cooldown was nil (Figure 6) prior to the pressure excursion. This is attributed to a negligible cooldown of the steam generator secondaries and no effect due to the pressurizer heaters since they were not modeled. Depletion of the coolant inventories (Figures 8 and 9) in both steam generators prior to SCRAM was in general agreement with data. However, degradation of the primary-to-secondary heat transfer in the steam generators[a] (Figures 10 and 11) as the secondary coolant inventories were depleted prior to SCRAM occurred only in the intact loop steam generator. This behavior is in contrast with data where primary-to-secondary heat transfer was degraded in both steam generators prior to SCRAM, with the exception of Test S-SF-2. In this test the intact loop steam generator heat transfer rate remained

---

a. The initial difference between the measured and calculated primary-to-secondary heat transfer is due to measurement uncertainty.

TABLE 3. SEQUENCE OF EVENTS FOR TESTS S-SF-1, 2, AND 3c

EVENT	TIME(s)					
	S-SF-1		S-SF-2		S-SF-3c	
	DATA	RELAP5	DATA	RELAP5	DATA	RELAP5
Break Initiation	0	0	0	0	0	0
Feedwater Valves Closed	0	0	0	0	0	0
Primary Pressure Excursion Begins	27	32	52	52	75	70
SCRAM	40	45	75	64	88	83
Maximum PCS Pressure	42	49	78	67	89	86
I.L. and B.L. Steam Valves Begin Closing	40	45	75	64	88	83
I.L. and B.L. Pump Coastdown Initiated	40	45	75	64	88	83
Auxiliary Feedwater Initiated	100	100	105	106	150	150
B. L. Auxiliary Feedwater Off	300	300	308	306	300	300

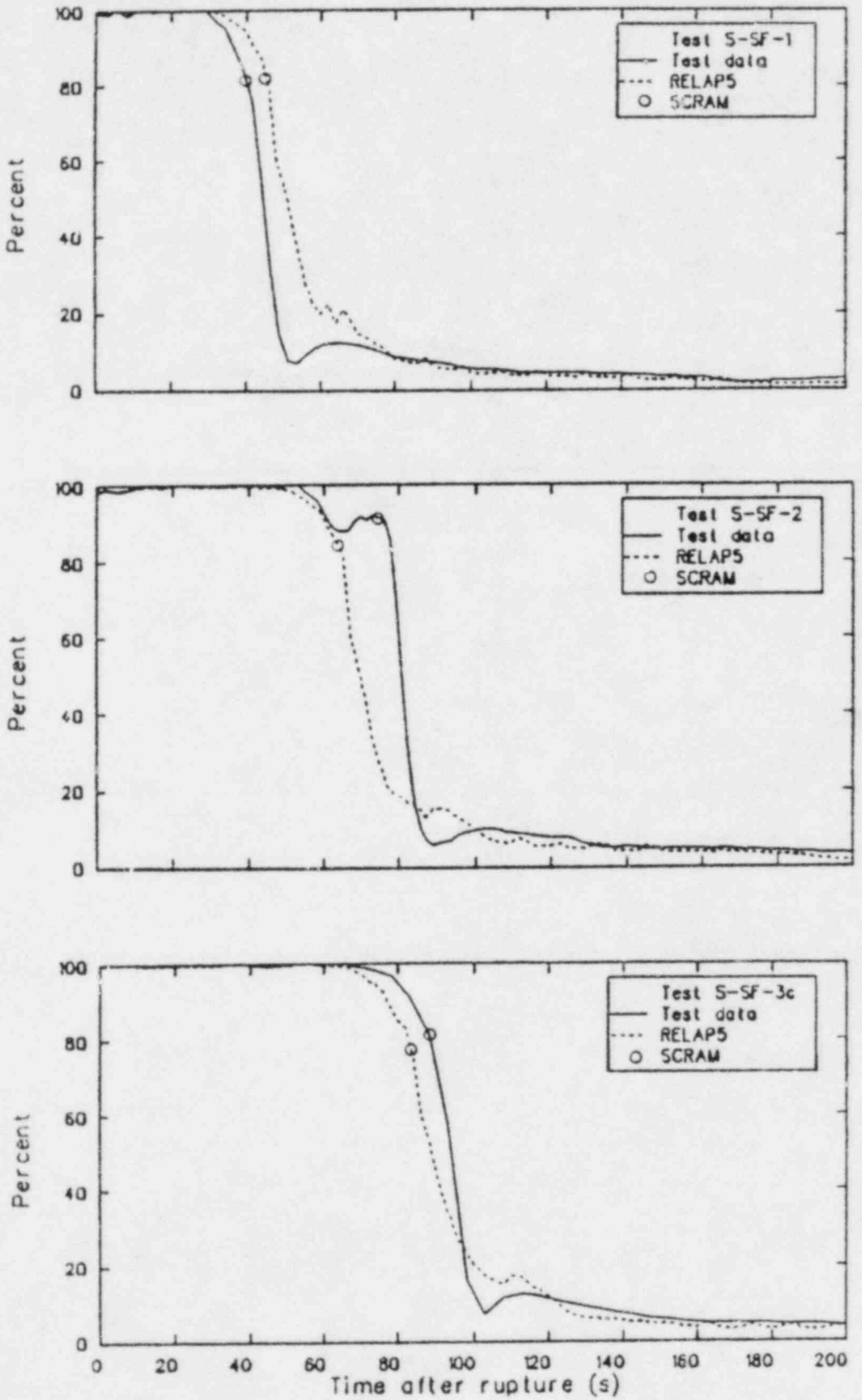

Figure 7. Percent total heat transferred to secondaries.

TABLE 4. TESTS S-SF-1, 2, AND 3c CALCULATED AND MEASURED TRANSIENT CONDITIONS

	S-SF-1		S-SF-2		S-SF-3c	
	Data	RELAP5	Data	RELAP5	Data	RELAP5
Heat transfer degradation begins[a]						
Steam generator masses (kg):						
Intact loop	51.8	53.3	18.3[b]	53.7	52.0	52.9
Broken loop	80.4	49.0[b]	73.5	39.0[b]	41.8	43.9[b]
SCRAM						
Pressure setpoint[c] (MPa)	15.7[d]	15.86	15.7[d]	15.86	15.5[d]	15.86
PCS pressure (MPa)	15.92	15.91	15.88	15.90	15.96	15.96
Steam generator masses (kg):						
Intact loop	42.1	39.5	18.3	39.8	33.9	37.5
Broken loop	76.2	49.0	52.8	39.0	36.9	43.9
Total heat sink degradation (%)	18.1	15.9	8.5	16.2	18.7	21.1
Maximum PCS pressure (MPa)	16.23	16.49	15.91	16.32	16.00	16.58

a. Heat transfer degrades at different times for each loop.

b. Heat transfer does not degrade until SCRAM.

c. Measured in the pressurizer.

d. SCRAM was initiated at 15.86 MPa as determined by process instrumentation.

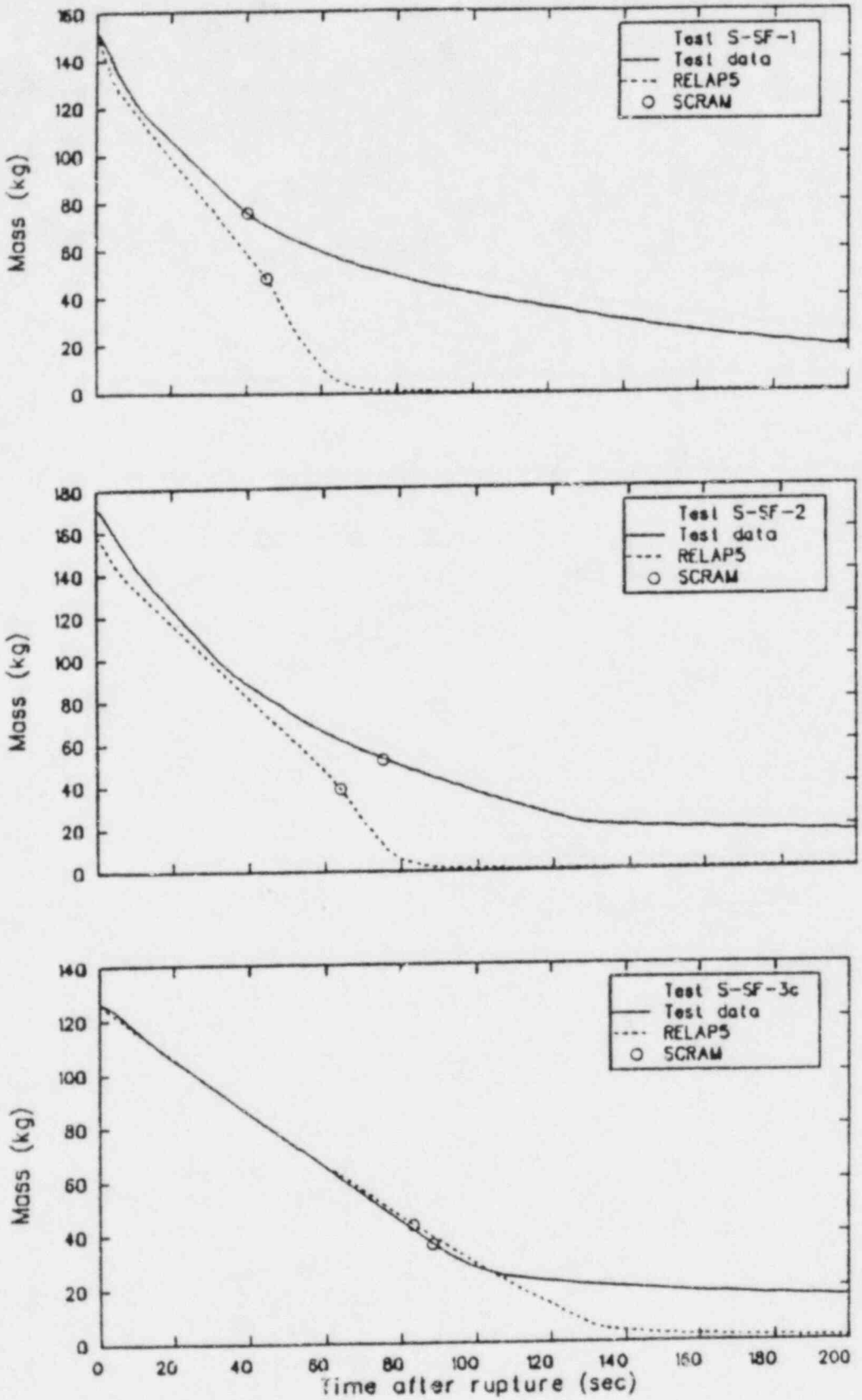

Figure 8. Mass in broken loop steam generator.

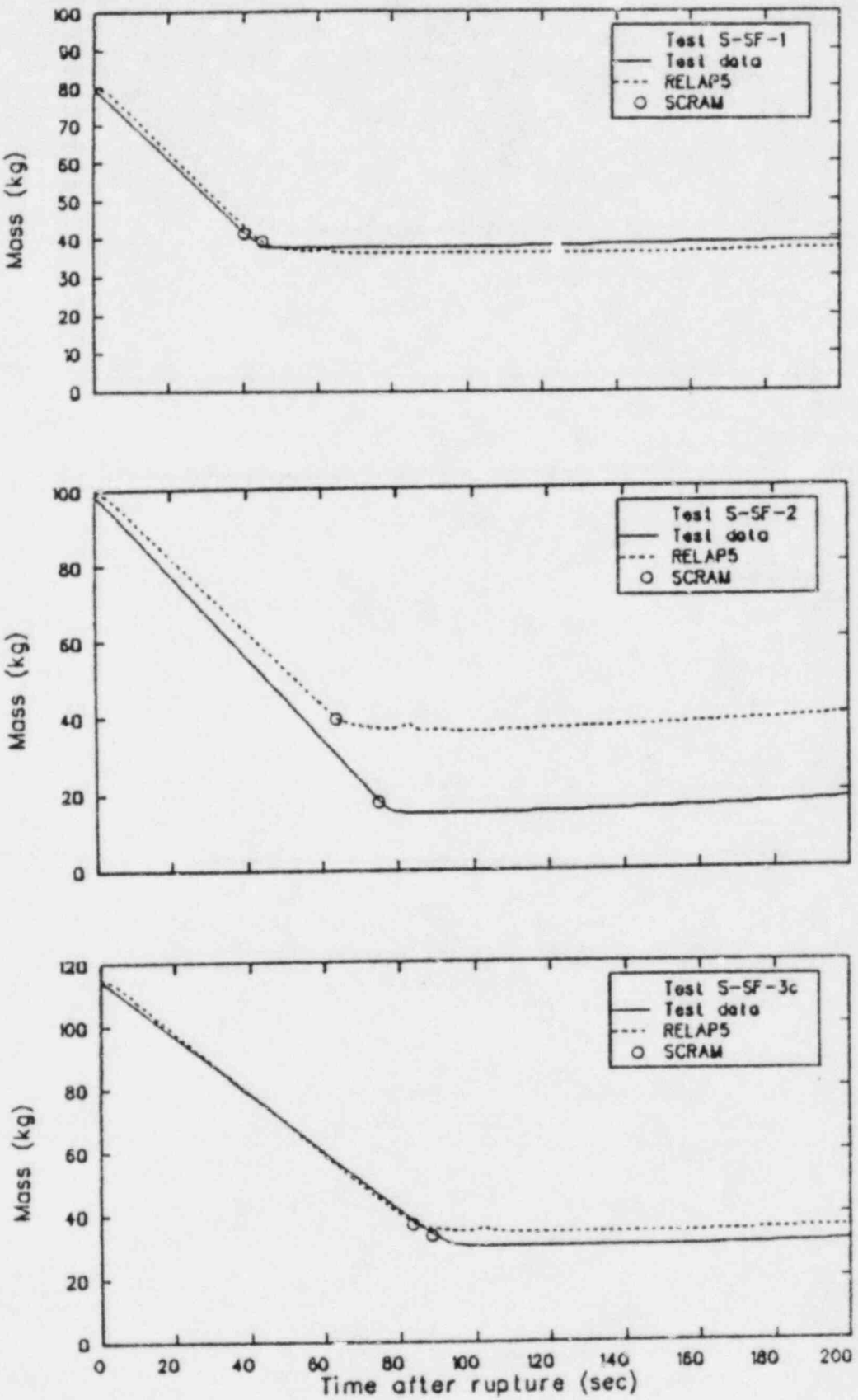

Figure 9. Mass in intact loop steam generator.

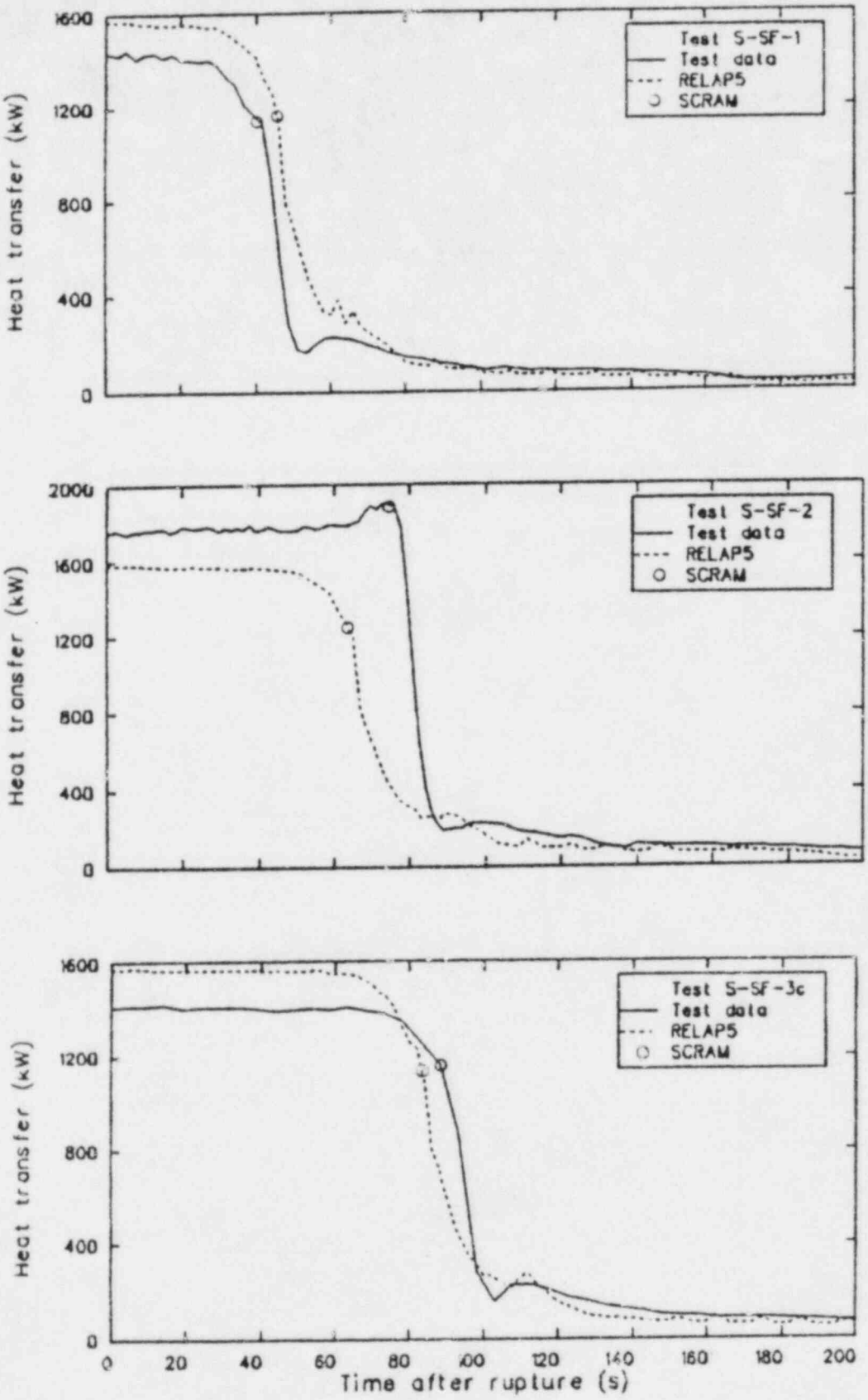

Figure 10. Heat transferred to intact loop secondary.

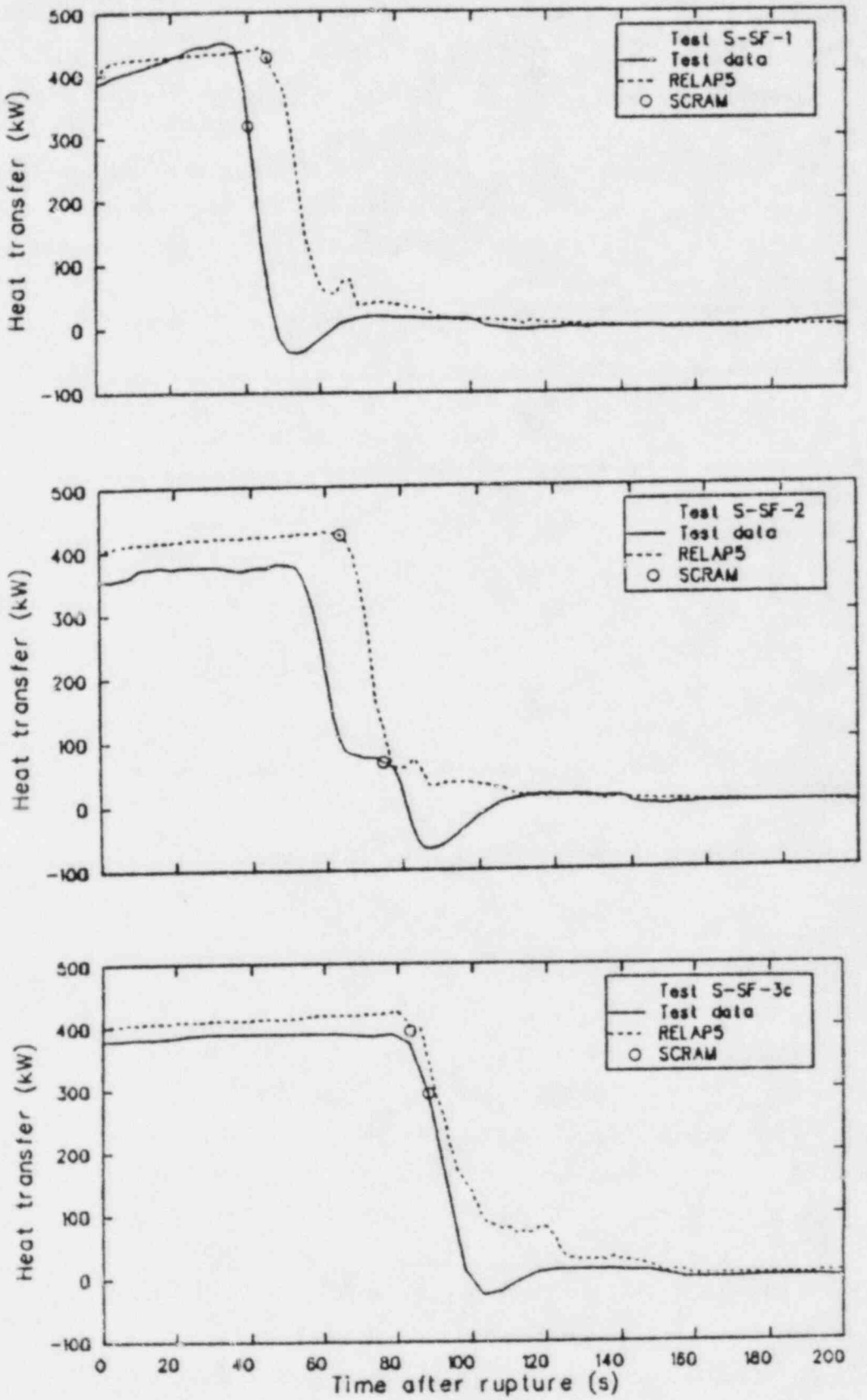

Figure 11. Heat transferred to broken loop secondary.

fairly constant and then picked up 41% of the load lost by the broken loop steam generator. Thus only the broken loop steam generator primary-to-secondary heat transfer rate was degraded prior to SCRAM.

After SCRAM had been calculated and the steam control valve closed in each steam generator a slight pressurization of the secondaries (Figure 12) occurred in all tests. Pressurization of both secondaries was observed in only the S-SF-3c test. The slight pressurization of the steam generator secondaries was due to primary-to-secondary heat transfer in conjunction with structural heat transfer to the coolant. A higher than measured break flow was calculated as a result of the pressurization after SCRAM in the broken loop steam generator. This caused the broken loop steam generator coolant inventory to be depleted at a higher rate than in the test just prior to auxiliary feedwater initiation. The differences in the measured and calculated coolant inventories in both steam generator secondaries and the associated primary-to-secondary heat transfer caused the calculated PCS pressure response after SCRAM to undershoot data.

The calculated primary coolant system and secondary coolant system behavior will be discussed in more detail in Sections 4.2 and 4.3.

4.2 Primary Coolant System Response

The calculated PCS pressure response (Figure 6) generally agreed with data within the measurement uncertainty prior to the PCS pressure excursion. The slight cooldown of the PCS observed in the tests during this period was due to terminating power to the pressurizer heaters and the depressurization of the steam generator secondaries. The cooldown was small enough, however, not to cause substantial disagreement with the calculated pressure responses. The PCS was not calculated to cooldown prior to the PCS pressure excursion in any of the tests.

PCS heatup and the associated pressurization of the PCS was caused, both in the tests and calculations, by degradation of the primary-to-secondary heat transfer (shown in Figure 7 in terms of percent of the initial total power transferred to both steam generator

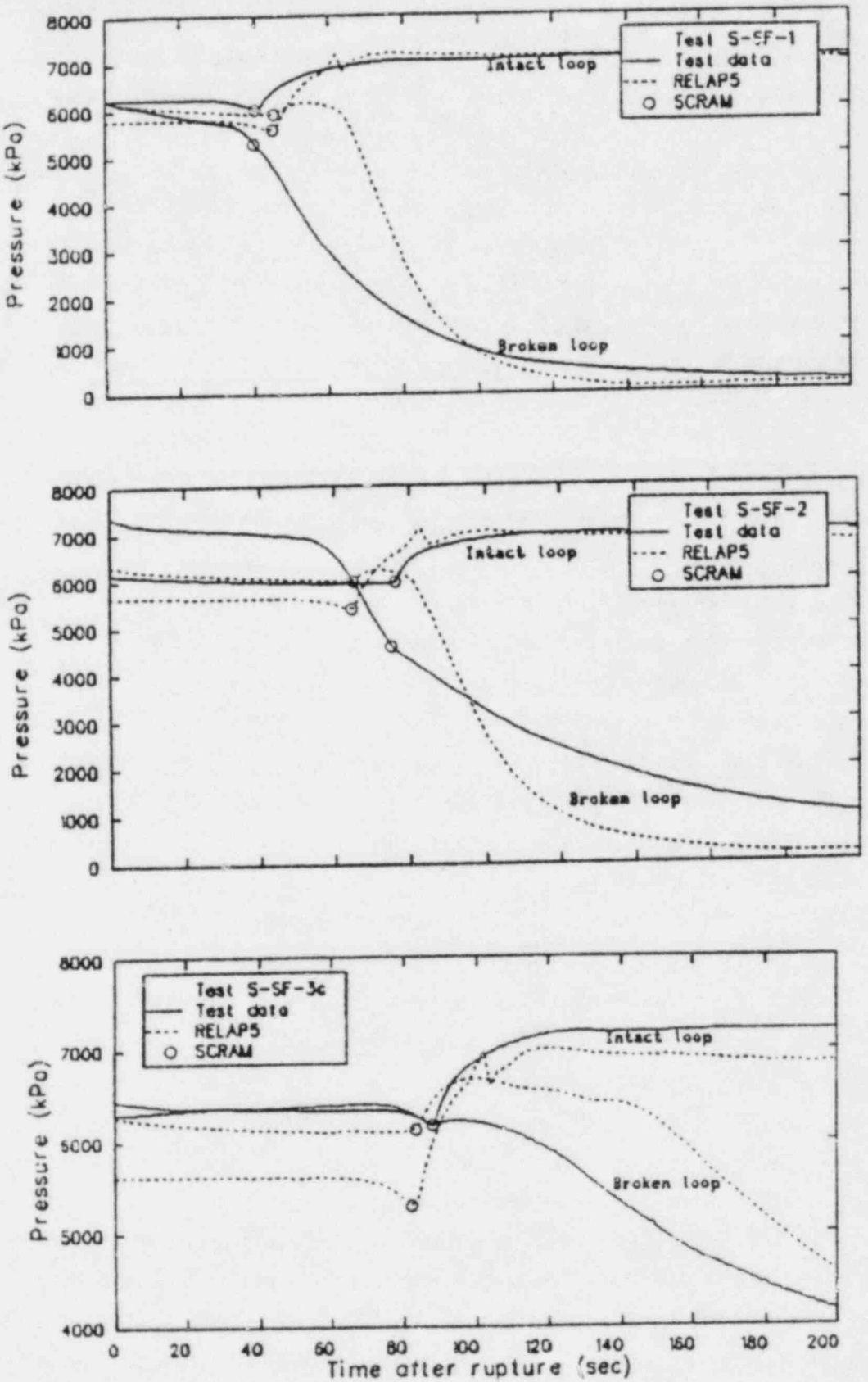

Figure 12. Steam generator secondary pressures.

secondaries). In Tests S-SF-1 and 3c both the intact and broken loop steam generator heat transfer rates (Figures 10 and 11, respectively) were reduced prior to SCRAM, thus causing a rather sharp continuous rise in PCS pressure. For Test S-SF-2 the intact loop steam generator heat transfer remained constant and even picked up some of the load lost by the broken loop steam generator. The PCS pressurization for this test had two distinguishable rates. A fast pressurization rate due to heat transfer degradation in the broken loop steam generator while the intact loop heat transfer remained fairly constant, and a slower pressurization rate due to a gradual increase in the heat transfer of the intact loop steam generator as the heat transfer of the broken loop steam generator decreased.

The calculated PCS pressurization rate for all tests was essentially the same. This is attributed to the fact that for all of the tests the heat transfer degradation in the intact loop steam generator as a function of secondary coolant inventory was approximately equivalent and the broken loop steam generator heat transfer remained constant prior to SCRAM. The rate that the secondary coolant inventory was depleted in the intact loop steam generator was the same between tests because the interloop heat transfer split and boiloff rate were approximately the same. The primary reason that the calculated PCS pressurizations occurred at different times is because the initial loop steam generator secondary coolant inventories were different between tests.

As the PCS heats up and the primary coolant expands the pressurizer coolant level increases (Figure 13) and compresses the pressurizer steam space. The magnitude of the calculated level increase agreed with data. The calculated compression was nearly adiabatic as was observed in the tests. Once the core was SCRAMed and shrinkage of the primary coolant occurred, the pressurizer level dropped as liquid flowed into the primary. In general, the calculated pressurizer levels after SCRAM were lower than observed in the tests because the PCS was cooled more and therefore there was more shrinkage of the primary coolant volume. The calculated and measured pressurizer pressures (Figure 14) were less than that of the PCS by an amount determined by the pressure drop across the surge line and the hydrostatic head of the fluid in the pressurizer.

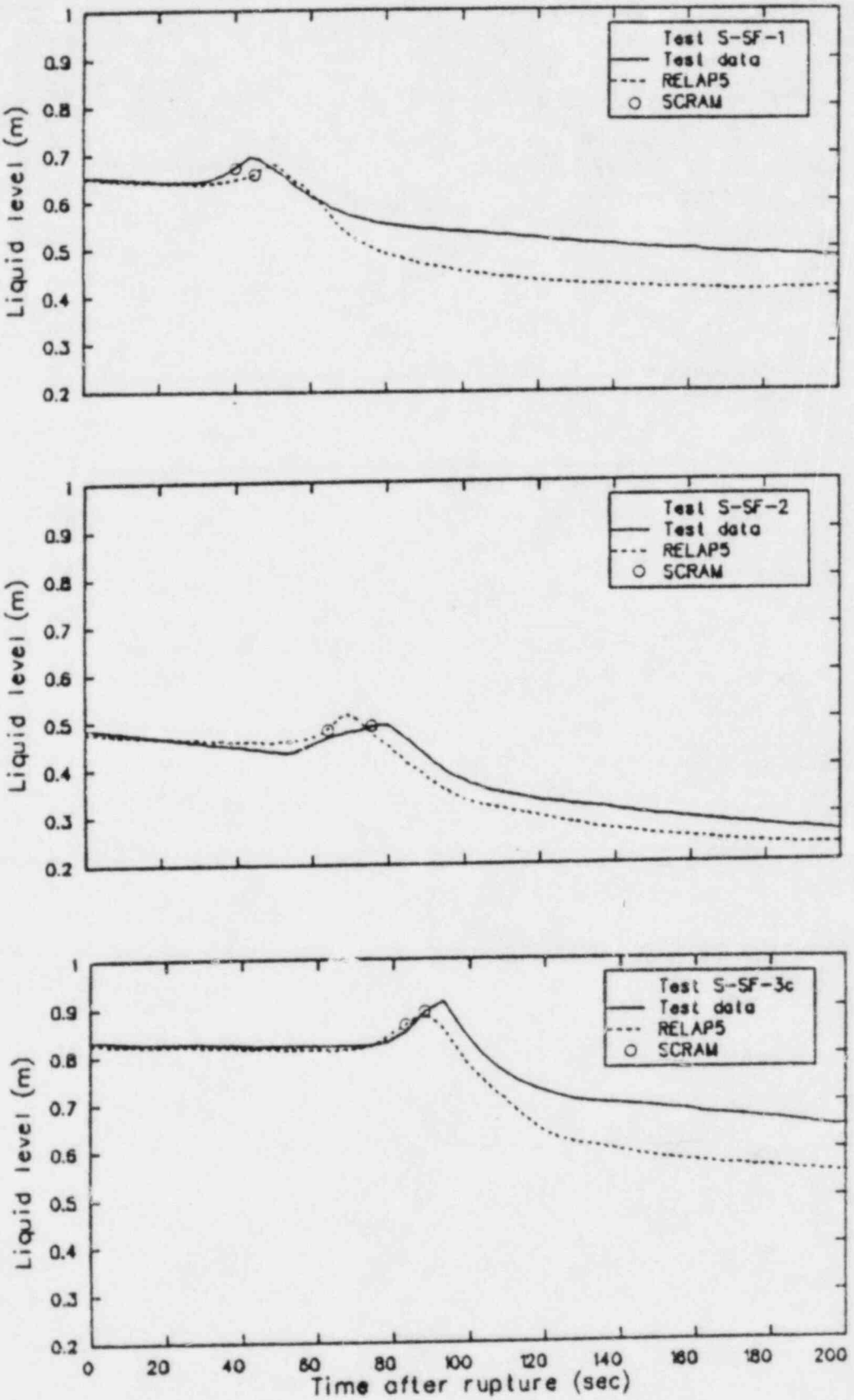

Figure 13. Pressurizer liquid level.

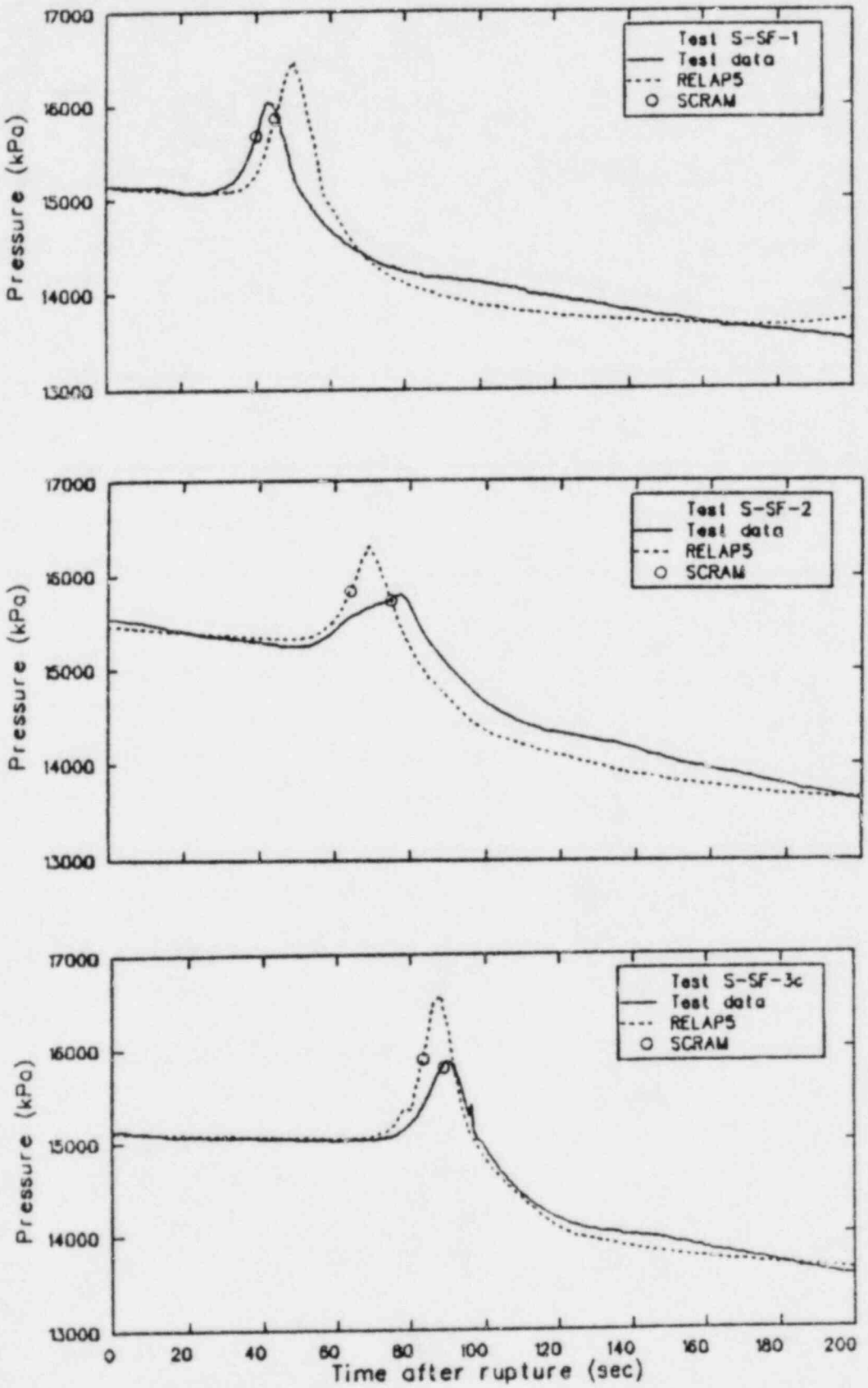

Figure 14. Pressurizer pressure.

4.3 Secondary Coolant System Response

Feedwater flow was terminated to both steam generators coincident with break initiation. The steam control valves were left in their respective steady-state positions until the high PCS pressure trip signal was received. The calculated and measured mass flow (Figure 15) out the steam lines remained nearly constant prior to closing the steam control valves. Auxiliary feedwater flow was started at the times indicated in Table 3 for the respective tests.

Prior to SCRAM neither steam generator secondary underwent any significant depressurization except for Test S-SF-2 (Figure 12). Generation of steam from boiling and flashing was sufficient to maintain pressure. This behavior was also observed in the calculations. The broken loop steam generator in Test S-SF-2 lost its heat transfer capability well before SCRAM so the broken loop secondary depressurized significantly prior to SCRAM. Following SCRAM and closing of the steam control valves the intact loop steam generator pressurized in all tests and the broken loop steam generator continued to depressurize in all but Test S-SF-3c. RELAP5 calculated that both steam generators in all of the tests pressurized after the steam control valves were closed. This is largely attributed to higher than measured heat transfer rates as a function of time (Figure 11) after closure of the steam control valve in the broken loop steam generator and, to a smaller degree, with lower than measured volumetric break flow (Figure 16) for a period after the steam control valve was closed.

Degradation of the heat transfer rate in the broken loop steam generator (Figure 17) started in the tests at different secondary coolant inventories (Table 4). The onset of heat transfer degradation occurred at smaller secondary coolant inventories as the break sizes were made smaller. Heat transfer degradation in the broken loop steam generator was not calculated at all prior to SCRAM. The principal reason for this is that the coolant inventory in the broken loop steam generator riser region (represented by the collapsed liquid level in Figure 18) remained unchanged after approximately 10 s for a significant period prior to SCRAM. Enough flow was calculated to enter the riser from the downcomer to make up for

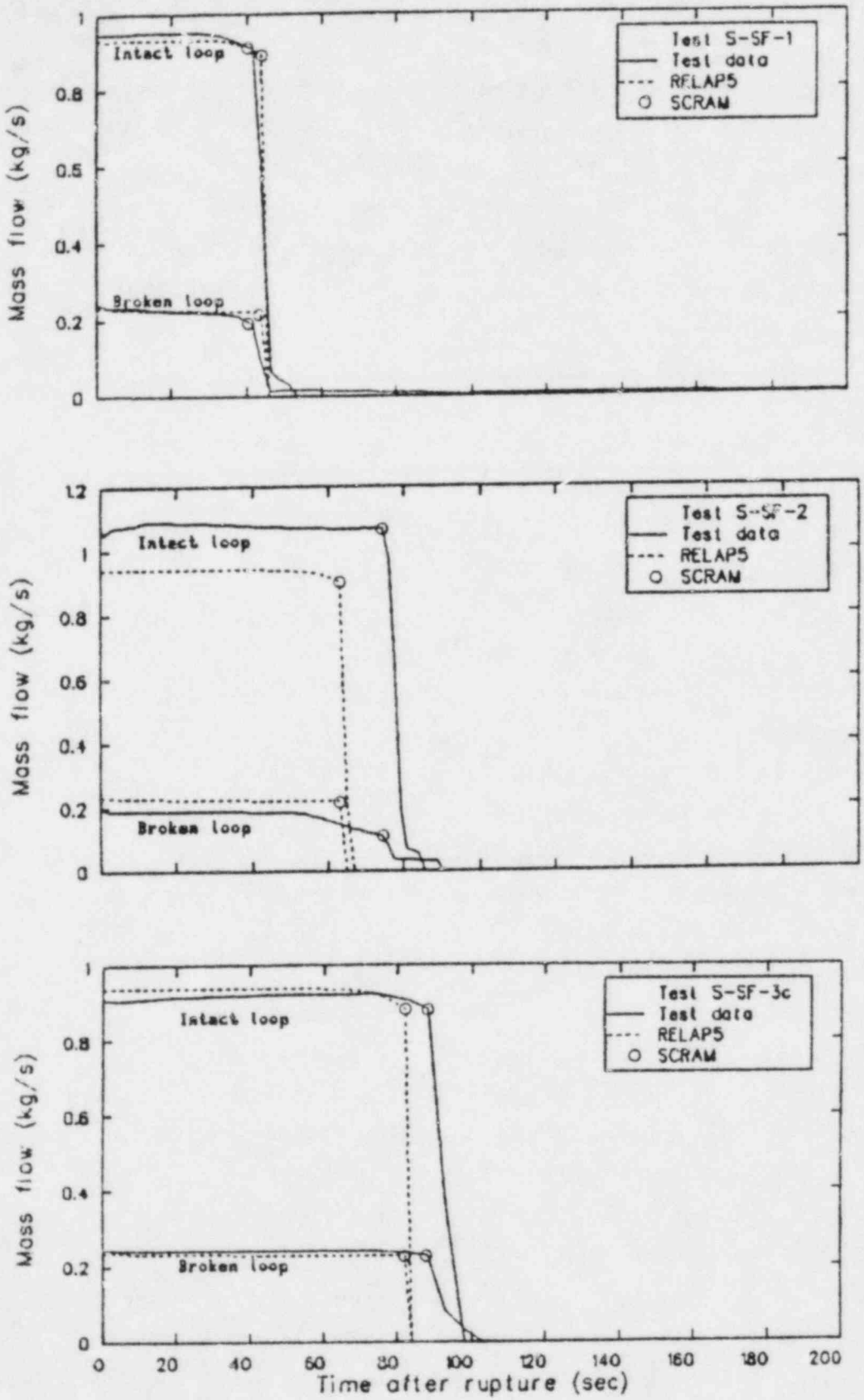

Figure 15. Steam flow rate out steam generators.

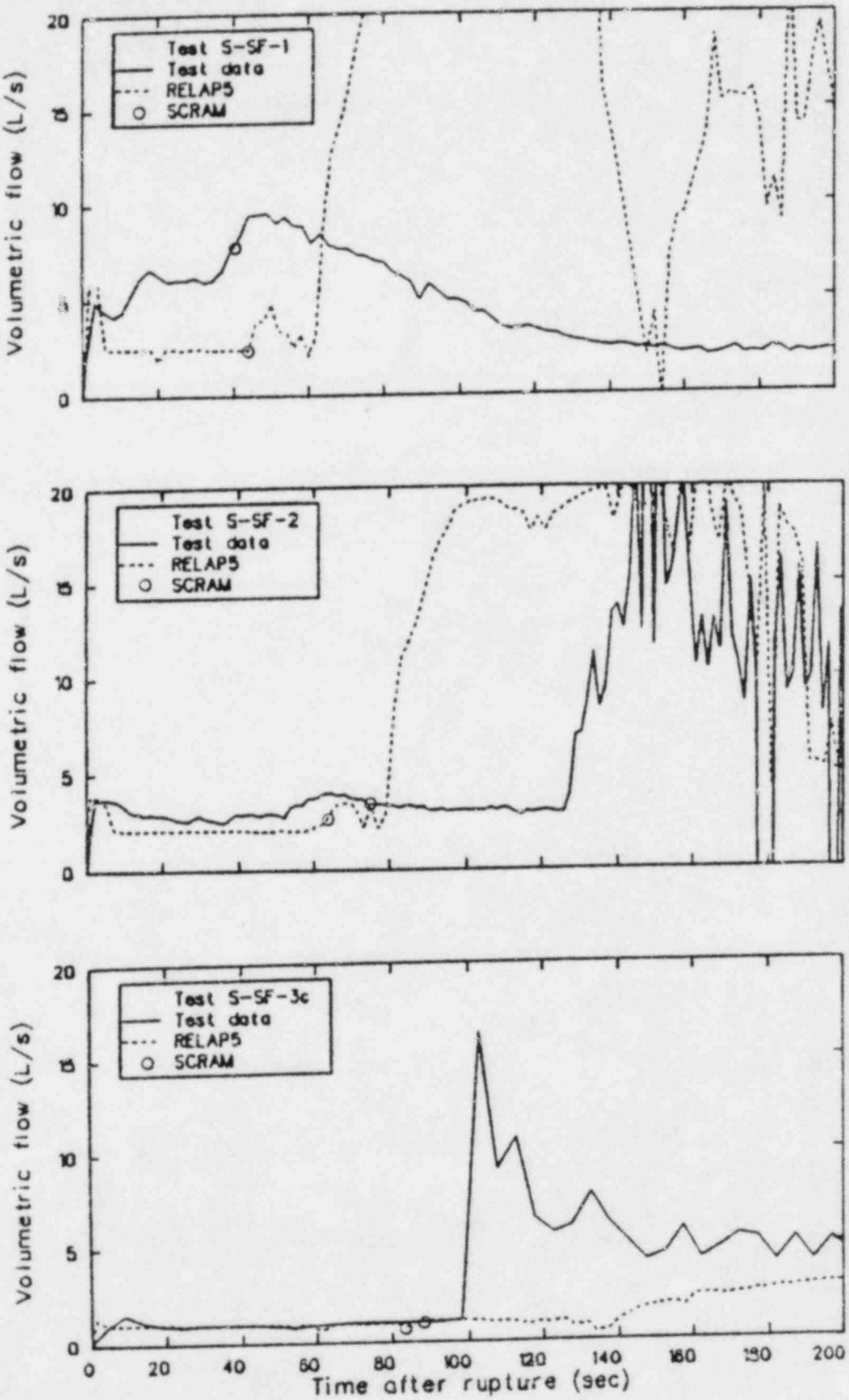

Figure 16. Volumetric break flow rate.

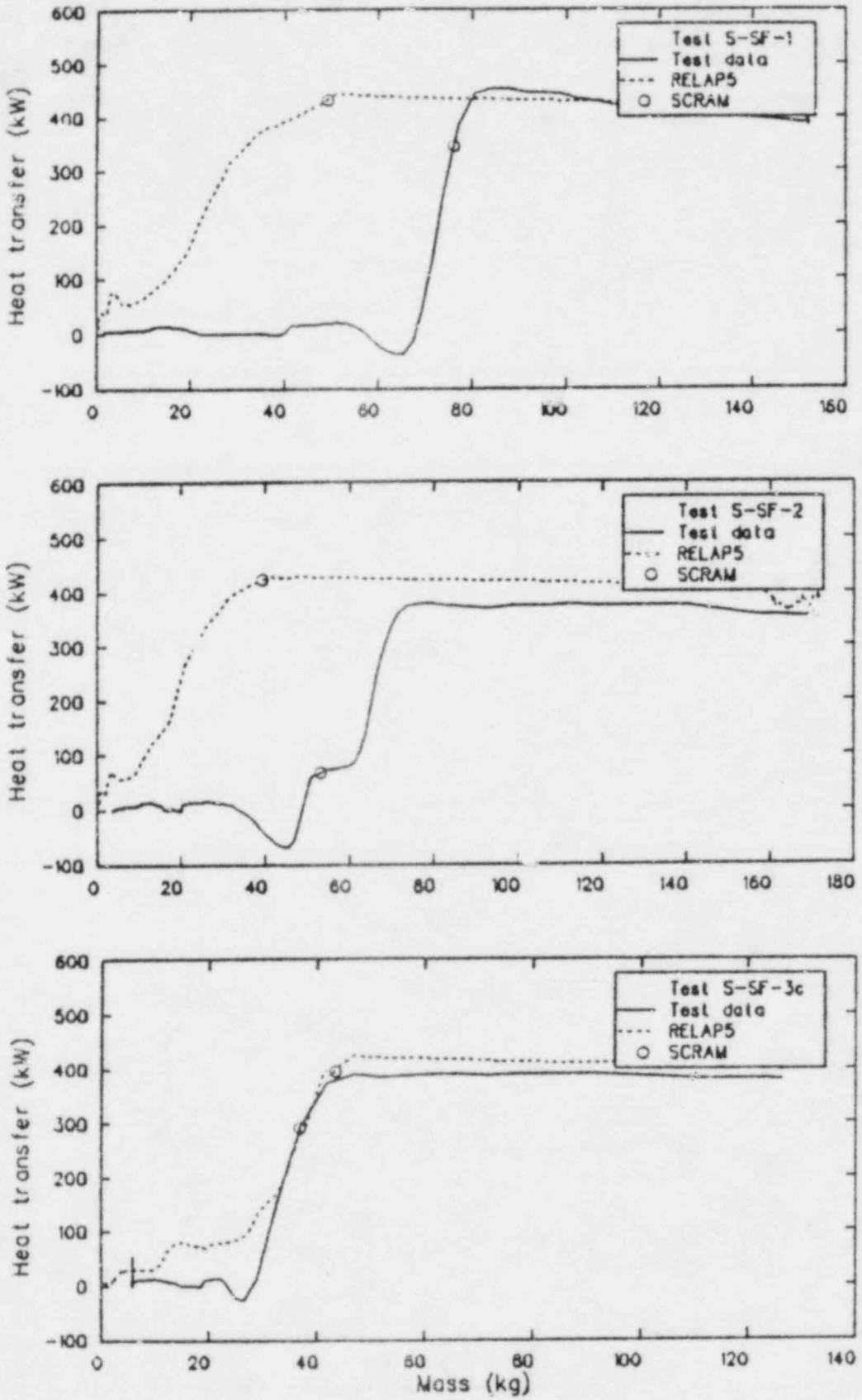

Figure 17. Heat transferred to broken loop secondary as a function of the mass in the broken loop secondary.

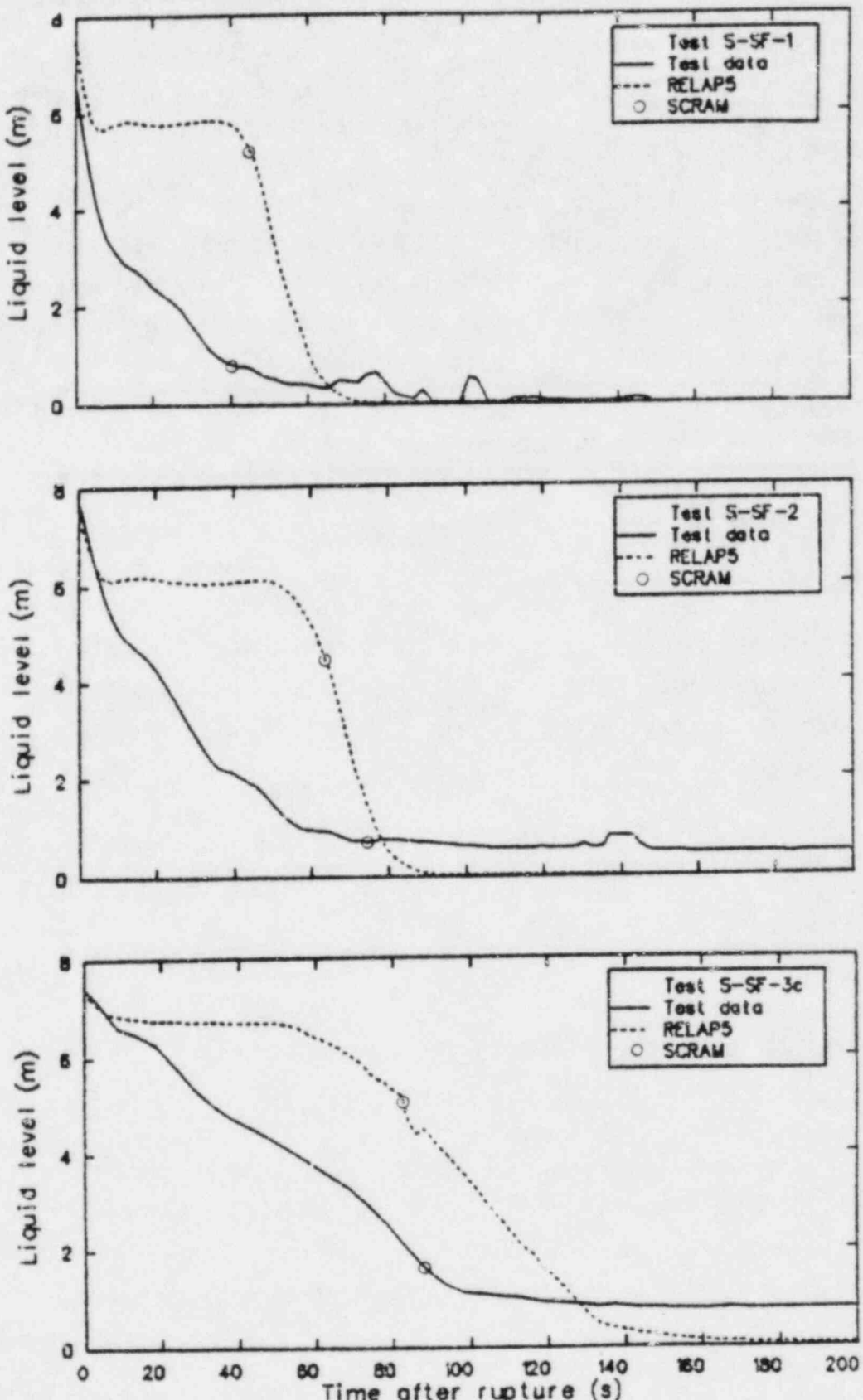

Figure 18. Broken loop steam generator riser level.

that steamed off and recirculated during this period to maintain the level in the riser. The calculated flow direction within the secondary was unchanged prior to SCRAM. Consequently, fluid out the break during this period came exclusively from the downcomer (a flow reversal in the riser would have been necessary to drain the riser and downcomer simultaneously).

Fluid densities calculated upstream of the break (Figure 19) were higher than that observed in Tests S-SF-1 and 2 for the early portion of the transients. Better agreement, however, was obtained between the calculation and data for Test S-SF-3c. Higher calculated fluid densities upstream of the break are in part a result of the fluid coming from the downcomer rather than the riser where the qualities are higher. Measured and calculated break mass flow differences (Figure 20) are due to differences in break upstream conditions. The RELAP5 subcooled and two-phase discharge coefficients were adjusted (see Appendix B) to agree with data for comparable upstream conditions. Although some of the data trends of the break mass flow rate were not calculated well because of the different upstream conditions (as a function of time) the calculated broken loop steam generator coolant inventory (Figure 8) prior to SCRAM was in fairly good agreement with data. This is particularly true for Test S-SF-3c.

Degradation of the primary-to-secondary heat transfer in the intact loop steam generator started at a secondary coolant inventory of approximately 52 kg (Figure 21) for Tests S-SF-1 and 3c. This is in excellent agreement with the calculated value of 53 kg for all three of the tests. Only Test S-SF-2 showed a significant difference between the observed and calculated secondary coolant inventories at which heat transfer degradation started.

Heat transfer in the intact loop steam generator degraded from top down. The heat transfer modes calculated as the heat transfer on the shell-side of the U-tubes degraded were: (a) nucleate boiling to saturated water in annular flow, (b) transition boiling to saturated water in transitional annular-mist flow, and (c) film boiling to saturated water in mist flow.

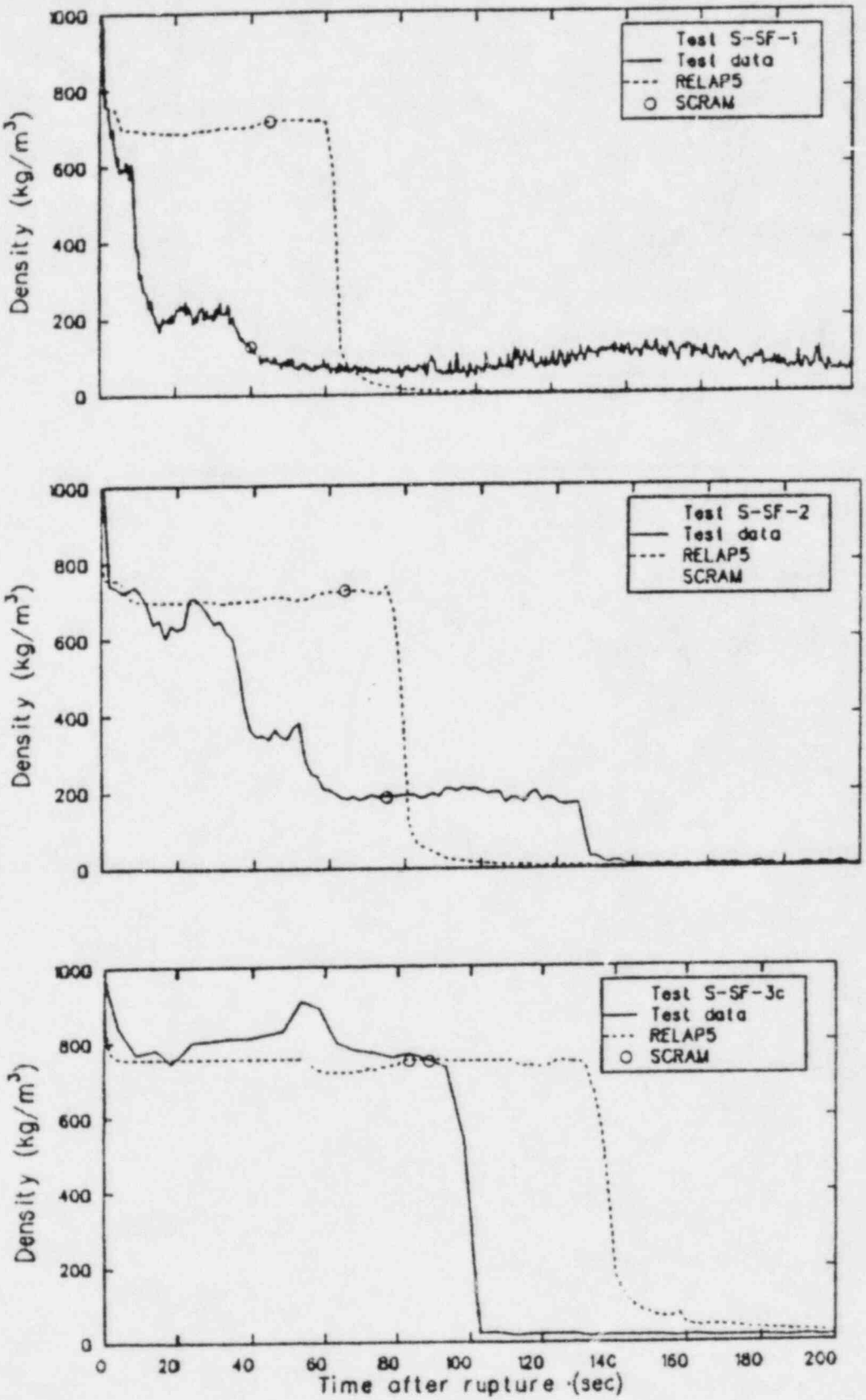

Figure 19. Density of fluid upstream of break.

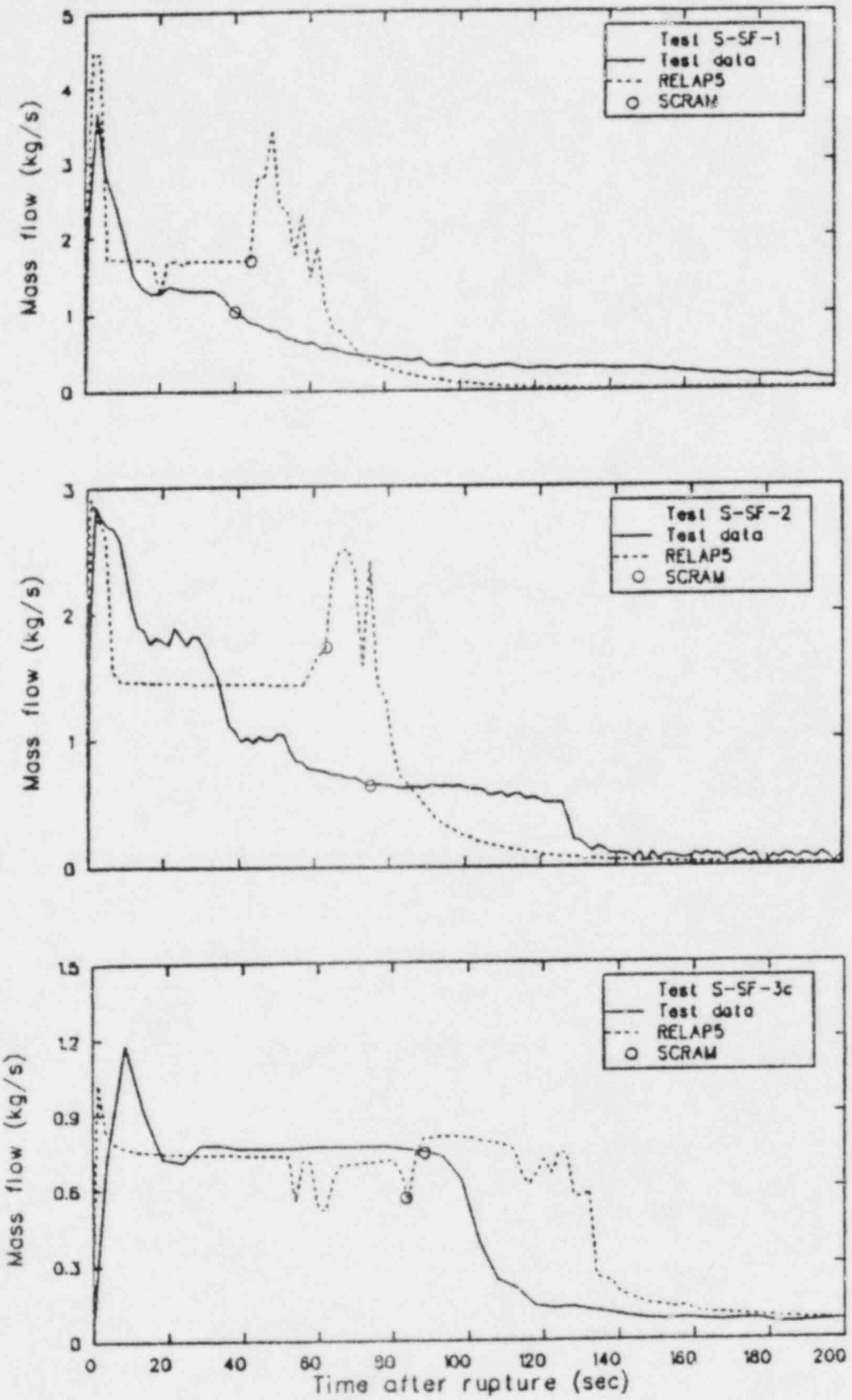

Figure 20. Break mass flow rate.

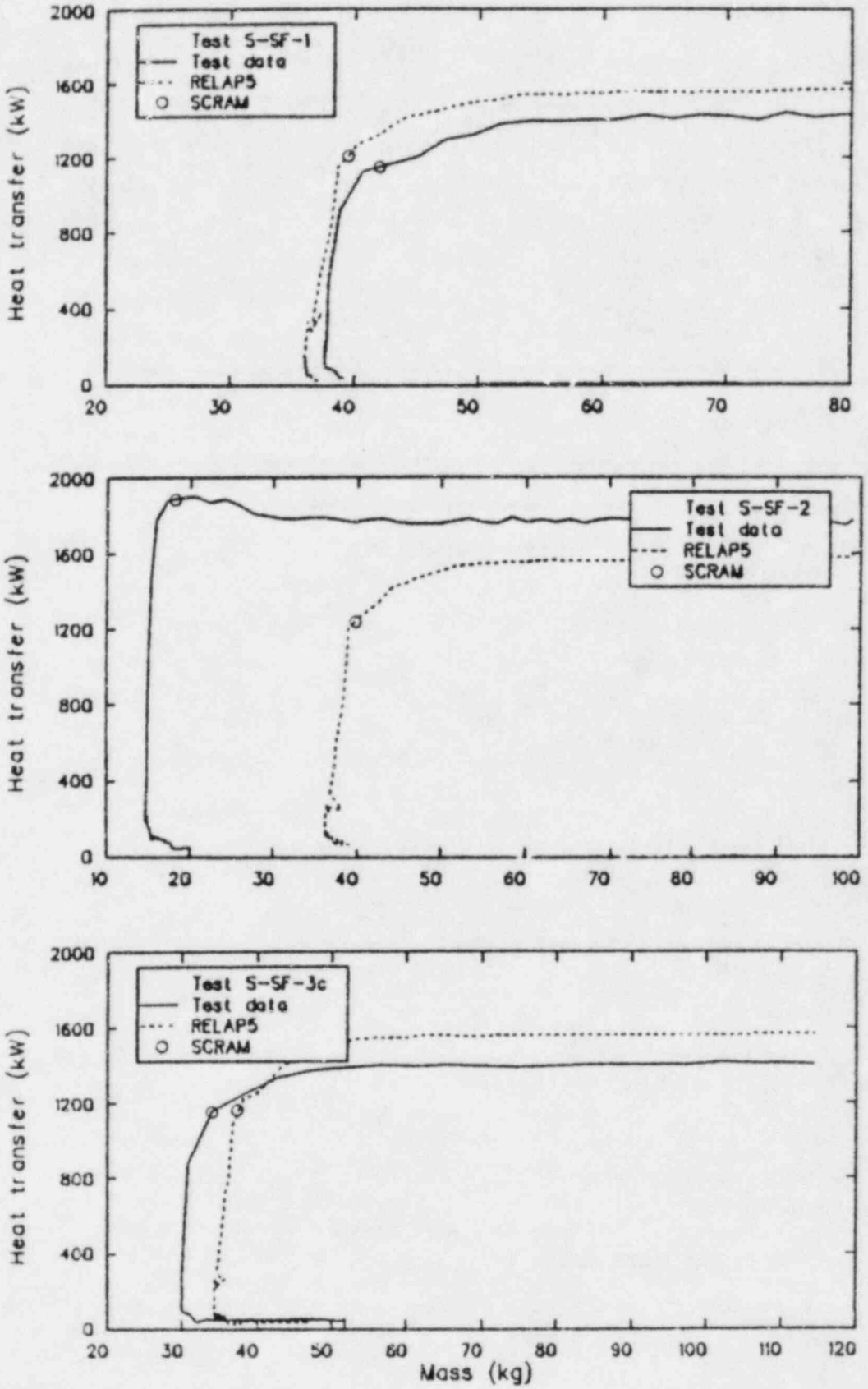

Figure 21. Heat transferred to intact loop secondary as a function of the mass in the intact loop secondary.

Selected measured and calculated "local" heat transfer rates[a,b] on the upside of the U-tubes for the intact loop steam generator are shown in Figures 22 through 24, and for the broken loop steam generator in Figures 25 through 27, for each of the respective tests. Both the measured and calculated responses show a gradual heat transfer degradation in the upper half of the intact loop steam generator prior to SCRAM for Tests S-SF-1 and S-SF-3c. In Test S-SF-2 the heat transfer remained uniform throughout the intact loop steam generator until SCRAM. The early heat transfer degradation observed between 152 and 211 cm in the broken loop steam generator during Tests S-SF-1 and S-SF-2 was not calculated. This behavior is not completely understood due to the limited instrumentation available to measure local phenomena in the steam generator. However, it is probably a result of the hydraulics induced by the double-ended blowdown of the steam generator through both the feedwater and steam line prior to steam control valve closure (i.e., a flow stagnation point probably existed in the riser).

---

a. The measured heat transfer rates were computed by multiplying the difference between available primary fluid temperature measurements by the mass flow rate and liquid specific heat then dividing by the distance between the temperature measurements.

b. The calculated heat transfer rates were computed by summing the average heat transferred by the volumes in the elevation range corresponding to measurements and then dividing by the elevation difference.

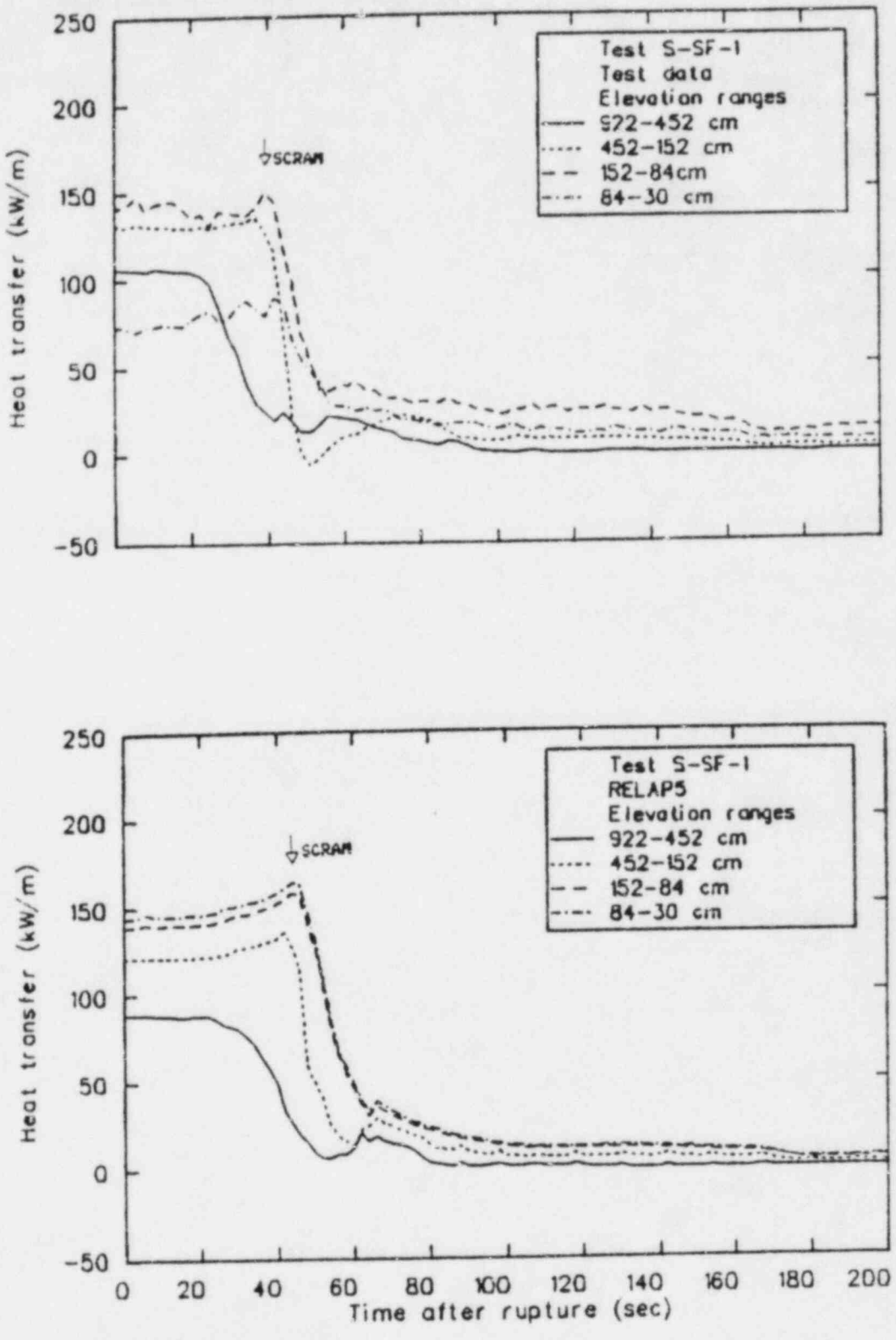

Figure 22. Local heat transfer rates in the intact loop steam generator for Test S-SF-1.

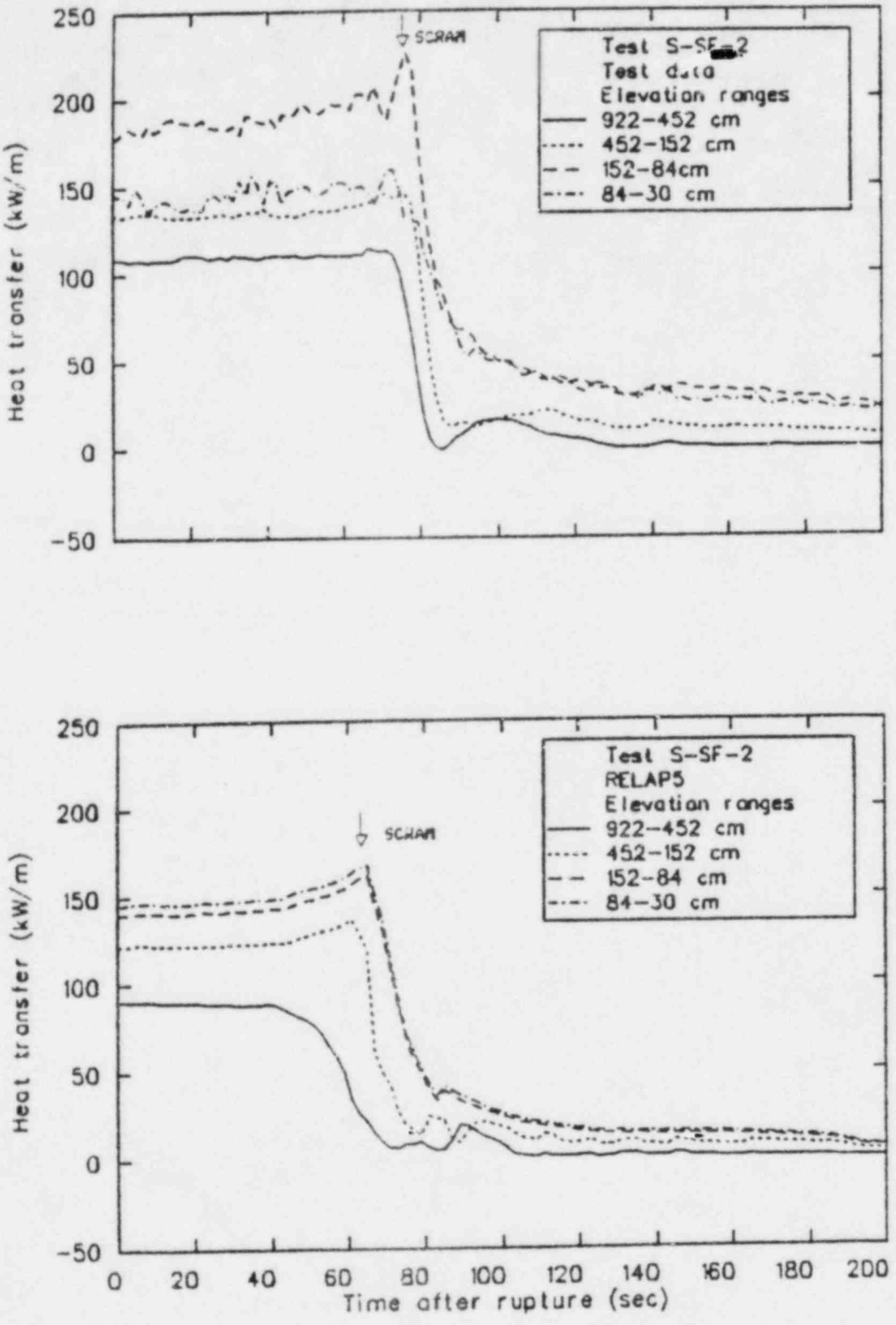

Figure 23. Local heat transfer rates in the intact loop steam generator for Test S-SF-2.

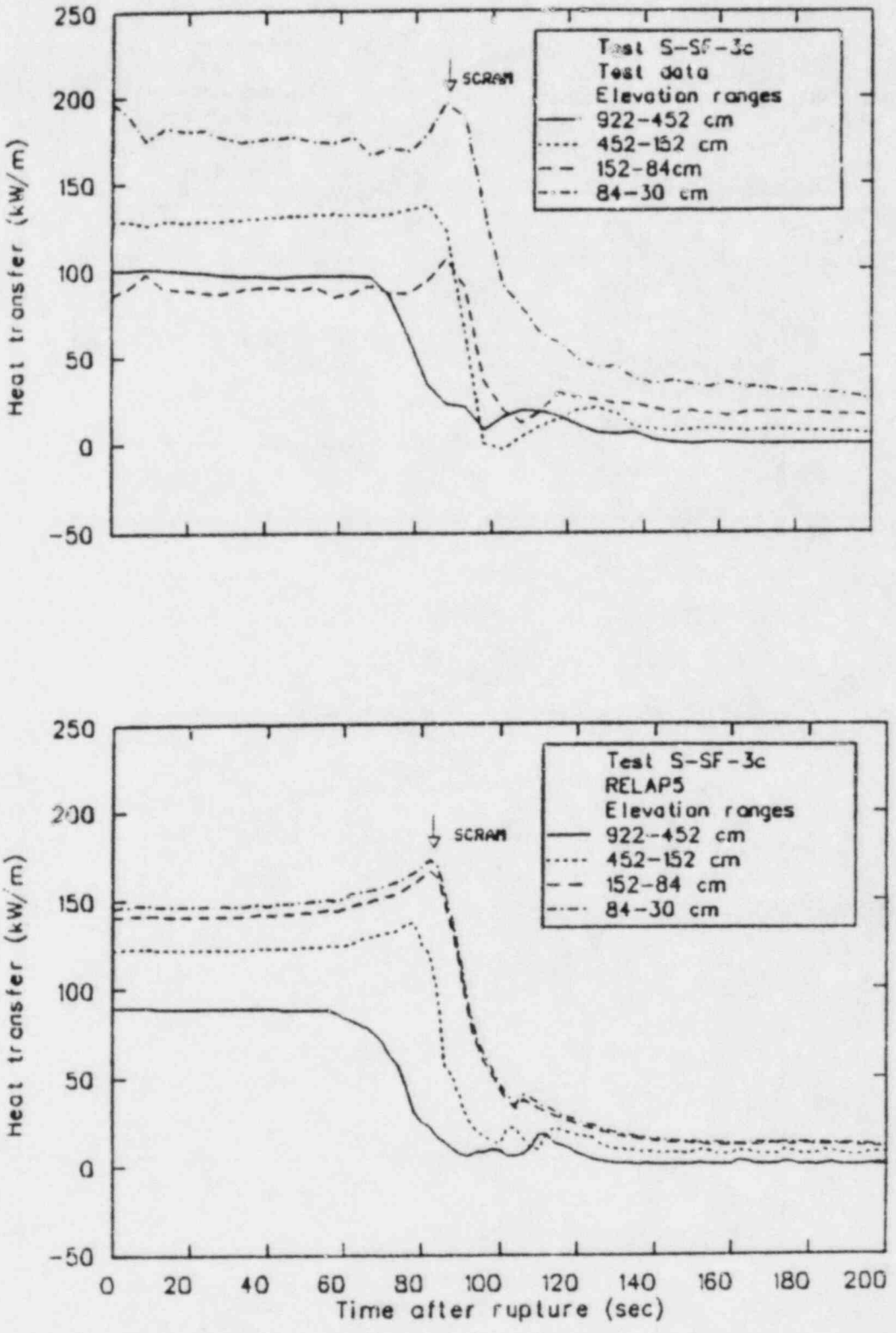

Figure 24. Local heat transfer rates in the intact loop steam generator for Test S-SF-3c.

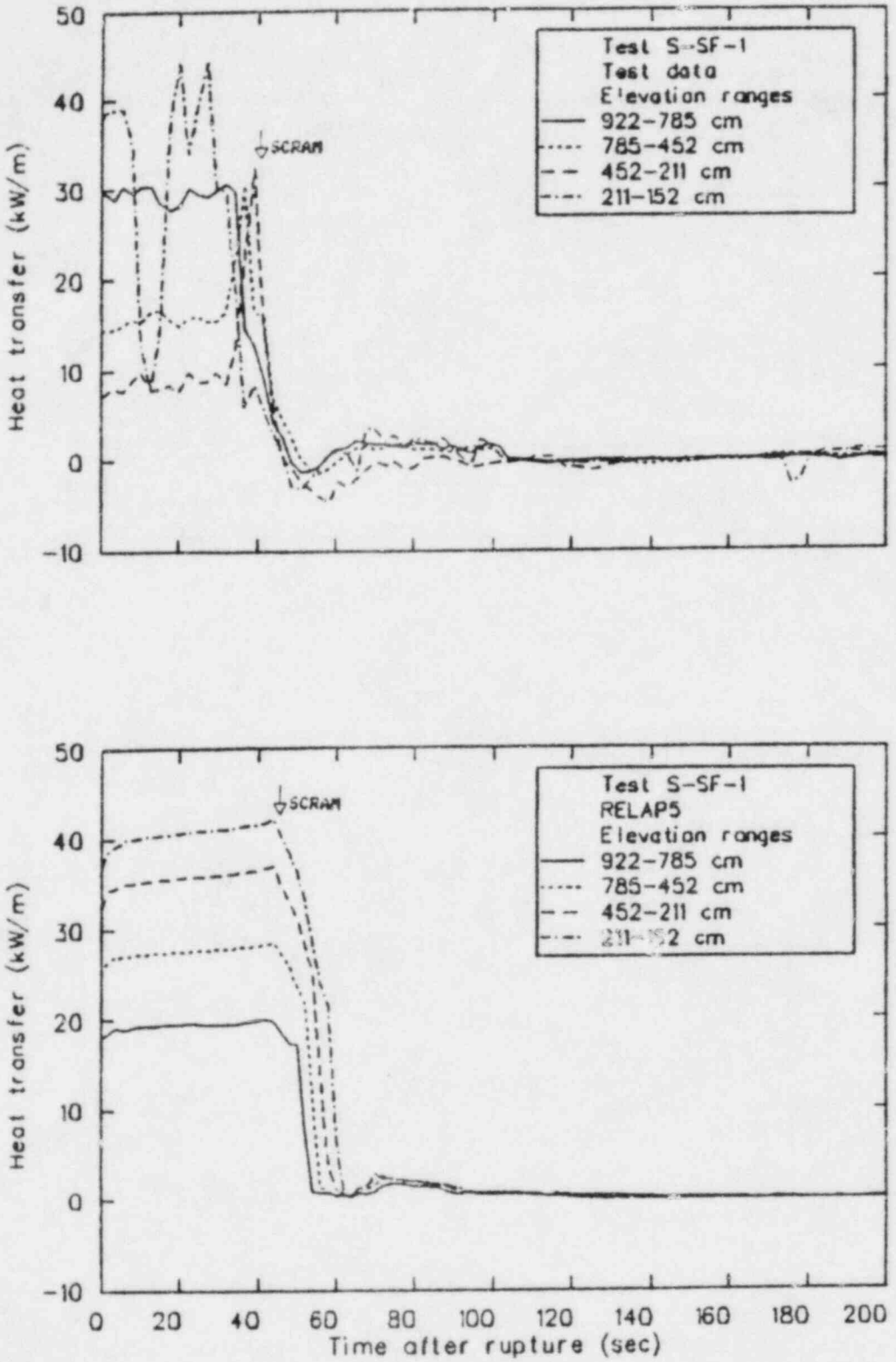

Figure 25. Local heat transfer rates in the broken loop steam generator for Test S-SF-1.

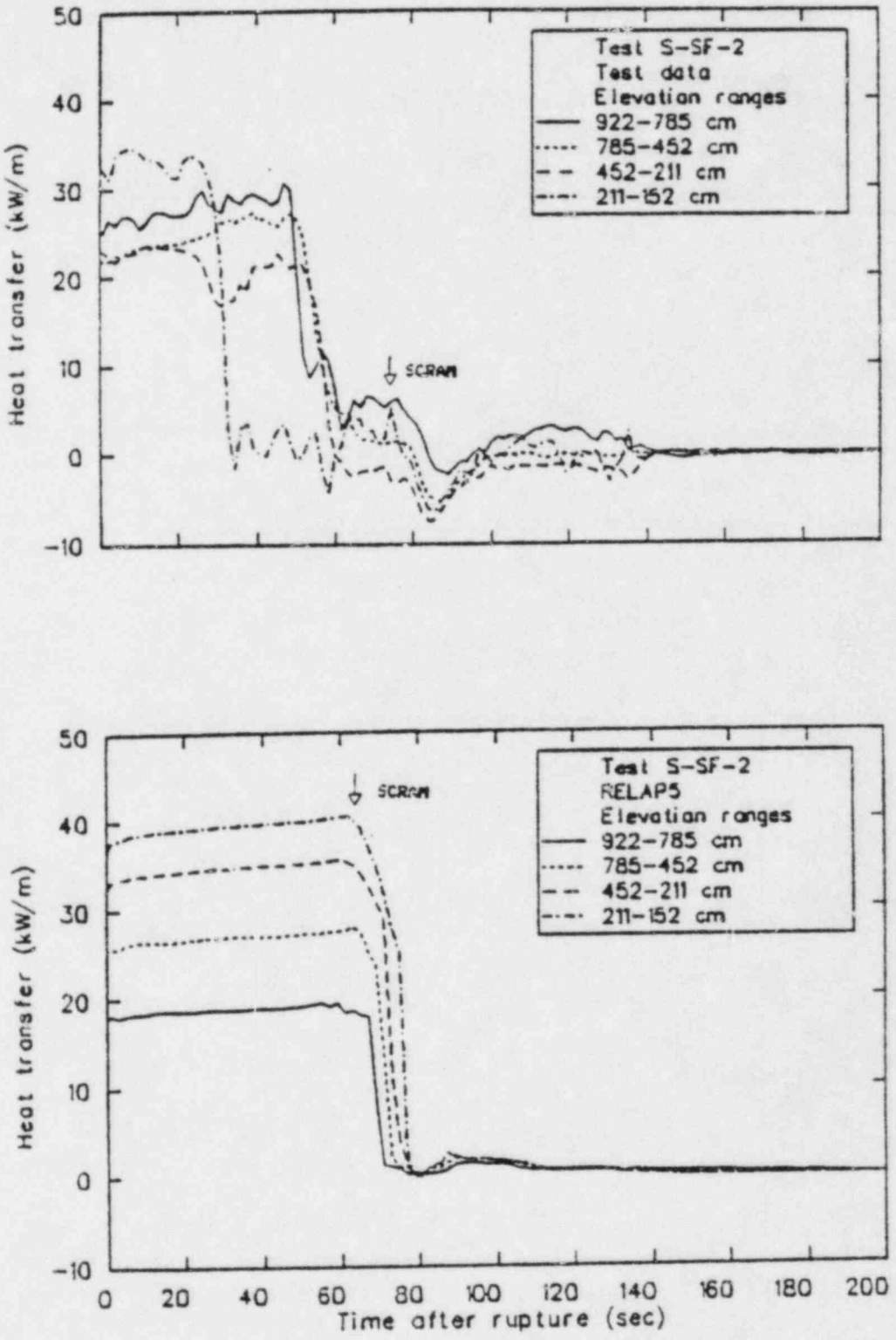

Figure 26. Local heat transfer rates in the broken loop steam generator for Test S-SF-2.

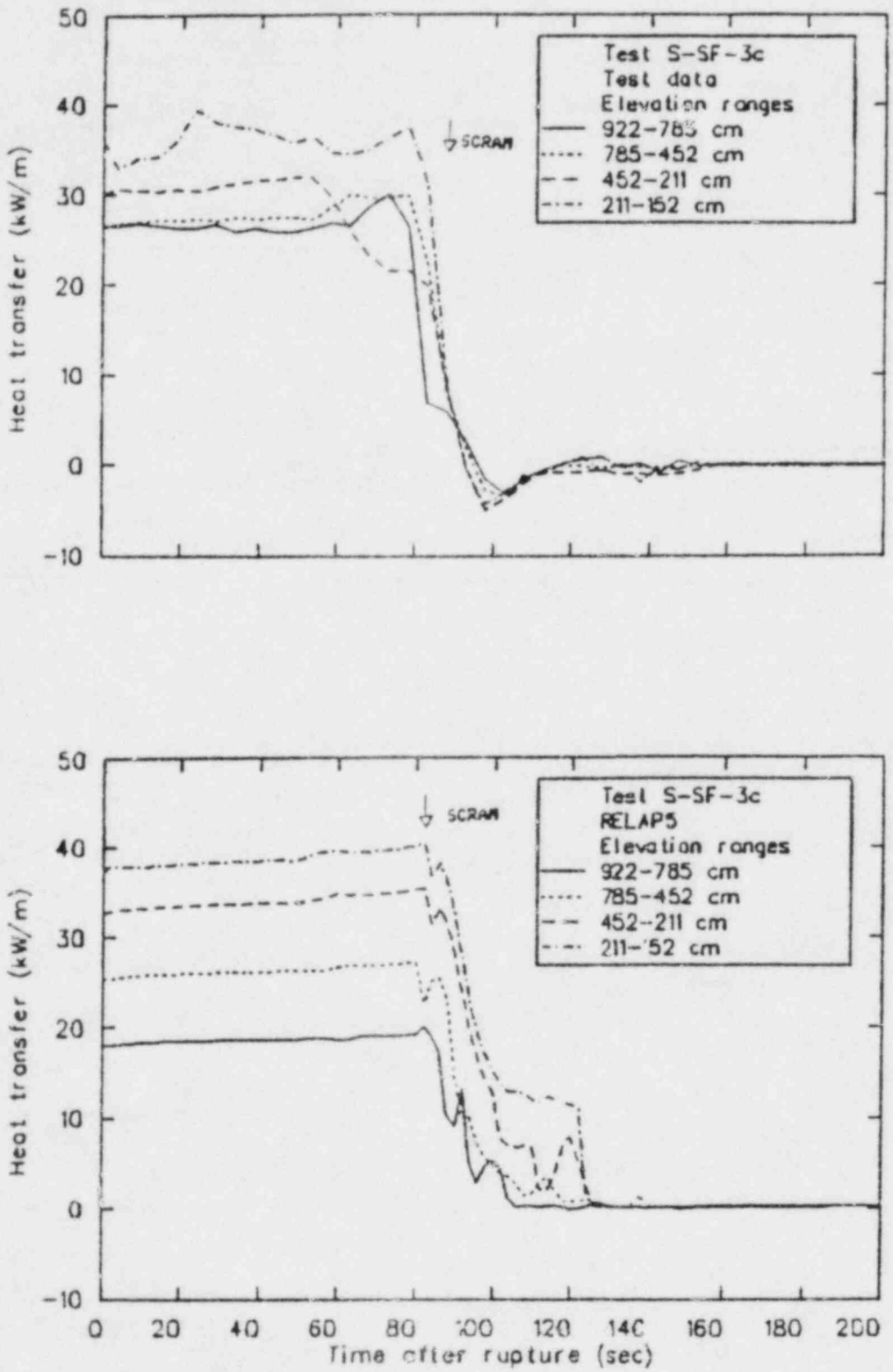

Figure 27. Local heat transfer rates in the broken loop steam generator for Test S-SF-3c.

5. CONCLUSIONS

The general characteristics and data trends of Tests S-SF-1, 2, and 3c were calculated by RELAP5. Degradation of the primary-to-secondary heat sink caused the PCS to heatup and pressurize to the SCRAM setpoint. The PCS pressure continued to rise momentarily after SCRAM, then depressurized continuously thereafter, aided by system heat losses to ambient and cooldown of the steam generator secondaries by injection of auxiliary feedwater. Details of the primary-to-secondary heat transfer degradation, however, were not calculated. In particular, degradation of the broken loop steam generator heat transfer prior to SCRAM as the secondary coolant inventory was depleted was not calculated due to preferential blowdown of the steam generator downcomer with respect to the riser. Consequently, degradation of the heat sink prior to SCRAM is attributed to the intact loop steam generator exclusively. The calculated degradation of the intact loop steam generator heat transfer as a function of secondary coolant inventory was in good agreement with data.

6. RECOMMENDATIONS

The following recommendations are made to improve the quality of future RELAP5 calculations of FWLB transients and to improve the assessment of the same calculations. These recommendations are based on the analysis results presented in this report.

1. For slightly subcooled upstream break conditions, such as those which typically exist for a considerable time during a FWLB transient, the RELAP5 computer code underpredicts the break flow rate. Available critical flow data having upstream subcooled conditions less than approximately 10 K should be used to benchmark the code.

2. Preferential blowdown of the broken loop steam generator secondary downcomer with respect to the riser was calculated. This behavior is sensitive to the nodalization density (number of control volumes used), use of smooth or abrupt area change models, and use of "pipe" or "annulus" components in the riser and downcomer (or more specifically the magnitude of the calculated interphase drag). More sensitivity studies are needed to determine the modeling approach that best simulates the observed phenomena.

3. More instrumentation are need in the steam generator secondaries such that the effects on heat transfer of separator efficiency, recirculation ratio, riser void distribution, and the respective contributions to the break flow from the downcomer and the riser regions can be determined.

7. REFERENCES

1. D. J. Shimeck, Experiment Operating Specification for Semiscale Mod-2A Steam and Feedwater Line Break Scoping Experiment Series, EGG-SEMI-5830, March 1982.

2. V. H. Ransom et al., RELAP5/MOD1 Code Manual, Volumes 1 and 2, NUREG/CR-1826, March 1982.

3. M. T. Leonard, RELAP5 Standard Model Description for the Semiscale Mod-2A System, EGG-SEMI-5692, December 1981.

4. D. J. Shimeck, L. J. Martinez, G. R. Berglund, Quick Look Report for Semiscale Mod-2A Feedwater Line Tests S-SF-1, S-SF-2, and S-SF-3, EG&G-SEMI-5940, July 1982.

APPENDIX A

TESTS S-SF-1, 2, AND 3c RELAP5 CALCULATION TO DATA COMPARISONS

APPENDIX A

TESTS S-SF-1, 2, AND 3c RELAP5 CALCULATION TO DATA COMPARISONS

Contained in this appendix are RELAP5 calculation-to-data comparisons for Tests S-SF-1, 2, and 3c. These comparisons are presented to supplement those in the main body of this report. The RELAP5 output files for these calculations are stored at the Idaho National Engineering Laboratory in the Computer Code Configuration Management (CCCM) System. Archival reference numbers are F00950, F00949, F00948 for Tests S-SF-1, 2, and 3c, respectively.

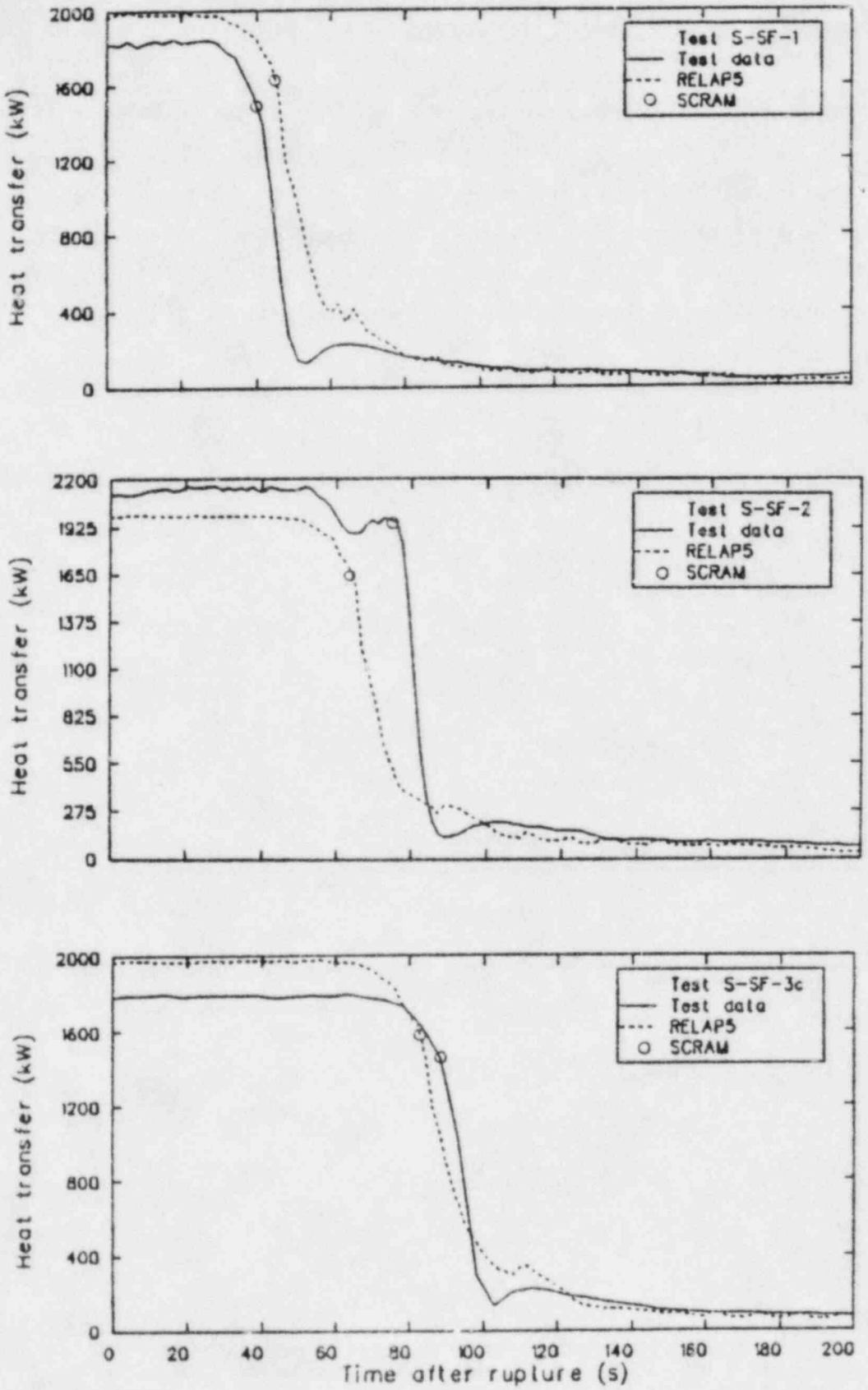

Figure A-1. Total heat transferred to secondaries.

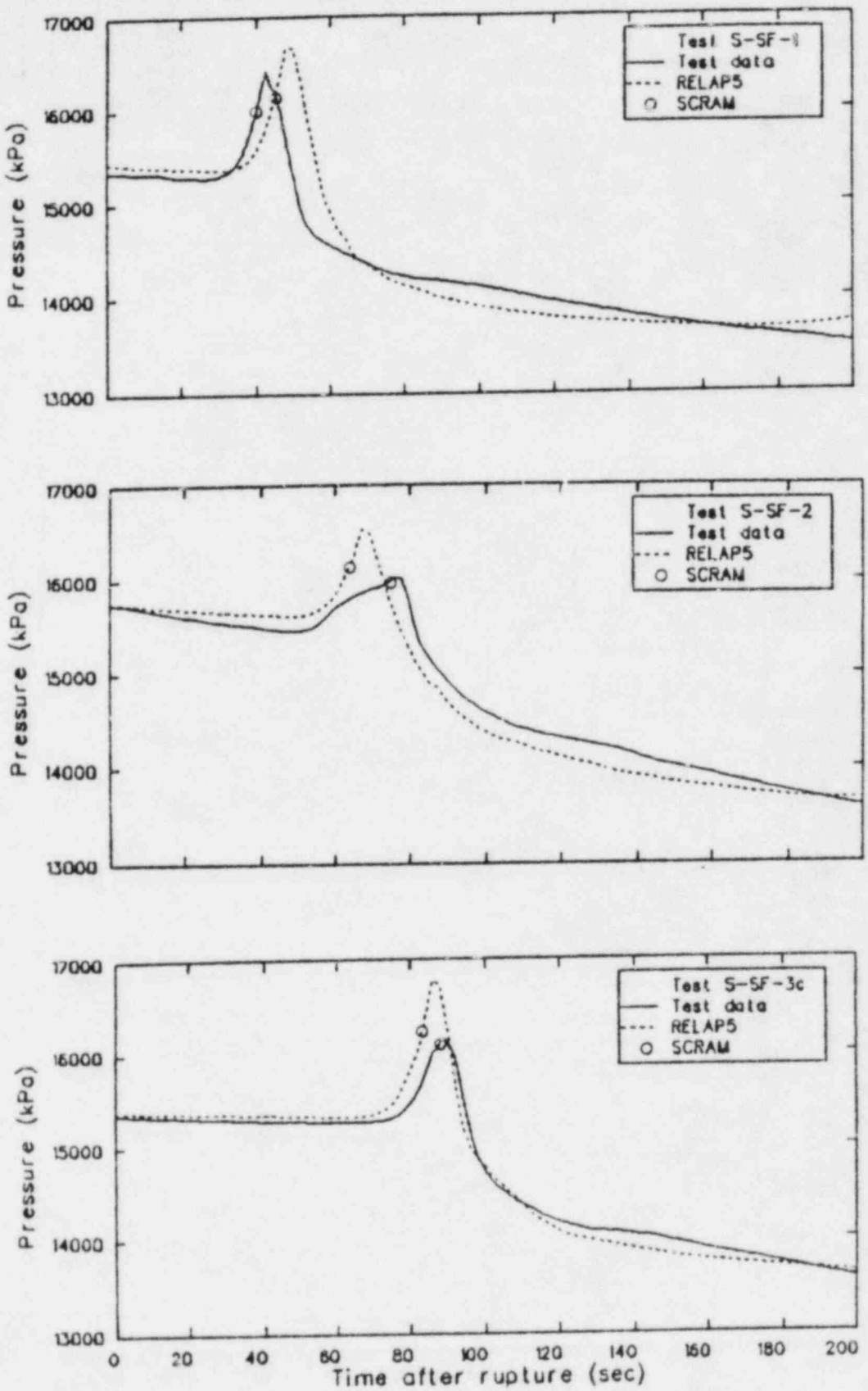

Figure A-2. Broken loop pump discharge pressure.

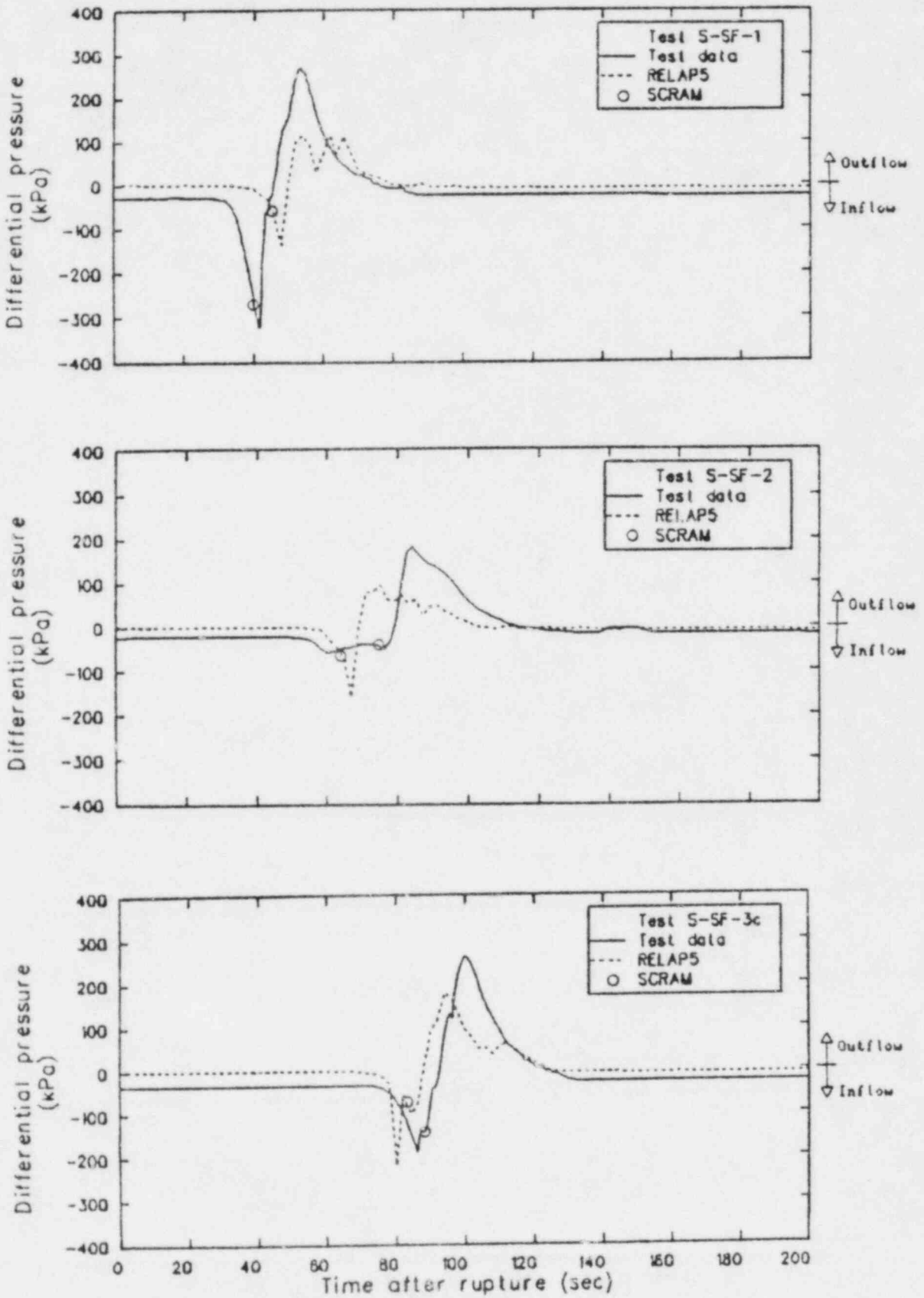

Figure A-3. Pressure difference across pressurizer surge line.

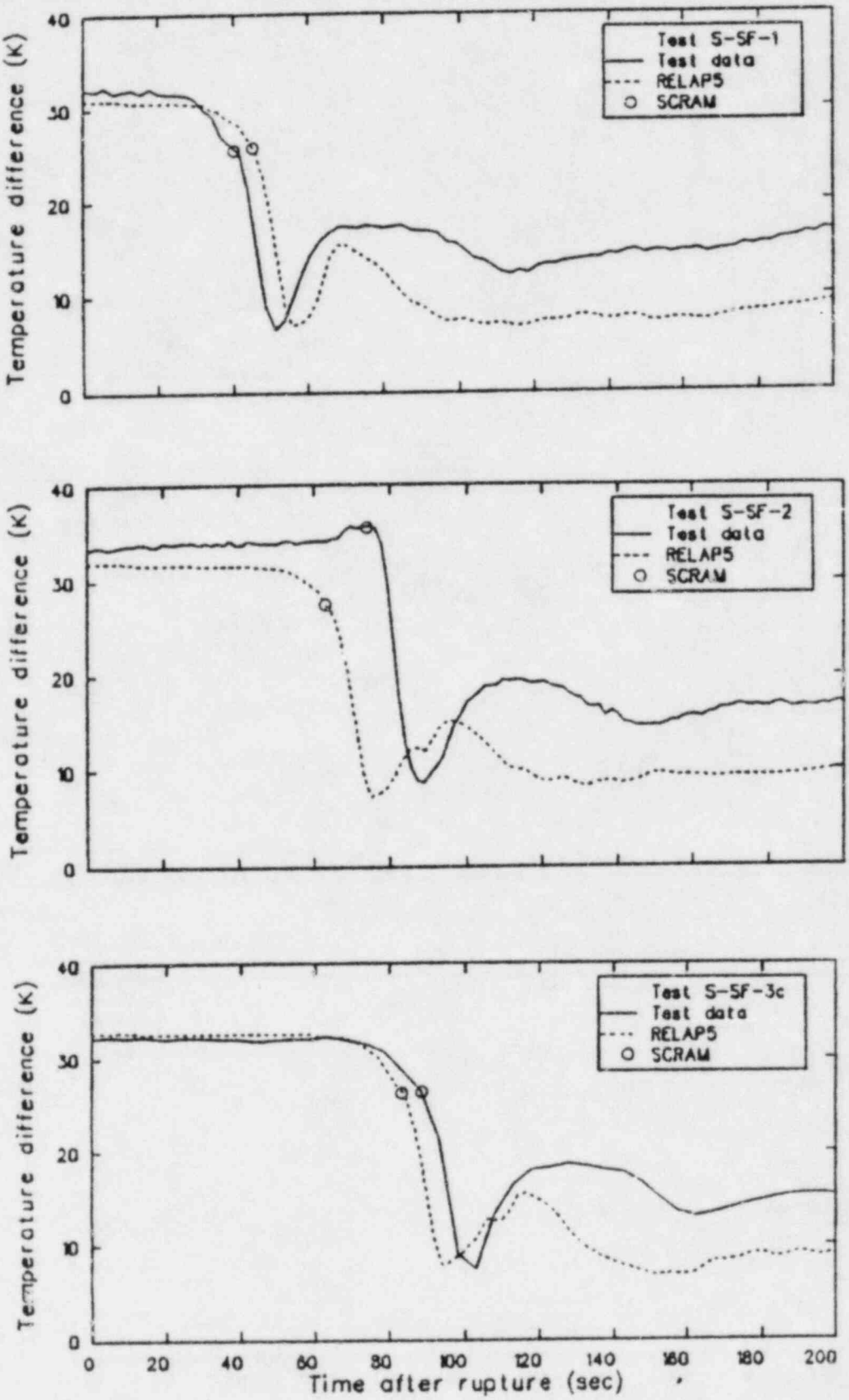

Figure A–4. Intact loop primary temperature difference between steam generator inlet and outlet.

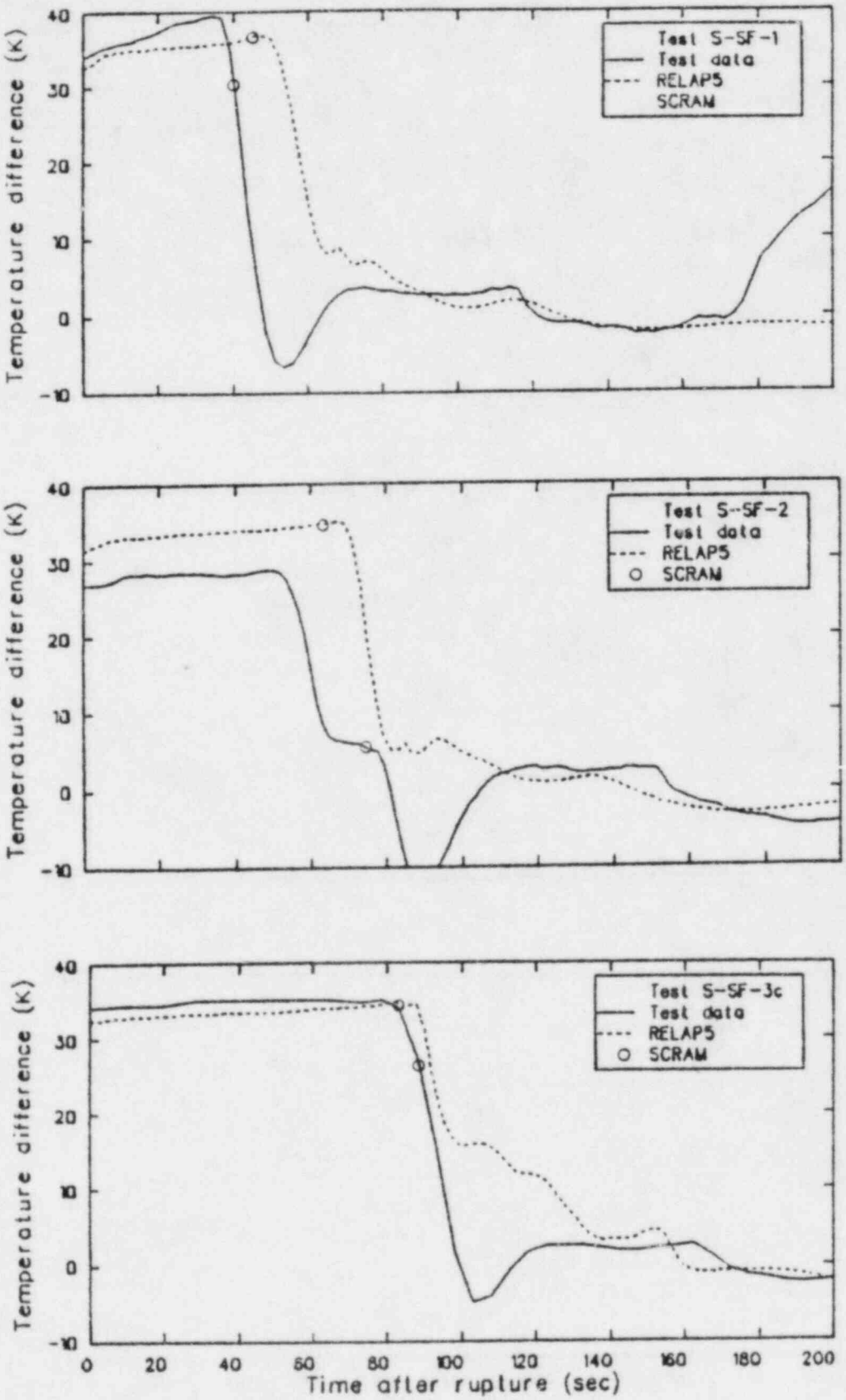

Figure A-5. Broken loop primary temperature difference between steam generator inlet and outlet.

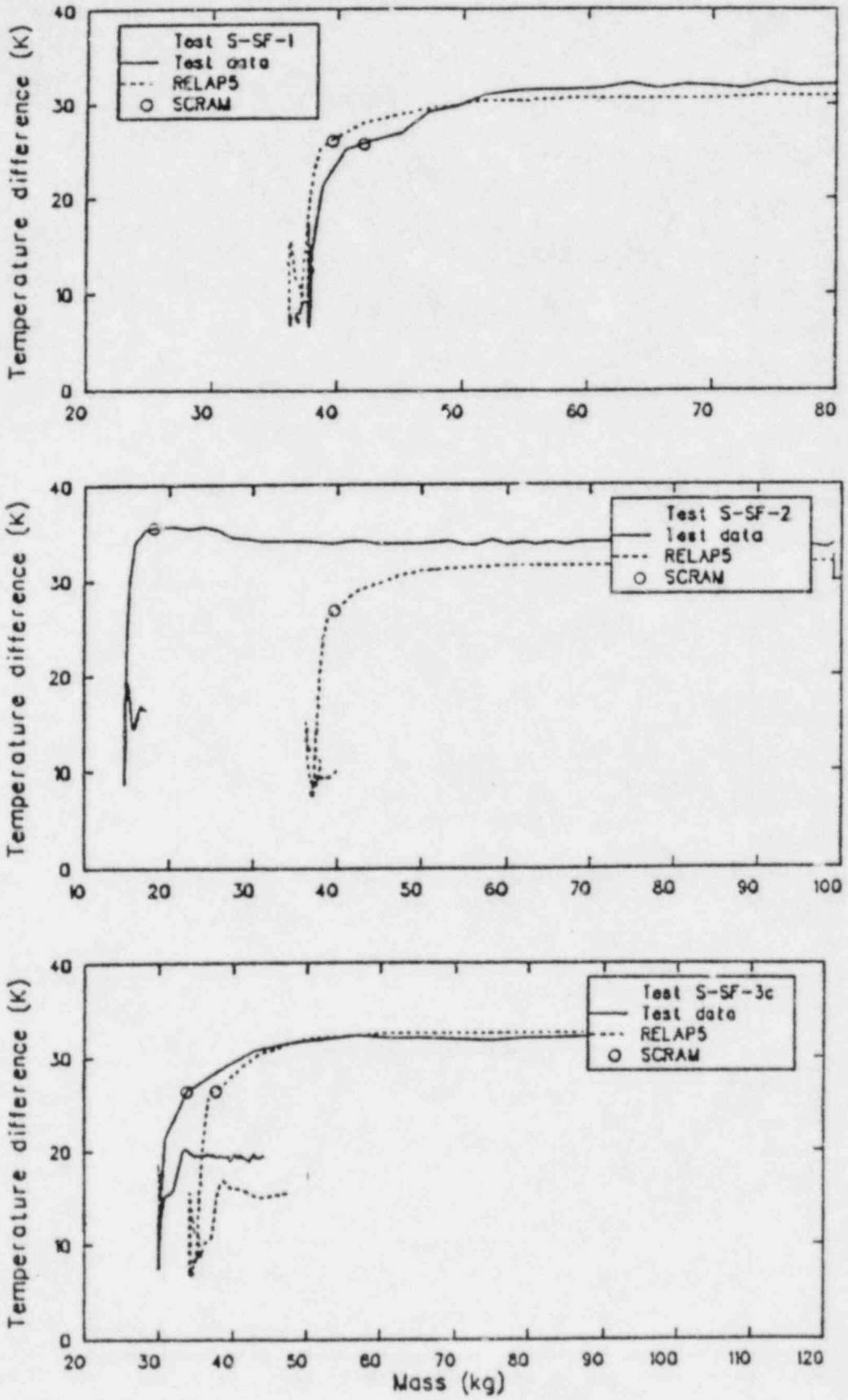

Figure A-6. Intact loop primary temperature difference between steam generator inlet and outlet as a function of the mass in the intact loop secondary.

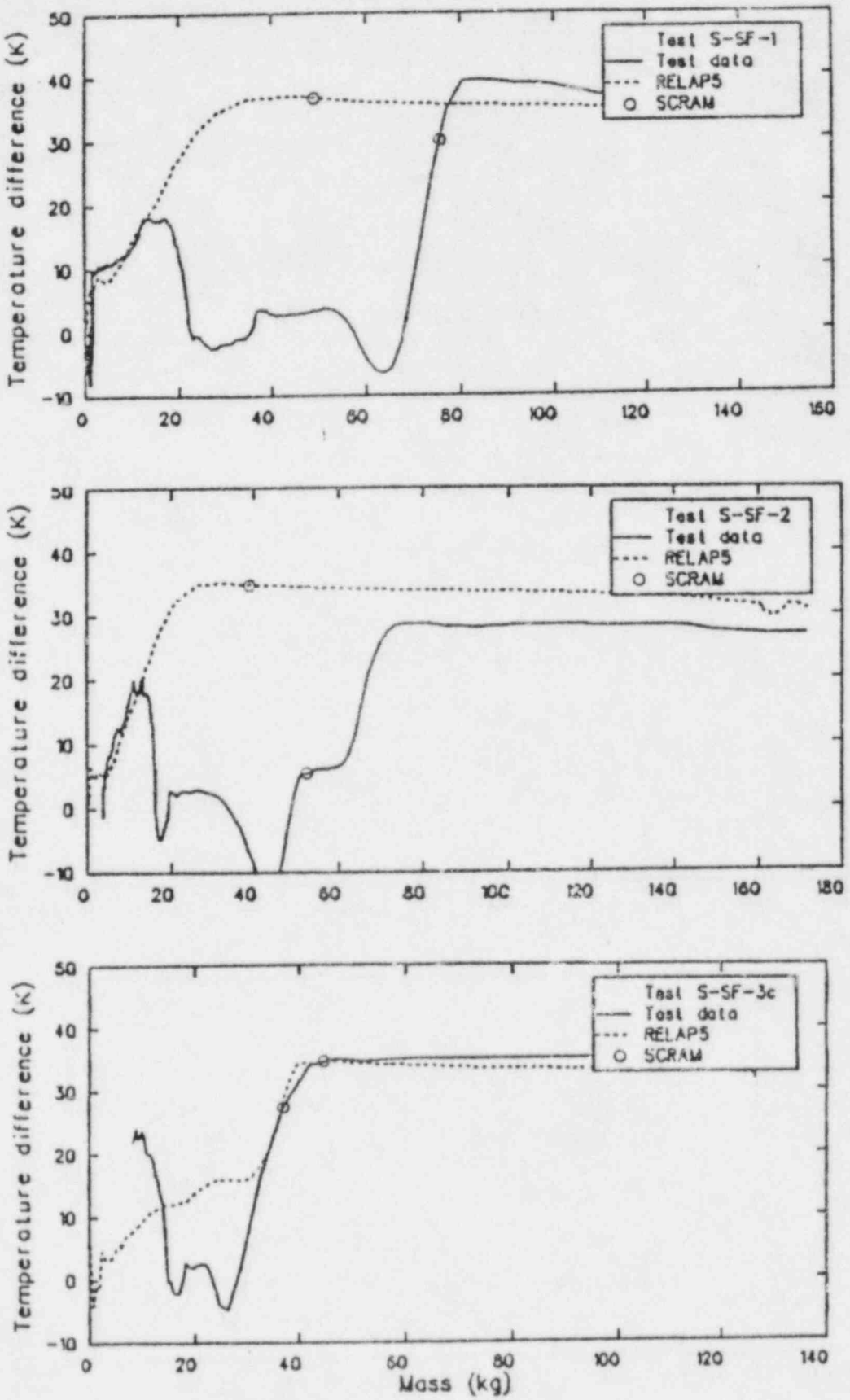

Figure A-7. Broken loop primary temperature difference between steam generator inlet and outlet as a function of the mass in the broken loop secondary.

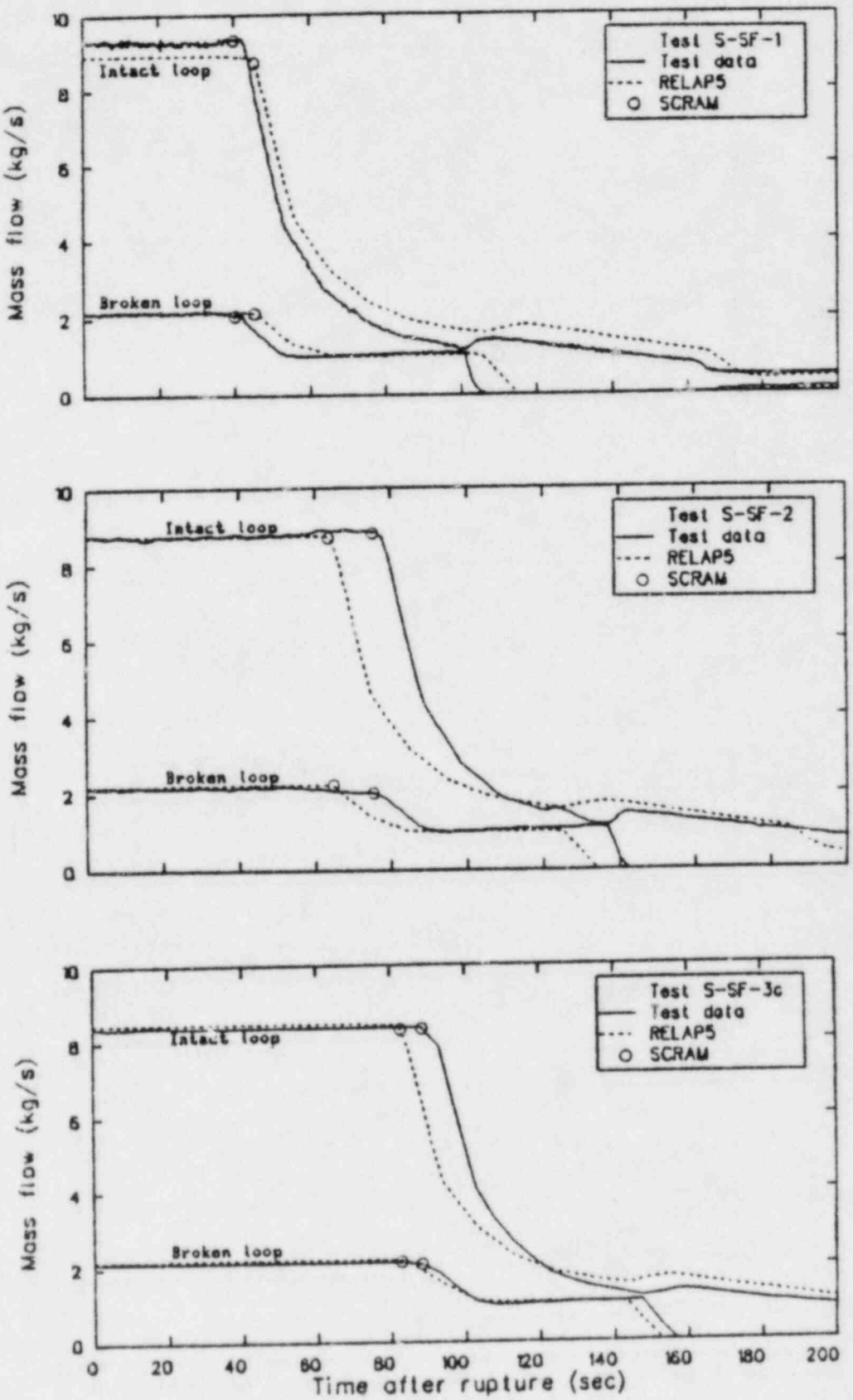

Figure A-8. Primary loop mass flow rates.

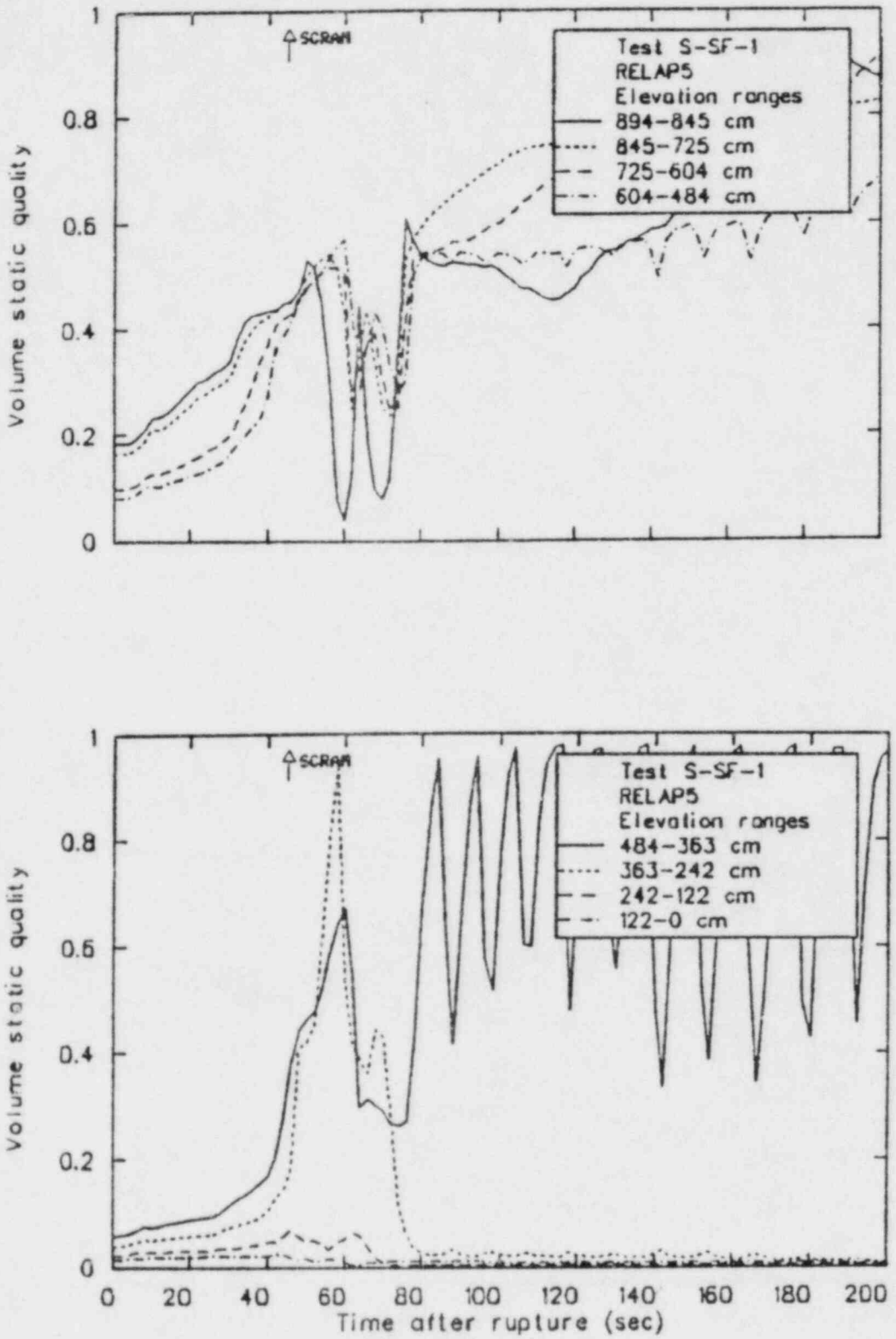

Figure A-9. Qualities in intact loop steam generator riser for Test S-SF-1.

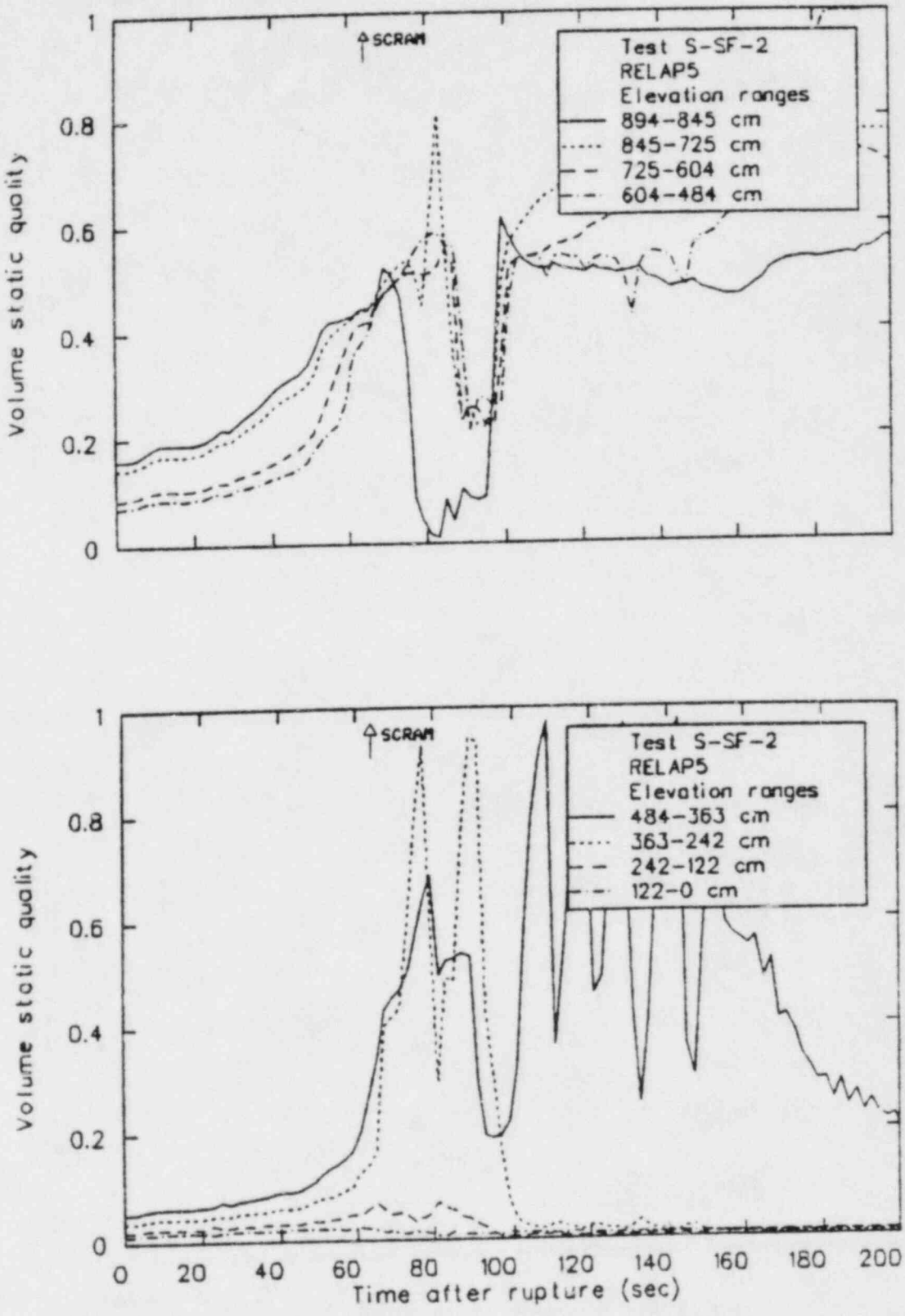

Figure A-10. Qualities in intact loop steam generator riser for Test S-SF-2.

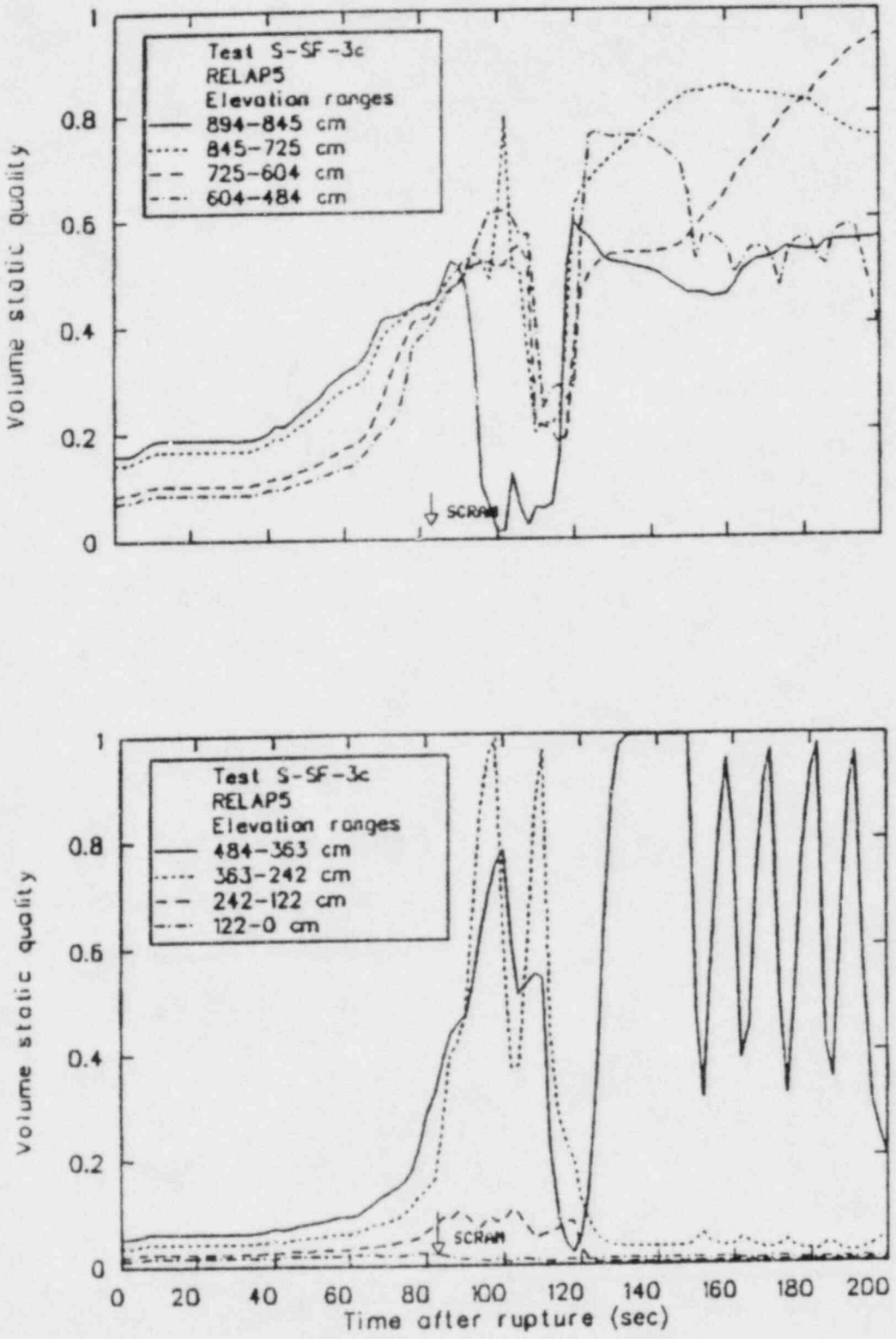

Figure A-11. Qualities in intact loop steam generator riser for Test S-SF-3c.

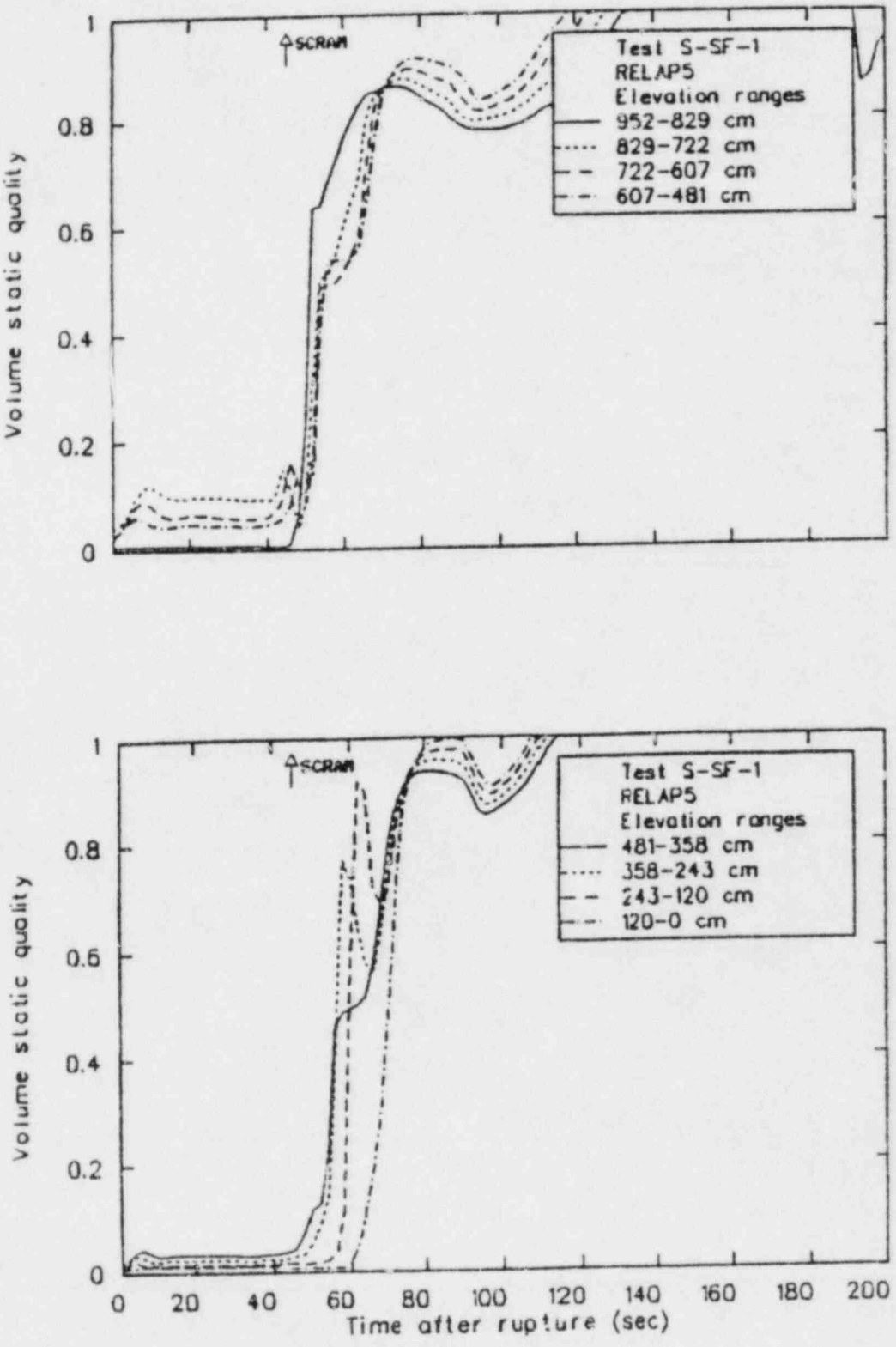

Figure A-12. Qualities in broken loop steam generator riser for Test S-SF-1.

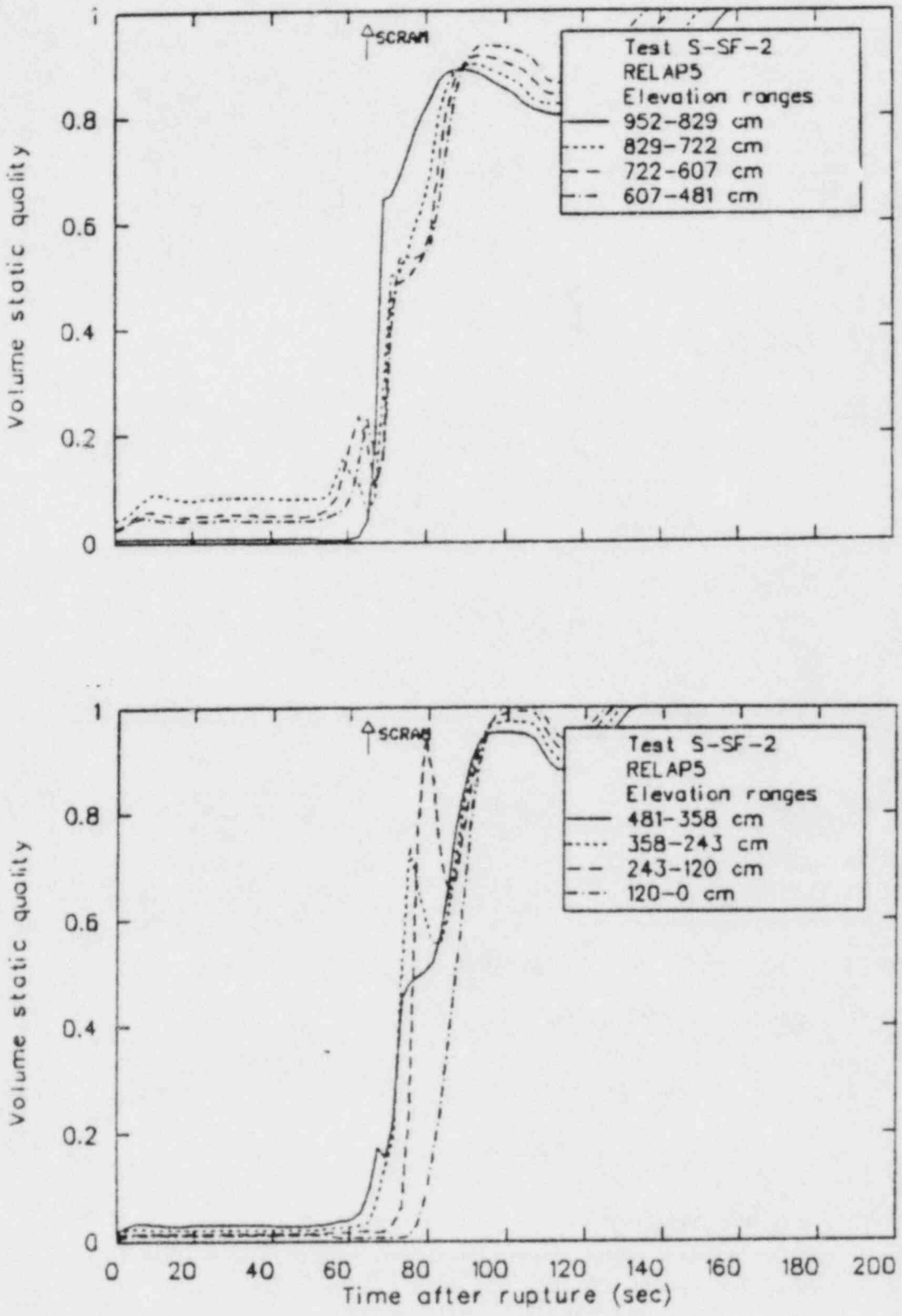

Figure A-13. Qualities in broken loop steam generator riser for Test S-SF-2.

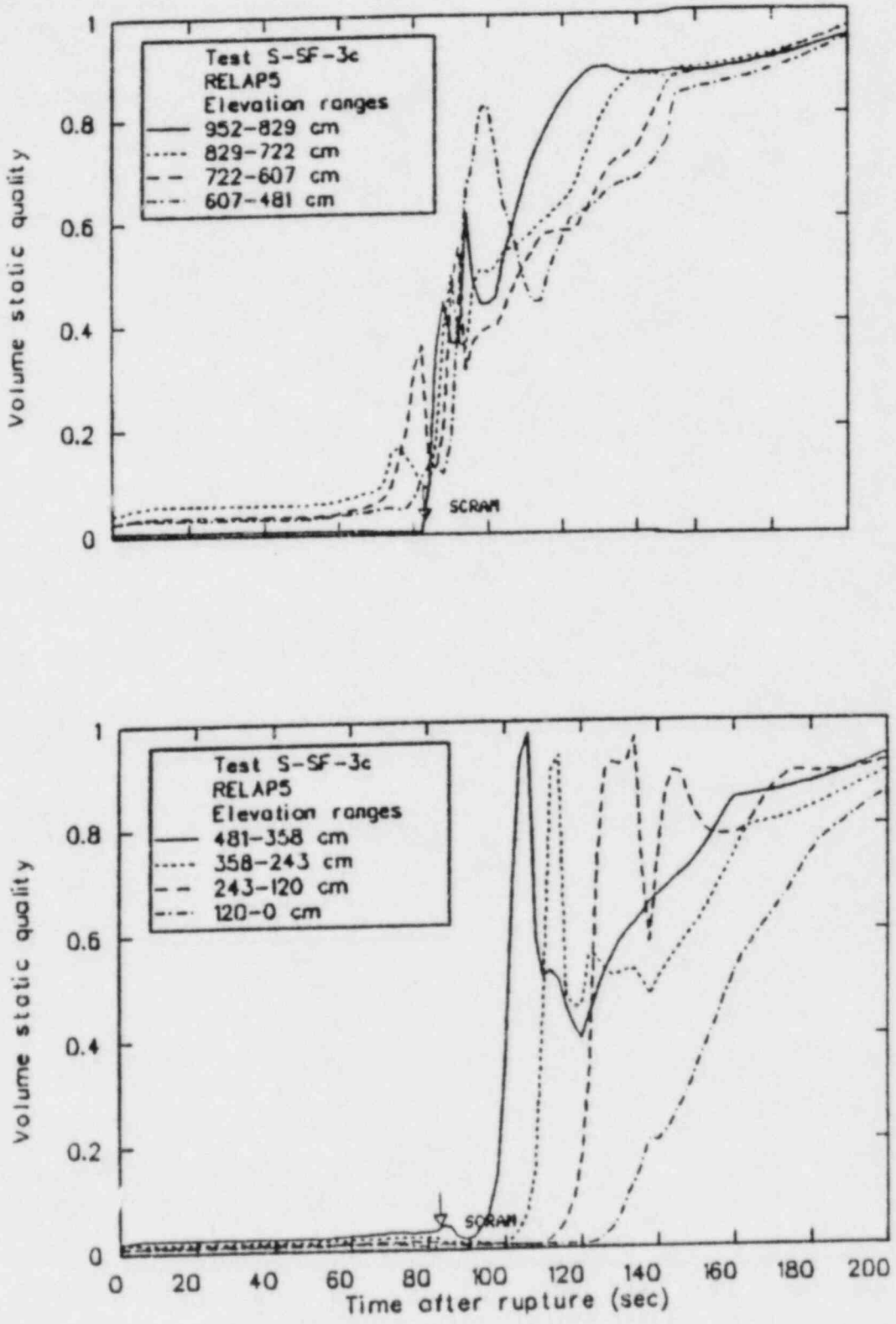

Figure A-14. Qualities in broken loop steam generator riser for Test S-SF-3c.

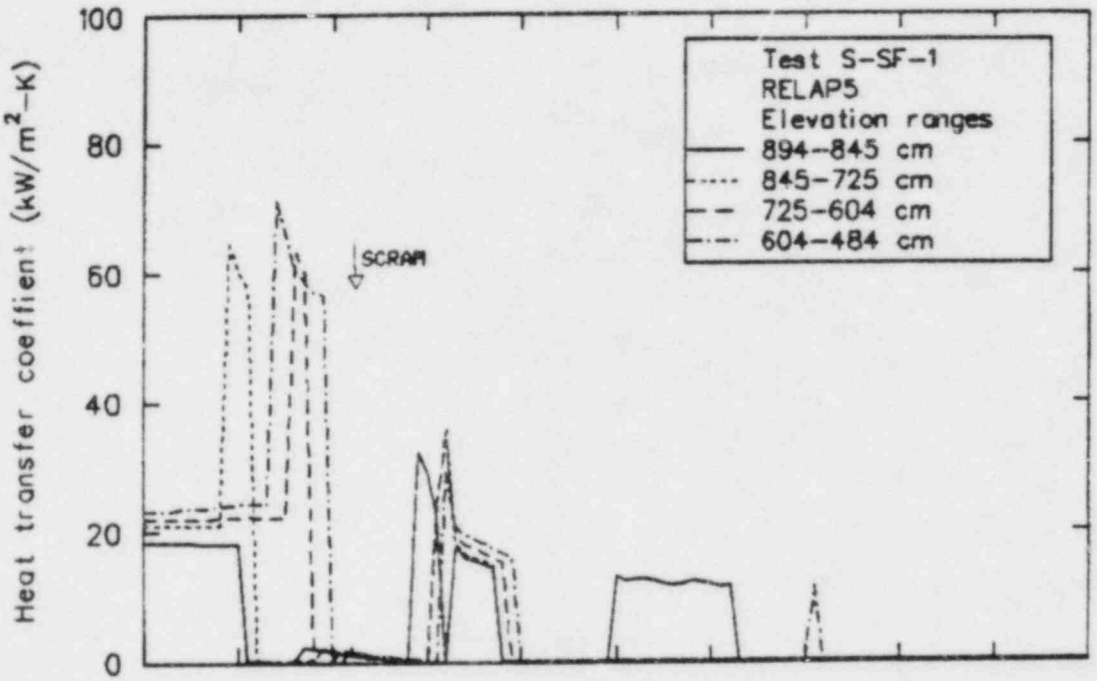

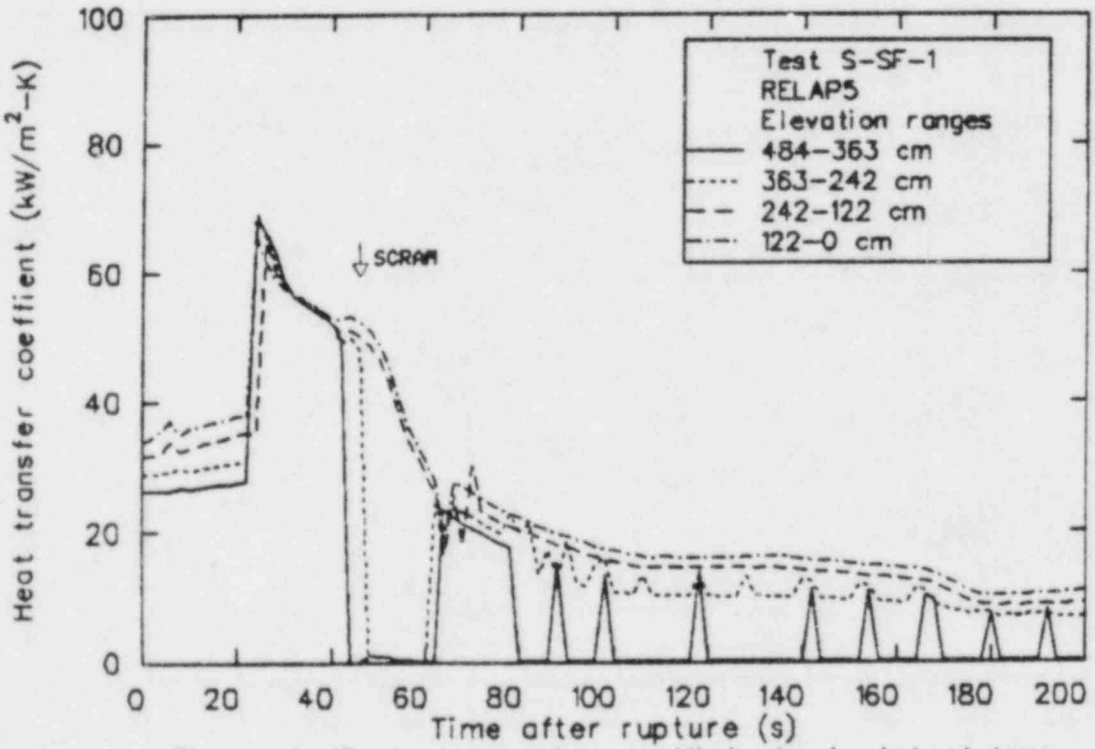

Figure A-15. Heat transfer coefficients in intact loop steam generator riser for Test S-SF-1.

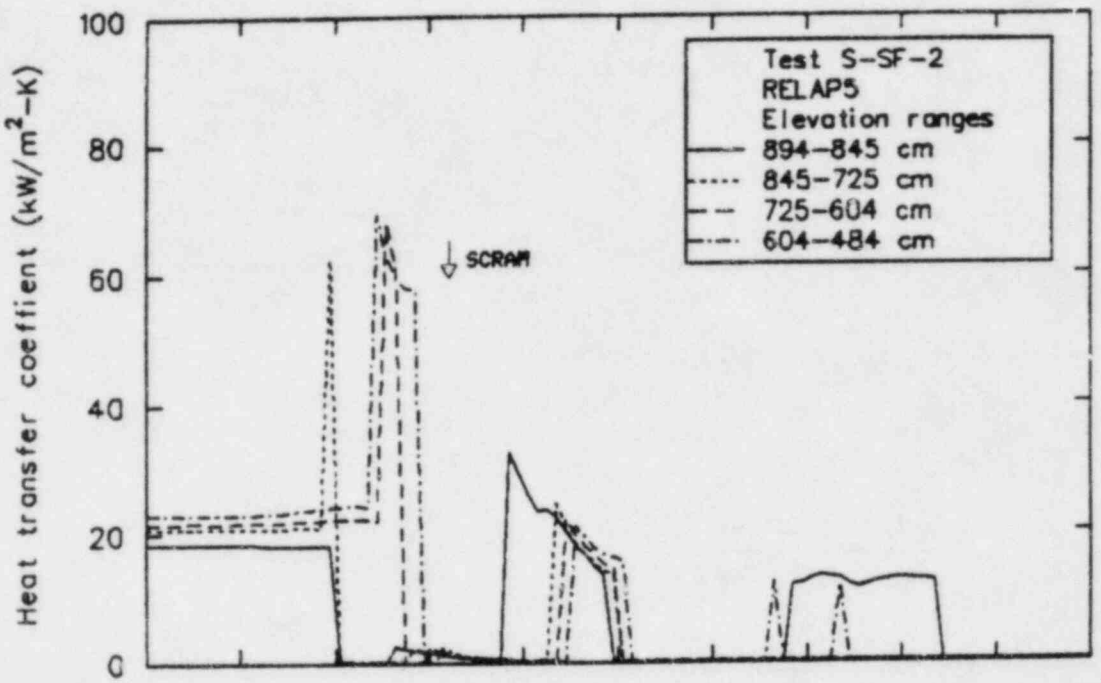

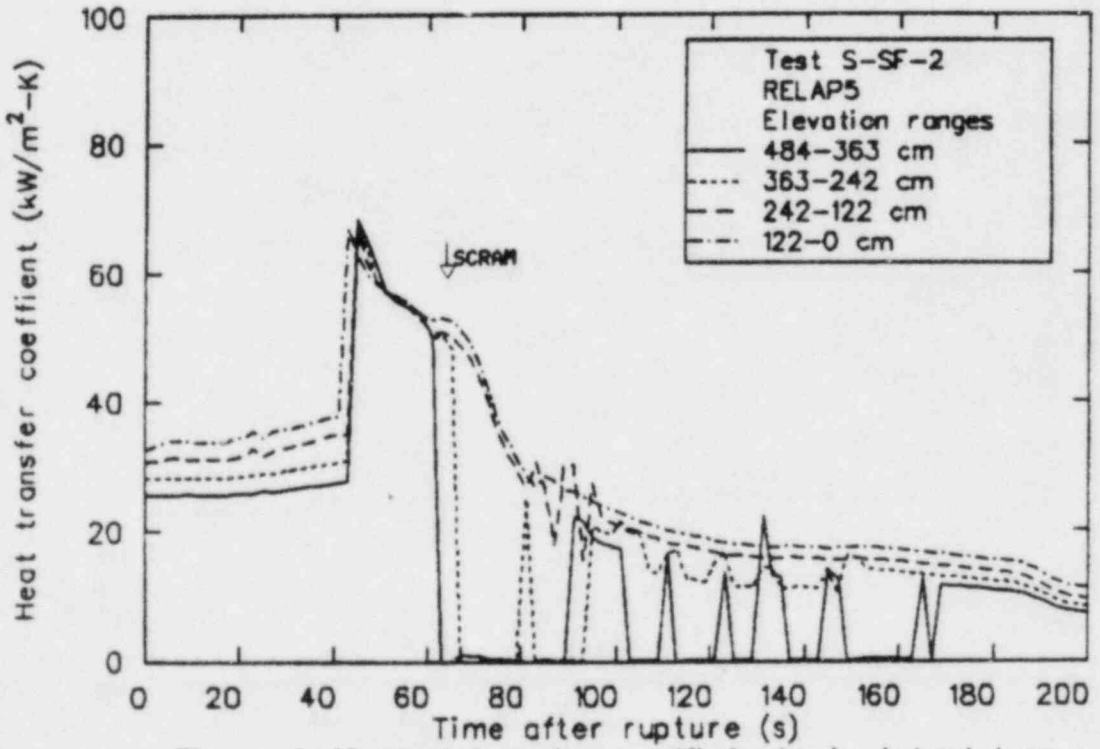

Figure A-16. Heat transfer coefficients in intact loop steam generator riser for Test S-SF-2.

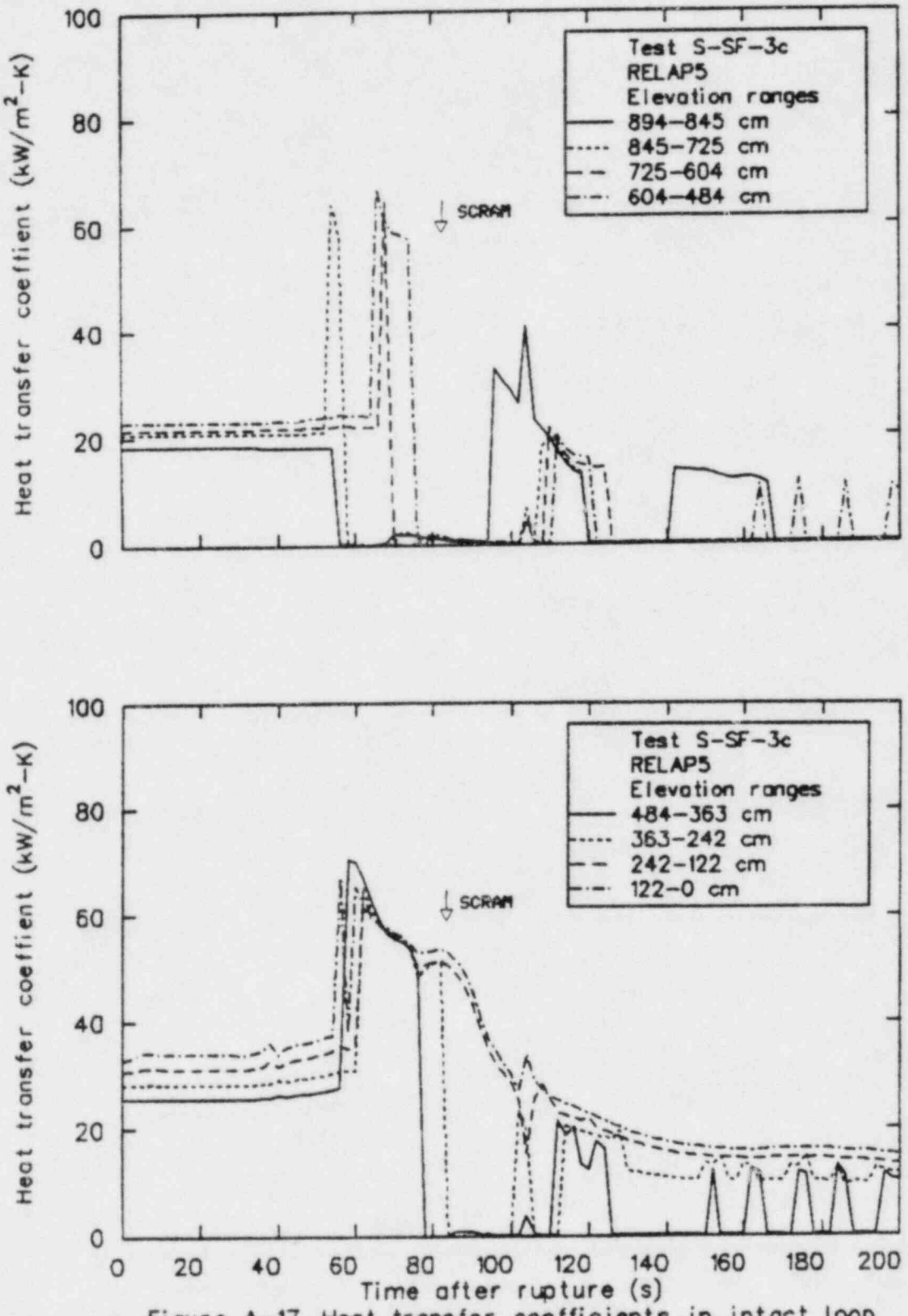

Figure A-17. Heat transfer coefficients in intact loop steam generator riser for Test S-SF-3c.

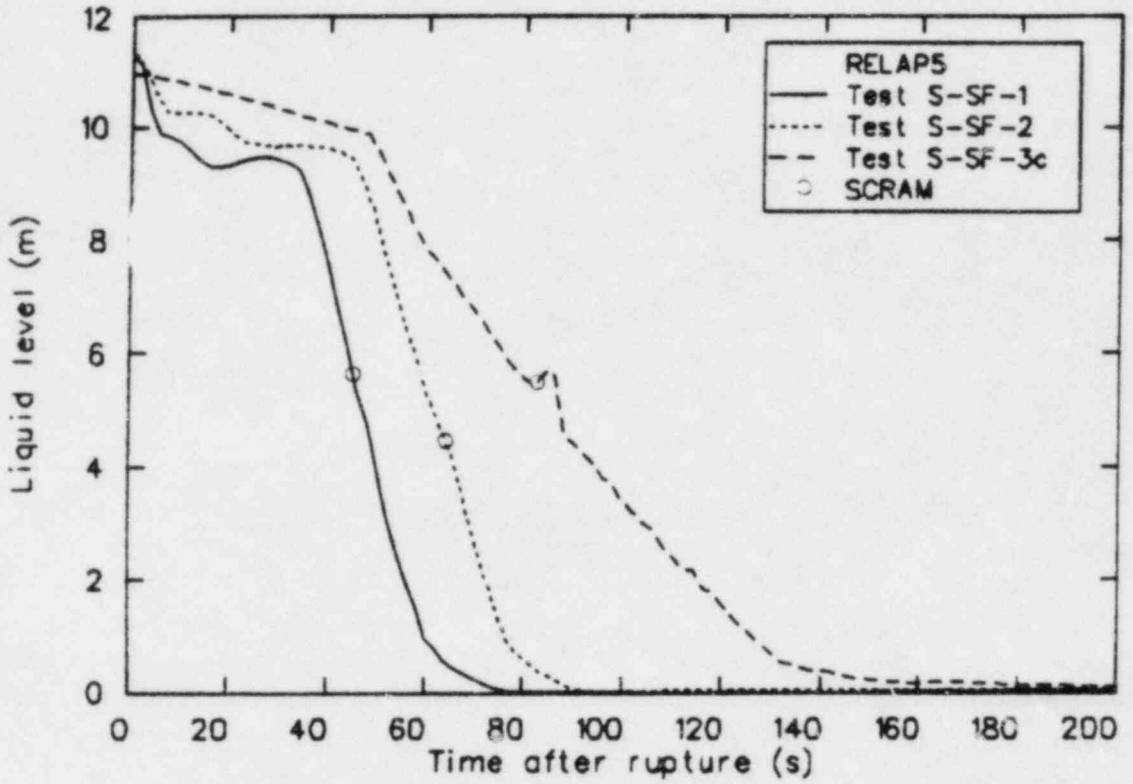

Figure A-18. Broken loop steam generator downcomer level.

APPENDIX B
RELAP5 SUBCOOLED CRITICAL FLOW MODEL ADJUSTMENT

APPENDIX B

RELAP5 SUBCOOLED CRITICAL FLOW MODEL ADJUSTMENT

Initial RELAP5 calculations of Test S-SF-3c showed that for most of the period preceeding SCRAM the fluid immediately upstream of the break was subcooled by less than 10 K. (This was also the case in the other calculations.) During this same period, use of a subcooled discharge coefficient (CD1) of 1.0 resulted in underpredicting the critical flow out the break by as much as 45%. Generally, use of a subcooled discharge coefficient of 1.0 results in good agreement with data for elliptical-entrance orifices of the type used for Tests S-SF-1, 2, and 3c. A study was then performed to determine whether the modified Burnell Critical Flow model[B-1] (formulated similarly to the critical flow calculation algorithm used in RELAP5), as implemented in the MASFLO[B-2] computer code and driven with measured break upstream conditions, resulted in better agreement with data. The results of this study indicated that the RELAP5 and modified Burnell model calculated mass flow rates (Figure B-1) were in agreement when the upstream conditions (Figures B-2 and B-3) were similar or from approximately 25 to 65 s, and less than observed in test data.

The undeprediction of test data is similar to the results reported in Reference B-3, in which the modified Burnell model as implemented in the MASFLO computer code was compared with Loss-of-Fluid Test (LOFT) Test Support Facility (LTSF) data for a 2.8 mm diameter rounded orifice nozzle. Figure B-4 shows a comparison of these data with the modified Burnell model expressed in terms of a mass flow ratio (MFR), which is defined as measured mass flow rate divided by the calculated mass flow rate. The temperature dependence of the MFR can be expressed by the following least-squares fit:

$$MFR = 1.642 - 7.1167 \times 10^{-2}\ SC + 2.9878 \times 10^{-3}\ (SC)^2 - 4.4289 \times 10^{-5}\ (SC)^3,$$

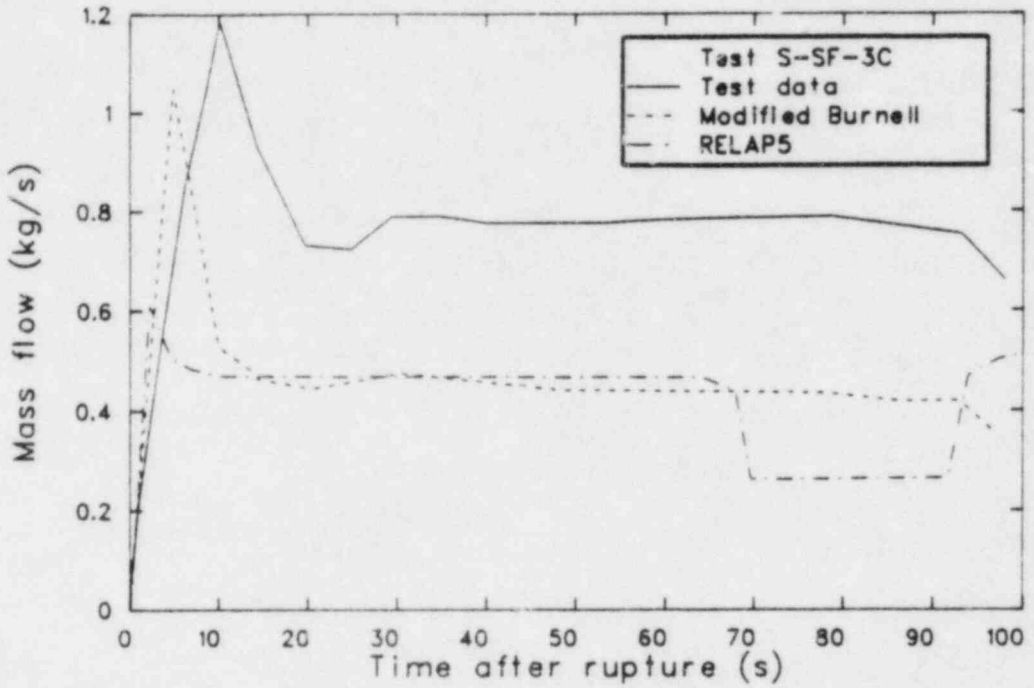

Figure B-1. Break flow model comparisons.

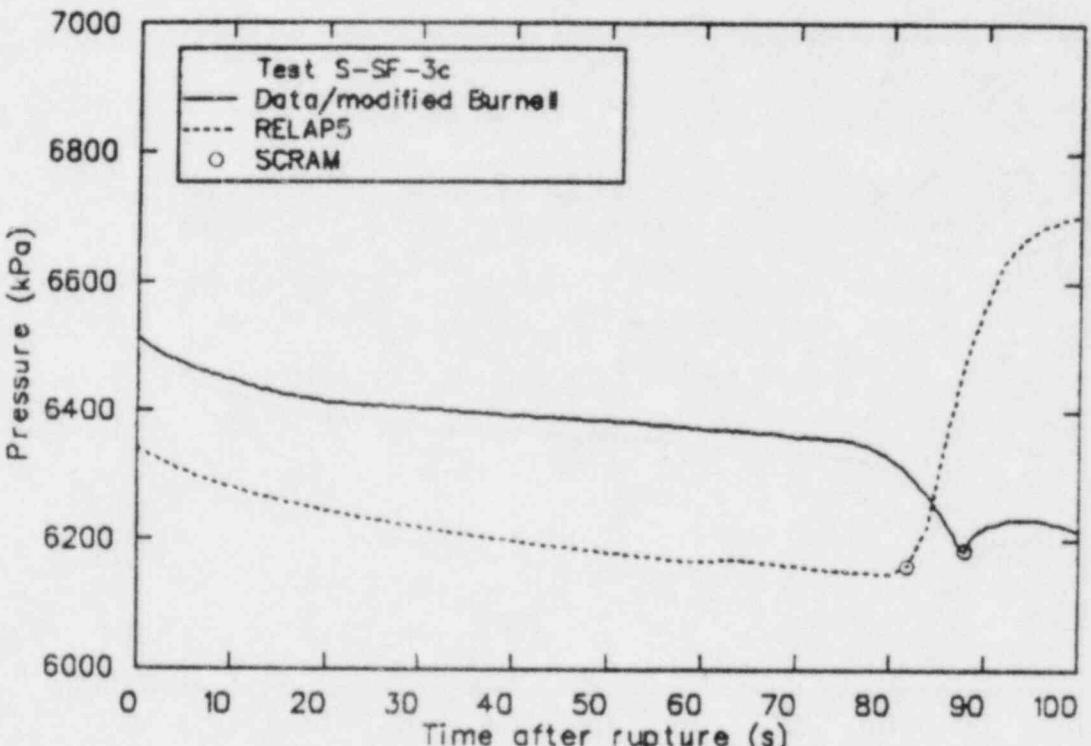

Figure B-2. Pressure of fluid upstream of break.

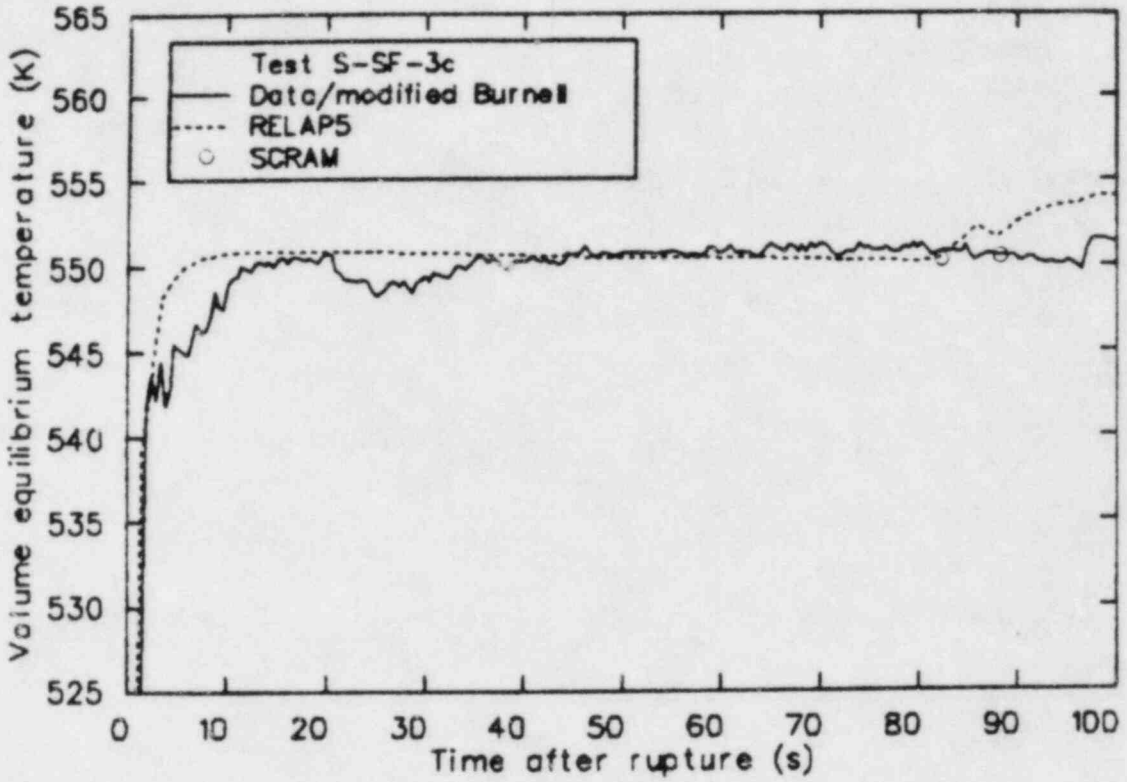

Figure B-3. Temperature of fluid upstream of break.

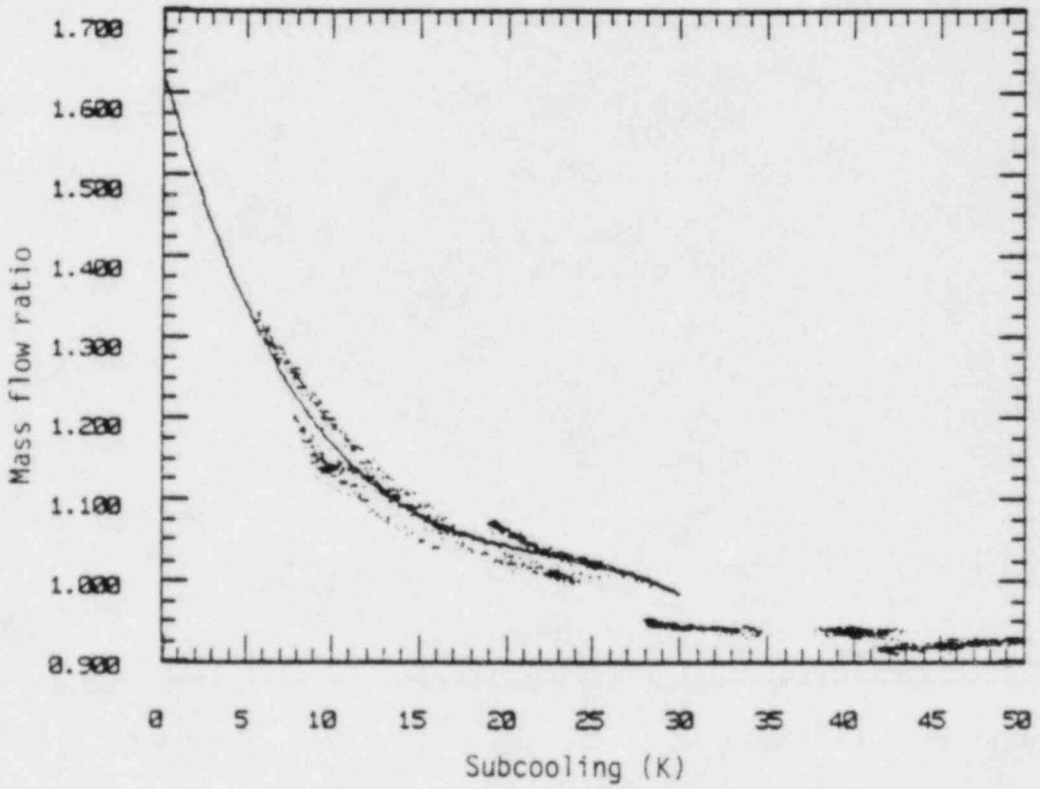

Figure B-4. Mass flow ratio as a function of subcooling.

where

SC = degrees K subcooling, $0\ K \leq SC \leq 30\ K$.

This MFR was used as the subcooled discharge coefficient, CD1, in the RELAP5 analysis of Tests S-SF-1, 2, and 3c.

REFERENCES TO APPENDIX B

B-1. L. S. Tong, Boiling Heat Transfer and Two-Phase Flow, New York: John Wiley and Sons, Inc., 1965, p. 110.

B-2. D. G. Hall, A Study of Critical Flow Prediction for Semiscale Mod-1 Loss of Coolant Accident Experiments, TREE-NUREG-1006, December 1976.

B-3. D. B. Jarrell and D. G. Hall, Determination of Scale Effect on Subcooled Critical Flow, NUREG/CR-2498, EGG-2127, February 1982.